

Push-pull dyes based on pyropheophorbide-a for nonlinear optical imaging

Anjul Khadria,^a Yovan de Coene,^b Przemyslaw Gawel,^a Cécile Roche,^a Koen Clays^b and Harry L. Anderson^a

^aOxford University, Department of Chemistry, Chemistry Research Laboratory, 12 Mansfield Road, Oxford OX1 3TA, UK

^bDepartment of Chemistry, University of Leuven, Celestijnenlaan 200 D, 3001 Leuven, Belgium

Table of Contents

1.0 Reverse-phase (RP) HPLC method used for monitoring reactions i, ii, iii and v.....	2
2.0 Synthesis.....	3
2.1 Synthetic Procedures.....	3
2.2 Experimental characterization (¹ H NMR spectra, ¹³ C NMR spectra, MALDI ToF mass spectra).....	9
3.0 Absorption and fluorescence measurements.....	30
3.1 Determination of molar absorptivity.....	30
3.2 Measurement of quantum yield.....	30
4.0 Electrochemistry.....	32
5.0 Hyper-Rayleigh scattering.....	34
6.0 Microscopy.....	37
6.1 Droplet experiments.....	37
6.2 Microscopy.....	37
6.3 Tilt angle experiments.....	37
6.4 Presence of different transition dipole moments at different wavelengths.....	41
7.0 Computational studies of pyropheophorbide a derivatives.....	42
7.1 Conformational search of donor-acceptor-substituted pyropheophorbide a.....	42
7.2 Calculated Optical and Electronic Properties of 1a, 2a, 3a, and 4a.....	43
7.3 Cartesian Coordinates and Structural Parameters of Compounds.....	57
8.0 References.....	63

1.0 Reverse-phase (RP) HPLC method used for monitoring reactions i, ii, iii and v.

Table S1: Triple eluent gradient system for monitoring reactions through RP-HPLC

Time (minutes)	H ₂ O (%) + 0.1% TFA	Acetonitrile (%)	Methanol (%)
0	30	70	0
2	10	60	30
10	0	50	50
25	0	75	25
26	95	5	0

The solvent flow rate was set to 1 mL/min and the oven temperature to 40 °C. A Zorbax Eclipse XDB C18 column (4.6 x 150 mm, 5 μM) was used to analyze the reaction mixtures and purity of compounds.

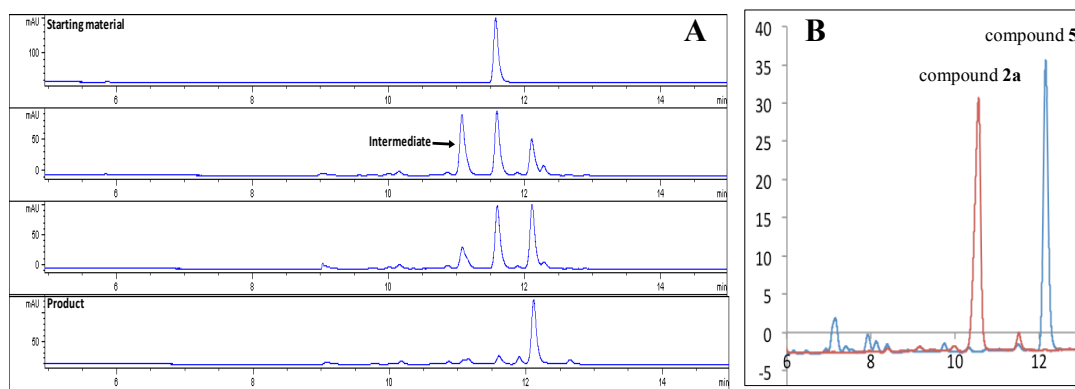


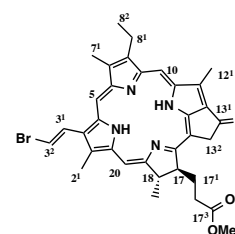
Figure S1: Reaction monitoring by RP-HPLC. : (A) Reaction (i) in Scheme 1 in main report to form compound **5**. The top chromatogram shows the starting material at a retention time of around 11.5 min. The second chromatogram shows formation of an intermediate at around 11 min and product at 12.2 min. The peaks in third chromatogram show the depletion of the intermediate and starting material along with the formation of product while the fourth row shows only the product peak at 12.2 min. (B) Reaction (ii) in Scheme 1 in main report to form compound **2a**. The retention time of compound **2a** is 10.5 min while that of compound **5** is 12.2 min. The method clearly shows formation of both the compounds **5** and **2a**. Peaks are detected at 665 nm.

2.0 Synthesis

General Procedure: Pyropheophorbide-a methyl ester (**1a**) was purchased from Chemieliva (China). All other chemicals were purchased from Sigma Aldrich and used without further purification; only *N*-bromosuccinimide, malononitrile and [Pd(PPh₃)₄] were purified before use. The chemical reactions were performed under inert atmosphere (Ar gas) unless otherwise stated. HPLC was performed on an Agilent 1100 instrument (Zorbax Eclipse XDB C18 column (4.6 x 150 mm, 5 μM). NMR spectra were acquired on 400 MHz (Bruker AVIIIHD 400), 500 MHz (Bruker AVII 500, Bruker AVIIIHD 500), 600 MHz (Bruker AVIIIHD 600), and 700 MHz (Bruker AVIII 700) spectrometers. Chemical shifts are reported in ppm relative to TMS and with the solvent (CDCl₃ unless otherwise stated) resonance as internal standard. The ¹H-NMR spectra of all the compounds were assigned using the spectrum of **1a** as reference, and also using COSY for some compounds. The ¹³C-NMR spectra of the compounds were assigned using their HSQC and HMBC spectra. MALDI-ToF (Waters MALDI micro) spectrometer was used for mass analysis. The UV-Vis (Perkin Elmer Lambda 20) and fluorescence (ISA instruments SA Inc., FluoroMax-2) measurements were performed in CH₂Cl₂ at 25 °C. The units of molar absorptivity are M⁻¹ cm⁻¹, and their logarithmic values are reported.

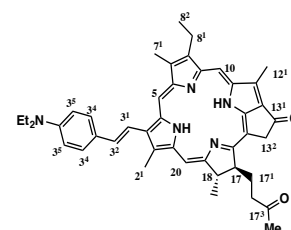
2.1 Synthetic Procedures

(E)-3²-Bromopyropheophorbide-a methyl ester 5. Pyropheophorbide-a methyl ester **1a** (25.0 mg, 45 μmol) was dissolved in 1,2-dichloroethane (15 mL) in a round bottom two-neck flask. *N*-Bromosuccinimide (8.2 mg, 45 μmol) was dissolved in 1,2-dichloroethane (1 mL) and added to the first solution. The reaction mixture was then heated to reflux under Ar at 84 °C. The reaction was monitored throughout using reverse phase HPLC (Table S1). After 3 h, an additional portion of *N*-bromosuccinimide (4.1 mg, 22 μmol) was added to the reaction mixture followed by the addition of another batch of *N*-bromosuccinimide (4.1 mg, 22 μmol) after 6.5 h. The heating was stopped after 9 h, and the reaction mixture was brought to room temperature. Two reactions were performed in parallel at 25 mg scale and then both mixtures were combined after the reaction was completed. The resultant mixture was passed through a plug of SiO₂ using 5% MeOH in CH₂Cl₂ as eluent, followed by purification through flash column chromatography using 5% EtOAc in CH₂Cl₂ as eluent to give **5**. **Yield:** 44.4 mg, 78 %. **¹H-NMR** (400 MHz, CDCl₃) δ/ppm: 9.17 (s, 1H; 10-H), 8.65 (s, 1H; 5-H), 8.44 (s, 1H; 20-H), 7.84 (d, ³J = 14.0 Hz, 1H; 3¹-H), 6.90 (d, ³J = 14.0 Hz, 1H; 3²-H), 5.23 (d, ²J = 19.6 Hz, 1H; 13²-CH₂), 5.08 (d, ²J = 19.6 Hz, 1H; 13²-CH₂), 4.47 (q, J = 7.3 Hz, 1H; 18-H), 4.27 (m, 1H; 17-H), 3.69 (q, ³J = 9.9 Hz, 2H; 8²-CH₂), 3.67 (s, 3H; 12-CH₃), 3.52 (s, 3H; 17³-CO₂CH₃), 3.11 (s, 3H; 2¹-CH₃), 2.90 (s, 3H; 7¹-CH₃), 2.76-2.20 (several m, 4H; 17-CH₂CH₂COOMe), 1.84 (d, ³J = 7.3 Hz, 3H; 18¹-CH₃), 1.57 (t, ³J = 7.6 Hz; 8²-CH₃), -0.08 (br s, 1H; NH) and -2.26 (br s, 1H; NH). **¹³C-NMR** (100 MHz, CDCl₃) δ/ppm: 196.4 (C13¹), 172.5 (C17³), 171.2 (C19), 160.8 (C16), 154.7 (C6), 150.8 (C9), 149.0 (C14), 144.9 (C8), 140.9 (C1), 138.1 (C12), 136.0 (C7), 134.9 (C4), 133.0 (C3), 131.3 (C11), 130.8 (C2), 129.5 (C3¹), 128.8 (C13), 112.1 (C3²), 106.4 (C15), 104.0 (C10), 96.7 (C5), 93.3 (C20), 52.0 (C17), 52.0 (C17⁵), 50.1 (C18), 48.3 (C13²), 31.3 (C17²), 30.1 (C17¹), 23.4 (C18¹), 19.5 (C8¹), 17.6 (C8²), 12.4 (C2¹), 12.2 (C12¹), 11.3 (C7¹). **m/z (MALDI-ToF)** 628.8 (C₃₄H₃₅N₄O₃⁸¹Br: [M+H]⁺ calculated 628.2).



(E)-3²-(4-(*N,N*-diethylaminophenyl)) pyropheophorbide-a methyl ester 2a.

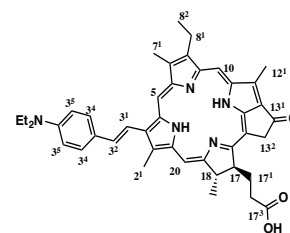
(*E*)-3²-Bromopyropheophorbide-a methyl ester **5** (44.0 mg, 67 μmol) was mixed with 4-(*N,N*-diethylaminophenyl) boronic acid (64.6 mg, 334 μmol), [Pd(PPh₃)₄] (7.8 mg, 6.7 μmol), tetrabutylammonium bromide (21.6 mg, 66.9 μmol), aq. sodium hydroxide (1.00 mL, 200 μmol) and toluene (4 mL) in a Schlenk tube. The mixture was degassed by three freeze-pump-thaw cycles and then stirred at 80 °C for 30 min under Ar atmosphere. The reaction was monitored by reverse-phase HPLC (Table S1, Figure S1). The reaction mixture was then washed with water and extracted with CH₂Cl₂, dried over Na₂SO₄ and concentrated. The crude was purified by flash column chromatography using 5% EtOAc in CH₂Cl₂ as eluent and then recrystallized (CH₂Cl₂/hexane) to give **2a** as a brown solid. **Yield:** 44.5 mg, 91 %. **¹H-NMR** (400 MHz, CDCl₃) δ/ppm: 9.41 (s, 1H; 10-H), 9.32 (s, 1H; 5-H), 8.49 (s, 1H; 20-H), 8.02 (d, ³J = 16.3 Hz, 1H; 3²-H), 7.79 (d, ³J = 8.4 Hz, 2H; 3⁴-H and 3⁸-H), 7.48 (d, ³J = 16.3 Hz, 1H; 3¹-H), 6.84 (d, ³J = 8.4 Hz, 2H;



3^5 -H and 3^7 -H), 5.23 (d, $^2J = 19.7$ Hz, 1H; 13^2 -CH₂), 5.09 (d, $^2J = 19.7$ Hz, 1H; 13^2 -CH₂), 4.47 (q, $J = 7.4$ Hz, 1H; 18-H), 4.26 (m, 1H; 17-H), 3.63 (m, 2H; 8^1 -CH₂), 3.63 (s, 3H; 12^1 -CH₃), 3.62 (s, 3H; 17^2 -CO₂CH₃), 3.50 (q, $^3J = 7.0$ Hz, 4H; N(CH₂CH₃)₂), 3.38 (s, 3H; 2^1 -CH₃), 3.17 (s, 3H; 7^1 -CH₃), 2.75-2.25 (several m, 4H; 17-CH₂CH₂COOMe), 1.82 (d, $^3J = 7.3$ Hz, 3H; 18^1 -CH₃), 1.68 (t, $^3J = 7.6$ Hz; 8^2 -CH₃), 1.29 (t, $^3J = 7.0$ Hz, 6H; N(CH₂CH₃)₂), 0.58 (br s, 1H; NH) and -1.63 (br s, 1H; NH). **¹³C-NMR** (100 MHz, CDCl₃) δ /ppm: 196.5 (C13¹), 173.8 (C17³), 171.6 (C19), 160.3 (C16), 155.4 (C6), 150.6 (C9), 149.3 (C14), 148.2 (C3⁶), 144.9 (C8), 142.3 (C1), 137.8 (C12), 137.3 (C3¹), 137.0 (C13), 136.8 (C4), 136.0 (C7), 130.4 (C3), 129.9 (C2), 128.5 (C3⁴), 128.0 (C11), 125.2 (C3³), 115.4 (C3²), 112.0 (C3⁵), 105.9 (C15), 104.1 (C10), 96.9 (C5), 92.8 (C20), 52.0 (C17), 51.8 (C17⁵-OCH₃), 50.2 (C18), 48.3 (C13²), 44.6 (NCH₂CH₃), 31.3 (C17¹), 30.1 (C17²), 23.4 (C18¹), 19.6 (C8¹), 17.7 (C8²), 13.0 (NCH₂CH₃), 12.6 (C2¹), 12.2 (C12¹), 11.4 (C7¹). ***m/z* (MALDI-ToF)** 696.6 (C₄₄H₄₉N₅O₃: [M+H]⁺ calculated 696.4). **UV-Vis** (CH₂Cl₂, 25 °C) λ_{max} (log ϵ): 678 nm (4.70), 621 nm (4.02), 550 nm (4.20), 515 nm (4.28) and 420 nm (4.94).

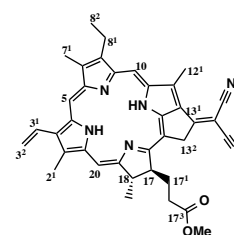
(*E*)-3²-4-(*N,N*-diethylaminophenyl) pyropheophorbide-a 2b: (*E*)-3²-4-(*N,N*-

diethylaminophenyl) pyropheophorbide-a methyl ester **2a** (30.0 mg, 42.6 μ mol) was dissolved in 37% concentrated HCl (18 mL) at 0 °C and stirred at 20 °C under Ar atmosphere for 3 h. After 3 h, the reaction mixture was poured in an ice/water bath and the compound was extracted with chloroform. The organic layer was washed with sat. NaHCO₃ (aq) and water. The organic layer was then dried over Na₂SO₄ and the solvent was evaporated under reduced pressure. The solid material was recrystallized (CH₂Cl₂/hexane) to give **2b** as a brown solid. **Yield:** 27.5 mg, 94 %. **¹H-NMR** (500 MHz, CDCl₃) δ /ppm: 9.35 (s, 1H; 10-H), 9.24 (s, 1H; 5-H), 8.45 (s, 1H; 20-H), 7.97 (d, $^3J = 16.3$ Hz, 1H; 3^2 -H), 7.69 (d, $^3J = 8.2$ Hz, 2H; 3^4 -H and 3^8 -H), 7.46 (d, $^3J = 16.3$ Hz, 1H; 3^1 -H), 6.83 (d, $^3J = 8.2$ Hz, 2H; 3^5 -H and 3^7 -H), 5.22 (d, $^2J = 19.3$ Hz, 1H; 13^2 -CH₂), 5.03 (d, $^2J = 19.3$ Hz, 1H; 13^2 -CH₂), 4.45 (m, 1H; 18-H), 4.24 (m, 1H; 17-H), 3.58 (m, 5H; 8^1 -CH₂; 12^1 -CH₃), 3.49 (q, $^3J = 7.0$ Hz, 4H; N(CH₂CH₃)₂), 3.34 (s, 3H; 2^1 -CH₃), 3.12 (s, 3H; 7^1 -CH₃), 2.72–2.18 (several m, 4H; 17-CH₂CH₂COOH), 1.78 (d, $^3J = 7.4$ Hz, 3H; 18^1 -CH₃), 1.65 (t, $^3J = 7.7$ Hz, 3H; 8^2 -CH₃), 1.28 (t, $^3J = 7.0$ Hz, 6H; N(CH₂CH₃)₂), -1.61 (br s, 1H; NH). **¹³C-NMR** (125 MHz, CDCl₃) δ /ppm: 196.7 (C13¹), 177.8 (C17³), 171.6 (C19), 160.3 (C16), 155.4 (C6), 150.6 (C9), 149.3 (C14), 147.9 (C3⁶), 144.9 (C8), 142.3 (C1), 137.7 (C12), 137.1 (C3¹), 137.0 (C13), 136.7 (C4), 135.9 (C7), 130.1 (C3), 129.9 (C2), 128.3 (C3⁴), 127.9 (C11), 125.3 (C3³), 115.4 (C3²), 112.0 (C3⁵), 105.7 (C15), 104.1 (C10), 96.9 (C5), 92.8 (C20), 51.6 (C17), 50.1 (C18), 48.1 (C13²), 44.8 (NCH₂CH₃), 31.0 (C17¹), 29.9 (C17²), 23.4 (C18¹), 19.5 (C8¹), 17.5 (C8²), 12.8 (NCH₂CH₃), 12.4 (C2¹), 12.0 (C12¹), 11.3 (C7¹). ***m/z* (MALDI-ToF):** 682.5 (C₄₃H₄₇N₅O₃: [M+H]⁺ calculated 682.4). **UV-Vis** (CH₂Cl₂, 25 °C) λ_{max} (log ϵ): 677 nm (4.62), 620 nm (3.98), 550 nm (4.14), 515 nm (4.23) and 420 nm (4.89).



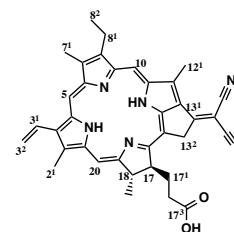
Methyl-13¹-Deoxo-13¹-(dicyanomethylene)pyropheophorbide-a 3a.¹ Pyropheophorbide-a methyl ester

1a (25 mg, 46 μ mol), malononitrile (301 mg, 4.5 mmol) and triethylamine (1.4 mL) were dissolved in anhydrous THF (6.9 mL). The reaction mixture was heated to reflux at 67 °C for 1 h under Ar atmosphere. The reaction was monitored through RP-HPLC. When small peaks of byproducts were observed after around 1 h, the heating and stirring was stopped, and the solvent was evaporated at 40 °C at 290 mbar pressure to complete the reaction. The residue obtained was added to an aq. HCl solution (1%) and extracted with CH₂Cl₂. The crude product was washed with water, dried over Na₂SO₄, filtered and the solvent was evaporated. The crude product was then purified by flash column chromatography (0.5–1% Et₂O in CH₂Cl₂) and recrystallized (CH₂Cl₂/hexane) to give **3a** as a dark green solid. **Yield:** 21.0 mg, 77%. **¹H-NMR** (400 MHz, CDCl₃) δ /ppm: 9.12, 8.82 and 8.37 (each s, 1H; meso H), 7.87 (dd, $^3J = 11.6$ Hz, $^3J = 17.9$ Hz, 1H; CH=CH₂), 6.26 (dd, $^3J = 17.9$ Hz, $^2J = 1.1$ Hz, 1H; CH=CH₂), 6.17 (dd, $^3J = 11.6$ Hz, $^2J = 1.1$ Hz, 1H; CH=CH₂), 5.20 (d, $^2J = 20.7$ Hz, 1H; 13^2 -CH₂, exocyclic ring), 5.09 (d, $^2J = 20.7$ Hz, 1H; 13^2 -CH₂, exocyclic ring), 4.30 (q, $^3J = 7.2$ Hz, 1H; 18-H), 4.02 (d, $^3J = 9.1$ Hz, 1H; 17-H), 3.67 (s, 6H; OCH₃), 3.47 (q, $^3J = 7.6$ Hz, 2H; 8^1 -CH₂-CH₃), 3.33, 3.14, and 3.09 (each s, 3H; 12^1 , 2^1 , 7^1 -CH₃), 2.61-1.91 (several m, 4H; CH₂CH₂COOMe), 1.75 (d, $^3J = 7.3$ Hz, 3H; 18-CH₃), 1.55 (t, $^3J = 7.6$ Hz, 3H; CH₂CH₃) and 0.89 (br s, 1H; NH) and -1.11 (br s, 1H; NH). **¹³C-NMR** (100 MHz, CDCl₃) δ /ppm: 173.3 (C19), 172.7 (C17³), 168.0 (C16), 160.9 (C6), 156.5



(C9), 151.3 (C14), 147.2 (C13¹), 145.3 (C8), 143.0 (C1), 138.4 (C12), 137.5 (C3¹), 136.6 (C13), 132.3 (C4), 129.5 (C7), 128.9 (C3), 127.7 (C2), 123.2 (C11), 116.1 (13¹-CN), 115.5 (C3²), 105.0 (C15), 103.4 (C10), 97.6 (C5), 93.4 (C20), 70.2 (CCN), 52.0(17⁵-OMe), 51.5 (C17), 50.0 (C18), 45.8 (C13²), 31.2 (C17¹), 30.0 (C17²), 23.0 (C18¹), 19.4 (C8¹), 17.3 (C8²), 14.0 (C2¹), 12.2 (C12¹), 11.3 (C7¹). **m/z** (MALDI-ToF) 596.7 (C₃₇H₃₆N₆O₂, [M]⁺ calculated 596.3). **UV-Vis** (CH₂Cl₂, 25 °C) λ_{max} (log ε): 704 nm (4.97), 645 nm (4.39), 574 nm (4.19), 534 nm (4.05) and 453 nm (4.93), 432 nm (4.91), 385 nm (4.91), 351 nm (4.81).

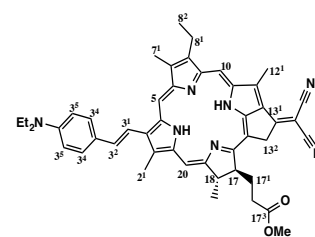
13¹-Deoxo-13¹-(dicyanomethylene)pyropheophorbide-a 3b. Pyropheophorbide-a **1b** (11 mg, 20 μmol), malononitrile (135 mg, 1.9 mmol) and triethylamine (617 μL, 4.42 mmol) were dissolved in anhydrous THF (3 mL). The reaction mixture was degassed by freeze-pump-thaw and then heated to reflux at 67 °C for 1 h under Ar atmosphere. After 1 h, the solvent was evaporated at 40–45 °C at 300 mbar pressure to complete the reaction. TLC (49% CHCl₃, 49% EtOAc, 2% MeOH, 0.1% CH₃COOH) and MALDI mass spectrometry of the crude product confirmed the completion of the reaction. The residue obtained was added to an aq. HCl solution (1%) and extracted with CH₂Cl₂. The crude product was washed with water, dried over Na₂SO₄, filtered and the solvent was evaporated. The residue was then purified by flash column chromatography using the same eluent system used for TLC and recrystallized (CH₂Cl₂/hexane) to give **3b** as a green solid. **Yield:** 6.0 mg, 51%.



Alternatively, **3b** was synthesized by hydrolyzing the ester of **3a** (21.0 mg, 35 μmol) by following the protocol used to synthesize **2b** from **2a**. **Yield:** 19.0 mg, 93%. **¹H-NMR** (700 MHz, CDCl₃, TFA added) δ/ppm: 10.05, 9.77, and 8.69 (each s, 1H; meso H); 7.76 (dd, ³J = 11.6 Hz, ³J = 17.7 Hz, 1H; 3¹-H); 6.36 (d, ³J = 11.6 Hz, 1H; 3²-H); 6.16 (d, ³J = 17.7 Hz, 1H; 3²-H); 5.83 (d, ²J = 21.0 Hz, 1H; 13²-H; exocyclic ring); 5.69 (d, ²J = 21.0 Hz, 1H; 13²-H; exocyclic ring); 4.68 (m, 2H; 18-H; 17-H); 3.86 (s, 3H; 12¹-CH₃); 3.84 (q, ³J = 9.7 Hz, 2H; 8¹-CH₂CH₃); 3.30 and 3.24 (each s, 3H; 2¹-CH₃, 7¹-CH₃); 2.96-2.49 (several m, 4H; 17¹-CH₂, 17²-CH₂); 1.87 (d, ³J = 7.4 Hz, 3H; 18¹-CH₃); 1.63 (t, ³J = 7.6 Hz, 3H; 8²-CH₃). **¹³C-NMR** (175 MHz, CDCl₃, TFA added) δ/ppm: 179.7 (C17³), 168.0 (C19), 163.7 (C16), 154.4 (C6), 151.8 (C9), 151.1 (C14), 148.2 (C13¹), 144.8 (C8), 142.3 (C1), 141.6 (C12), 141.0 (C3¹), 139.7 (C13), 139.0 (C4), 137.5 (C7), 136.3 (C3), 133.8 (C2), 128.8 (C11), 127.0 (13¹-CN), 109.5 (C3²), 105.0 (C15), 103.5 (C10), 92.3 (C5), 86.6 (C20), 77.6 (CCN), 51.1 (C17), 47.0 (C18), 45.8 (C13²), 30.0 (C17¹), 29.9 (C17²), 22.1 (C18¹), 20.0 (C8¹), 16.1 (C8²), 15.2 (C2¹), 11.8 (C12¹), 11.1 (C7¹). **m/z** (MALDI-ToF) 582.6 (C₃₆H₃₄N₆O₂, [M]⁺ calculated 582.3). **UV-Vis** (CH₂Cl₂, 25 °C) λ_{max} (log ε): 709 nm (4.90), 644 nm (4.33), 574 nm (4.13), 534 nm (3.99) and 453 nm (4.87), 431 nm (4.86), 385 nm (4.86), 351 nm (4.76).

Methyl-13¹-deoxo-13¹-(dicyanomethylene)-(E)-3²-(4-(N,N-diethylaminophenyl)) pyropheophorbide-a **4a**

pyropheophorbide-a 4a. (E)-3²-(4-(N,N-diethylaminophenyl)) pyropheophorbide-a methyl ester **2a** (40.0 mg, 57.5 μmol), malononitrile (380 mg, 5.75 mmol) and triethylamine (1.72 mL, 12.3 mmol) were dissolved in anhydrous THF (11 mL). The reaction mixture was degassed by freeze-pump-thaw and then heated to reflux at 67 °C for 1 h under Ar atmosphere. After 1 h, the solvent was evaporated at 40 °C at 300 mbar pressure to complete the reaction. The completion of the reaction was confirmed by RP-HPLC using the gradient triple eluent system (Table S1) and TLC (2% Et₂O in CH₂Cl₂). The reaction mixture was added to an aq. HCl solution (1%) and extracted with CH₂Cl₂. The mixture was washed with water, dried over Na₂SO₄, filtered and then the solvent was evaporated. The crude product was then purified by flash column chromatography (1% Et₂O in CH₂Cl₂) and recrystallized (CH₂Cl₂/hexane) to give **4a** as a green solid. **Yield:** 35.3 mg, 82%. **¹H-NMR** (400 MHz, CDCl₃) δ/ppm: 9.19 (s, 1H; 10-H), 9.12 (s, 1H; 5-H), 8.30 (s, 1H; 20-H), 7.94 (d, ³J = 16.3 Hz, 1H; 3²-H), 7.69 (d, ³J = 8.8 Hz, 2H; 3⁴-H and 3⁸-H), 7.45 (d, ³J = 16.3 Hz, 1H; 3¹-H), 6.84 (d, ³J = 8.8 Hz, 2H; 3⁵-H and 3⁷-H), 5.58 (d, ²J = 20.9 Hz, 1H; 13²-CH₂), 5.46 (d, ²J = 20.9 Hz, 1H; 13²-CH₂), 4.34 (m, 1H; 18-H), 4.15 (m, 1H; 17-H), 3.70 (s, 3H; 12¹-CH₃), 3.64 (s, 3H; 17²-OMe), 3.58 (q, ³J = 7.6 Hz, 2H; 8¹-CH₂), 3.51 (q, ³J = 7.1 Hz, 4H; N(CH₂CH₃)₂), 3.30 (s, 3H; 2¹-CH₃), 3.10 (s, 3H; 7¹-CH₃), 2.63-2.09 (several m, 4H; 17-CH₂CH₂COOMe), 1.76 (d, ³J = 7.3 Hz, 3H; 18¹-CH₃), 1.64 (t, ³J = 7.6 Hz, 3H; 8²-CH₃), 1.29 (t, ³J = 7.1 Hz, 6H; N(CH₂CH₃)₂), -0.76 (br s, 1H; NH). **¹³C-NMR** (175 MHz, CDCl₃) δ/ppm: 173.4 (C17³), 173.0 (C19), 168.7 (C16), 161.1 (C6), 156.8 (C9), 151.5 (C14), 148.2 (C3⁶), 147.8 (C13¹), 145.4 (C8), 143.7 (C1), 138.6 (C12), 138.2 (C3¹), 137.7 (C13), 137.4 (C4), 136.4 (C7), 130.3 (C3), 129.7 (C2), 128.5 (C3⁴), 127.8 (C11), 124.8 (13¹-CN), 116.5 (C3³), 115.8 (13¹-CN), 114.7

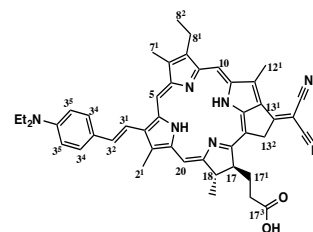


(C3²), 111.8 (C3⁵), 104.9 (C15), 103.7 (C10), 97.2 (C5), 93.1 (C20), 69.9 (CCN), 52.0 (C17), 51.5 (C17⁵), 50.0 (C18), 46.0 (C13²), 44.7 (NCH₂CH₃), 31.7 (C17¹), 30.0 (C17²), 23.0 (C18¹), 19.4 (C8¹), 17.4 (C8²), 14.4 (C2¹), 12.9 (NCH₂CH₃), 12.4 (C12¹), 11.3 (C7¹). **m/z** (MALDI-ToF) 744.9 (C₄₇H₄₉N₇O₂, [M+H]⁺ calculated 744.4). **UV-Vis** (CH₂Cl₂, 25 °C) λ_{max} (log ε): 716 nm (4.76), 658 nm (4.29), 589 nm (4.15), 541 nm (4.02) and 458 nm (4.79), 433 nm (4.74), 354 nm (4.60).

13¹-Deoxo-13¹-(dicyanomethylene)-(E)-3²-(4-(N,N-diethylaminophenyl)) pyropheophorbide-a

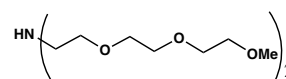
4b. Methyl-13¹-deoxo-13¹-(dicyanomethylene)-(E)-3²-(4-(N,N-diethylaminophenyl))

pyropheophorbide-a **4a** (7.0 mg, 9.4 μmol) was dissolved in 37% concentrated HCl (4.5 mL) at 0 °C and stirred at 20 °C under Ar atmosphere for 3 h. After 3 h, the reaction mixture was poured in an ice/water bath and the compound was extracted with chloroform. The organic layer was washed with sat. NaHCO₃ (aq.) and water. The organic layer was then dried over Na₂SO₄ and the solvent was evaporated under reduced pressure. The solid material was recrystallized (CH₂Cl₂/hexane) to give **4b** as a dark green solid. **Yield:** 5.5 mg, 80%. **¹H-NMR** (600 MHz, CDCl₃) δ/ppm: 9.19 (s, 1H; 10-H), 9.11 (s, 1H; 5-H), 8.30 (s, 1H; 20-H), 7.93 (d, ³J = 16.3 Hz, 1H; 3²-H), 7.68 (d, ³J = 8.3 Hz, 2H; 3⁴-H and 3⁸-H), 7.44 (d, ³J = 16.3 Hz, 1H; 3¹-H), 6.84 (d, ³J = 8.3 Hz, 2H; 3⁵-H and 3⁷-H), 5.59 (d, ²J = 20.3 Hz, 1H; 13²-CH₂), 5.45 (d, ²J = 20.3 Hz, 1H; 13²-CH₂), 4.35 (q, ³J = 7.5 Hz, 1H; 18-H), 4.17 (m, 1H; 17-H), 3.71 (s, 3H; 12¹-CH₃), 3.57 (q, ³J = 7.3 Hz, 2H; 8¹-CH₂), 3.50 (q, ³J = 7.1 Hz, 4H; N(CH₂CH₃)₂), 3.26 (s, 3H; 2¹-CH₃), 3.03 (s, 3H; 7¹-CH₃), 2.68-2.11 (several m, 4H; 17-CH₂CH₂COOH), 1.76 (d, ³J = 7.4 Hz, 3H; 18¹-CH₃), 1.63 (t, ³J = 7.7 Hz, 3H; 8²-CH₃), 1.28 (t, ³J = 7.1 Hz, 6H; N(CH₂CH₃)₂), -0.77 (br s, 1H; NH). **¹³C-NMR** (125 MHz, CDCl₃) δ/ppm: 174.6 (C17³), 173.2 (C19), 169.2 (C16), 161.4 (C6), 157.0 (C9), 151.7 (C14), 148.3 (C3⁶), 148.2 (C13¹), 145.6 (C8), 143.9 (C1), 139.0 (C12), 138.4 (C3¹), 137.9 (C13), 137.7 (C4), 136.5 (C7), 130.5 (C3), 130.0 (C2), 128.5 (C3⁴), 128.1 (C11), 125.0 (13¹-CN), 116.6 (C3³), 115.9 (13¹-CN), 114.9 (C3²), 111.9 (C3⁵), 105.0 (C15), 104.0 (C10), 97.3 (C5), 93.3 (C20), 70.0 (CCN), 51.5 (C17), 50.3 (C18), 46.4 (C13²), 44.7 (NCH₂CH₃), 31.7 (C17¹), 30.3 (C17²), 23.1 (C18¹), 19.5 (C8¹), 17.4 (C8²), 14.6 (C2¹), 12.9 (NCH₂CH₃), 12.4 (C12¹), 11.4 (C7¹). **m/z** (MALDI-ToF) 730.9 (C₄₆H₄₇N₇O₂, [M+H]⁺ calculated 730.4). **UV-Vis** (CH₂Cl₂, 25 °C) λ_{max} (log ε): 717 nm (4.75), 659 nm (4.28), 589 nm (4.15), 543 nm (4.02) and 459 nm (4.77), 433 nm (4.73), 412 nm (4.70), 354 nm (4.59).



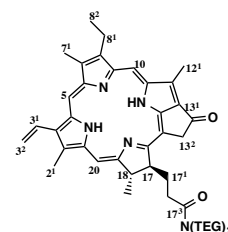
Bis-TEG amine.² *N,N*-Bis-(2-(2-(2-methoxyethoxy)ethoxy)ethyl)aniline or bis-TEG benzyl

amine (1.0 g, 2.6 mmol) was dissolved in ethanol (3 mL; deoxygenated by repeated evacuation), Pd/C (10% w/w Pd; 100 mg) was added, and the mixture placed under Ar atmosphere. H₂ gas (1 atm, approx. 2 L, 89 mmol) was introduced through a balloon and the reaction mixture was stirred at 20 °C for 24 h. The mixture was filtered through Celite, and the solvent was removed under reduced pressure to isolate bis-TEG amine as yellow liquid. **Yield:** 745.0 mg, 97%. **¹H-NMR** (400 MHz, CDCl₃) δ/ppm: 3.57 (m, 20H; CH₂), 3.36 (s, 6H; CH₃), 2.80 (t, ³J = 5.3 Hz, 4H; CH₂-NH); 2.10 (br s, 1H; NH) as literature.²



17³-(bis-(TEG)amide) pyropheophorbide-a 1c³. Pyropheophorbide-a **1b** (22.0 mg, 41.1 μmol) was

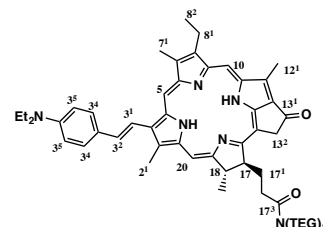
dissolved in a mixture of *N,N*-diisopropylethylamine (15 μL, 82 μmol) in DMF (1.4 mL) followed by addition of (1-cyano-2-ethoxy-2-oxoethylideneaminoxy)dimethylamino-morpholino-carbenium hexafluorophosphate (COMU, 18 mg, 41.1 μmol) at 0 °C under Ar atmosphere. After stirring the reaction mixture for 3 min, bis-TEG amine (13 mg, 41.1 μmol) was added. The mixture was stirred at 0 °C under Ar atmosphere for 2 h. After completion (monitored by RP-HPLC), the reaction mixture was diluted with water and extracted with CH₂Cl₂. The organic phase was dried over Na₂SO₄ and solvent was evaporated. The crude product was purified by flash column chromatography (1% MeOH in CH₂Cl₂). The product was then washed with water to remove oxyma, the leaving group of COMU. The product **1c** was obtained as dark green solid. **Yield:** 22.5 mg, 66%. **¹H-NMR** (400 MHz, CDCl₃) δ/ppm: 9.46, 9.35 and 8.57 (each s, 1H; meso H), 8.00 (dd, ³J = 11.6 Hz, ³J = 17.9 Hz, 1H; CH=CH₂), 6.29 (dd, ³J = 17.9 Hz, ²J = 1.1 Hz, 1H; CH=CH₂), 6.17 (dd, ³J = 11.6 Hz, ²J = 1.1 Hz, 1H; CH=CH₂), 5.29 (d, ²J = 19.8 Hz, 1H; 13²-CH₂), 5.12 (d, ²J = 19.8 Hz, 1H; 13²-CH₂), 4.53 (q, ³J = 7.2 Hz, 1H; 18-H), 4.35 (d, ³J = 6.0 Hz, 1H; 17-H), 3.68 (m, 2H; 8¹-CH₂-CH₃), 3.66, 3.41 and 3.27 (each s, 3H; 2¹, 7¹, 12¹-CH₃);



3.45–2.94 (several m, 24H; CH₂ of TEG chains), 3.22 (s, 6H; -OCH₃ of TEG chains), 2.77–2.24 (several m, 4H; CH₂CH₂CO-N(TEG)₂), 1.81 (d, ³J = 7.2 Hz, 3H; 18-CH₃), 1.69 (t, ³J = 7.5 Hz, 3H; CH₂CH₃) and -1.71 (br s, 1H; NH). ¹³C-NMR (100 MHz, CDCl₃) δ/ppm: 196.5 (C13¹), 172.8 (C17³), 171.9 (C19), 161.1 (C16), 155.2 (C6), 150.8 (C9), 149.0 (C14), 145.0 (C8), 141.5 (C1), 137.9 (C12), 136.2 (C3¹), 136.1 (C13), 135.9 (C4), 131.6 (C7), 130.6 (C3), 129.3 (C2), 128.4 (C11), 122.6 (C3²), 106.3 (C15), 104.0 (C10), 97.2 (C5), 93.2 (C20), 71.9–68.9 (CH₂ of bis-TEG), 59.0–59.0 (OCH₃ of bis-TEG), 52.0 (C17), 50.1 (C18), 48.6–48.3 (NCH₂ of bis-TEG), 46.2 (C13²), 30.0 (C17¹), 29.5 (C17²), 23.3 (C18¹), 19.6 (C8¹), 17.6 (C8²), 12.3 (C2¹), 12.2 (C12¹), 11.4 (C7¹). *m/z* (MALDI-ToF) 825.1 (C₄₇H₆₃N₅O₈, [M]⁺ calculated 825.5). **UV-Vis** (solvent: MeOH): λ_{max} = 414 nm (Soret band) and 670 nm (Q band).

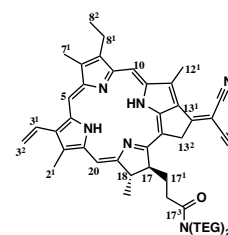
(E)-3²-(4-(N,N-diethylaminophenyl))-17³-(bis-(TEG)amide) pyropheophorbide-a 2c.

(E)-3²-(4-(N,N-diethylaminophenyl))-pyropheophorbide-a **2b** (9.0 mg, 14 μmol) was dissolved in a mixture of *N,N*-diisopropylethylamine (5 μL, 30 μmol) in DMF (0.1 mL) followed by addition of COMU (6.2 mg, 14 μmol) at 0 °C under Ar atmosphere and stirred for 3 min. Bis-TEG amine (4.5 mg, 14 μmol) was then added to the reaction mixture. The mixture was stirred at 0 °C under Ar atmosphere for 2 h followed by stirring at 20 °C for 3 h. After completion (monitored by TLC (47% CHCl₃, 47% EtOAc, 5% MeOH and 1% CH₃COOH)), the reaction mixture was diluted with ethyl acetate and extracted successively with 1 N HCl, 1 N NaHCO₃ and brine. The mixture was dried over Na₂SO₄ followed by the removal of solvent under reduced pressure. The crude product was purified by flash column chromatography using the same eluent as TLC and recrystallized (CH₂Cl₂/hexane) to give **2c** as a dark brown solid. **Yield:** 5.1 mg, 40%. ¹H-NMR (600 MHz, CDCl₃) δ/ppm: 9.48 (s, 1H; 10-H), 9.43 (s, 1H; 5-H), 8.53 (s, 1H; 20-H), 8.15 (d, ³J = 15.8 Hz, 1H; 3²-H), 7.76 (m, 2H; 3⁴-H and 3⁸-H), 7.58 (d, ³J = 15.8 Hz, 1H; 3¹-H), 6.86 (d, 2H; 3⁵-H and 3⁷-H), 5.28 (d, ²J = 18.9 Hz, 1H; 13²-CH₂), 5.11 (d, ²J = 18.9 Hz, 1H; 13²-CH₂), 4.53 (m, 1H; 18-H), 4.35 (m, 1H; 17-H), 3.70 (m, 2H; 8¹-CH₂), 3.67 (s, 3H; 12¹-CH₃), 3.58–3.33 (several m, 24H; CH₂ of TEG chains), 3.27 (q, ³J = 7.1 Hz, 4H; N(CH₂CH₃)₂), 3.24 (s, 3H; 2¹-CH₃), 3.22 (s, 3H; 7¹-CH₃), 2.74–2.24 (several m, 4H; 17-CH₂CH₂CON(TEG)₂), 1.81 (d, ³J = 7.4 Hz, 3H; 18¹-CH₃), 1.70 (t, ³J = 7.7 Hz, 8²-CH₃), 1.60 (t, ³J = 7.1 Hz, 6H; N(CH₂CH₃)₂), -1.54 (br s, 1H; NH). ¹³C-NMR (125 MHz, CDCl₃) δ/ppm: 196.5 (C13¹), 172.8 (C17³), 172.0 (C19), 161.1 (C16), 155.3 (C6), 150.7 (C9), 149.2 (C14), 148.1 (C3⁶), 145.0 (C8), 142.2 (C1), 137.8 (C12), 137.5 (C3¹), 137.0 (C13), 136.1 (C4), 134.5 (C7), 130.5 (C3), 130.0 (C2), 128.5 (C3⁴), 128.2 (C11), 125.2 (C3³), 115.5 (C3²), 111.9 (C3⁵), 106.0 (C15), 104.1 (C10), 97.0 (C5), 93.0 (C20), 71.9–68.9 (CH₂ of bis-TEG), 59.0–59.0 (OCH₃ of bis-TEG), 51.6 (C17), 50.1 (C18), 48.6–48.3 (NCH₂ of bis-TEG), 46.2 (C13²), 44.7 (NCH₂CH₃)₂, 30.0 (C17¹), 29.5 (C17²), 23.3 (C18¹), 19.6 (C8¹), 17.6 (C8²), 12.9 (NCH₂CH₃)₂, 12.6 (C2¹), 12.2 (C12¹), 11.5 (C7¹). *m/z* (MALDI-ToF) 972.9 (C₅₇H₇₆N₆O₈, [M]⁺ calculated 972.6).



13¹-Deoxo-13¹-(dicyanomethylene)-17³-(bis-(TEG)amide) pyropheophorbide-a 3c.

13¹-Deoxo-13¹-(dicyanomethylene)pyropheophorbide-a **3b** (19.0 mg, 32.6 μmol) was dissolved in a mixture of *N,N*-diisopropylethylamine (11.5 μL, 66 μmol) in DMF (1.1 mL) followed by addition of COMU (14 mg, 32 μmol) at 0 °C under Ar atmosphere and stirred for 3 min. Bis-TEG amine (10.2 mg, 32 μmol) was then to the reaction mixture followed by stirring at 0 °C under Ar atmosphere for 2 h. After completion (monitored by RP-HPLC), the reaction mixture was diluted with few drops of water and then extracted using CH₂Cl₂. The organic layer was dried over Na₂SO₄ followed by solvent evaporation. The crude product was purified by flash column chromatography (1% MeOH in CH₂Cl₂) and recrystallized (CH₂Cl₂/hexane) to give **3c** as a dark green solid. **Yield:** 6.0 mg, 21%. ¹H-NMR (400 MHz, CDCl₃) δ/ppm: 9.19 (s, 1H; 10-H), 9.16 (s, 1H; 5-H), 8.40 (s, 1H; 20-H), 7.91 (dd, ³J = 11.6 Hz, ³J = 17.8 Hz, 1H; 3¹-H), 6.26 (dd, ³J = 17.8 Hz, ²J = 1.4 Hz, 1H; *trans* 3²-H), 6.16 (dd, ³J = 11.6 Hz, ²J = 1.4 Hz, 1H; *cis*-3²-H), 5.67 (d, ²J = 21.0 Hz, 1H; 13²-CH₂), 5.47 (d, ²J = 21.0 Hz, 1H; 13²-CH₂), 4.44 (m, 1H; 18-H), 4.24 (m, 1H; 17-H), 3.70–3.00 (m, 45H; 12¹-CH₃, 8¹-CH₂, CH₂ of TEG chains, 2¹-CH₃, and 7¹-CH₃), 2.72–2.24 (several m, 4H; 17-CH₂CH₂CONTEG)₂), 1.77 (d, ³J = 7.3 Hz, 3H; 18¹-CH₃), 1.63 (t, ³J = 7.6 Hz, 3H; 8²-CH₃), -0.92 (br s, 1H; NH). ¹³C-NMR (125 MHz, CDCl₃) δ/ppm: 173.5 (C19), 172.6 (C17³), 168.9 (C16), 162.0 (C6), 156.6 (C9), 151.6 (C14), 147.9 (C13¹), 145.6 (C8), 143.0 (C1), 138.9 (C12), 137.6 (C3¹), 136.5 (C13), 132.4 (C4), 130.1 (C7), 129.0 (C3), 128.4 (C2), 123.1 (C11), 116.5 (13¹-CN), 115.7 (C3²), 105.6 (C15), 103.9 (C10), 97.4 (C5), 93.7 (C20), 71.9–70.4 (bis-TEG), 70.3 (CCN), 69.5–68.9 (bis-TEG), 59.1–59.0 (OCH₃ of bis-

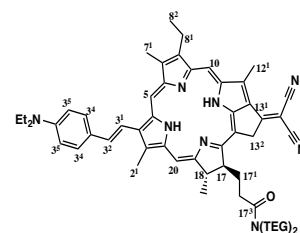


TEG), 52.0 (C17), 50.2 (C18), 48.6–46.4 (bis-TEG), 46.2 (C13²), 30.2 (C17¹), 29.7 (C17²), 23.2 (C18¹), 19.5 (C8¹), 17.5 (C8²), 14.5 (C2¹), 12.2 (C12¹), 11.3 (C7¹). **m/z (MALDI-ToF)** 873.4 (C₅₀H₆₃N₇O₇, [M]⁺ calculated 873.5)

13¹-Deoxo-13¹-(dicyanomethylene)-(E)-3²-(4-(N,N-diethylaminophenyl))-17³-(bis-(TEG)amide)-

pyropheophorbide-a 4c. 13¹-Deoxo-13¹-(dicyanomethylene)-(E)-3²-(4-(N,N-diethylaminophenyl))-

pyropheophorbide-a **4b** (15.0 mg, 20 μmol) was dissolved in a mixture of *N,N*-diisopropylethylamine (71.2 μL, 42 μmol) in DMF (0.67 mL) followed by addition of COMU (8.9 mg, 20 μmol) at 0 °C under Ar atmosphere. Bis-TEG amine (6.5 mg, 20 μmol) was then added to the



reaction mixture followed by stirring at 0°C under Ar atmosphere for 3 h. After completion, the solvent was evaporated under reduced pressure and the residue was washed with water. The crude product was purified by flash column chromatography. Initially, pure CH₂Cl₂ was used as eluent to remove a light green band and then 1.5% MeOH in CH₂Cl₂ was used as eluent to elute the desired product as dark green band. The starting material was then eluted using a mixture of solvents as eluent (47% CH₂Cl₂, 47% EtOAc, 5% MeOH and 1% CH₃COOH). The product was recrystallized (CH₂Cl₂/hexane) to give **4c** as a dark green solid. **Yield:** 9.0 mg, 43%. **¹H-NMR** (500 MHz, CDCl₃) δ/ppm: 9.22 (s, 1H; 10-H), 9.16 (s, 1H; 5-H), 8.34 (s, 1H; 20-H), 7.98 (d, ³J = 16.3 Hz, 1H; 3²-H), 7.71 (d, ³J = 8.5 Hz, 2H; 3⁴-H and 3⁸-H), 7.49 (d, ³J = 16.3 Hz, 1H; 3¹-H), 6.84 (d, ³J = 8.5 Hz, 2H; 3⁵-H; 3⁷-H), 5.70 (d, ²J = 21.1 Hz, 1H; 13²-CH₂), 5.51 (d, ²J = 21.1 Hz, 1H; 13²-CH₂), 4.41 (m, 1H; 18-H), 4.23 (m, 1H; 17-H), 3.74 (s, 3H; 12¹-CH₃), 3.59 (q, ³J = 7.6 Hz, 2H; 8¹-CH₂), 3.55–3.29 (several m, 22H; CH₂ of TEG chains, N(CH₂CH₃)₂), 3.34 (s, 3H; 2¹-CH₃), 3.33–3.13 (several m, 11H; CH₂, CH₃ of TEG chains), 3.12 (s, 3H; 7¹-CH₃), 2.69–2.28 (several m, 4H; 17-CH₂CH₂CON(TEG)₂), 1.77 (d, ³J = 7.3 Hz, 3H; 18¹-CH₃), 1.65 (t, ³J = 7.6 Hz, 8²-CH₃), 1.28 (t, ³J = 7.0 Hz, 6H; N(CH₂CH₃)₂), –0.74 (br s, NH). **¹³C-NMR** (125 MHz, CDCl₃) δ/ppm: 173.6 (C19), 172.6 (C17³), 169.0 (C16), 162.0 (C6), 156.9 (C9), 151.6 (C14), 148.3 (C3⁶), 148.1 (C13¹), 145.5 (C8), 143.7 (C1), 138.9 (C12), 138.4 (C3¹), 137.9 (C13), 137.5 (C4), 136.4 (C7), 130.5 (C3), 130.0 (C2), 128.5 (C3⁴), 128.0 (C11), 125.0 (13¹-CN), 116.7 (C3³), 115.8 (13¹-CN), 115.0 (C3²), 111.9 (C3⁵), 105.3 (C15), 104.0 (C10), 97.2 (C5), 93.3 (C20), 72.0–70.3 (bis-TEG), 70.2 (CCN), 69.5–68.9 (bis-TEG), 59.0 (OCH₃ of bis-TEG), 51.9 (C17), 50.2 (C18), 48.6–46.4 (bis-TEG), 46.2 (C13²), 44.7 (NCH₂CH₃)₂, 30.1 (C17¹), 29.7 (C17²), 23.2 (C18¹), 19.5 (C8¹), 17.5 (C8²), 14.6 (C2¹), 12.9 (NCH₂CH₃)₂, 12.5 (C12¹), 11.4 (C7¹). **m/z (MALDI-ToF)** 1021.1 (C₆₀H₇₇N₈O₇, [M]⁺ calculated 1020.6).

2.2 Experimental characterization (¹H NMR spectra, ¹³C NMR spectra, MALDI ToF mass spectra)

(E)-3²-Bromopyropheophorbide-a methyl ester 5

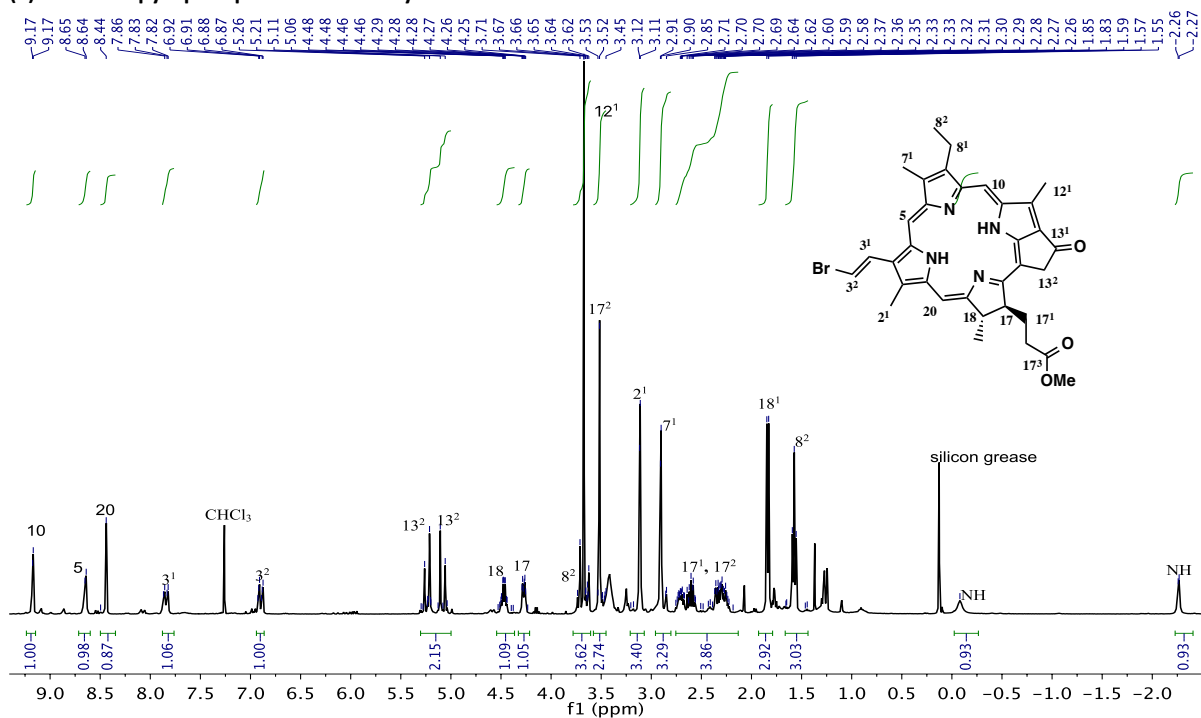


Figure S2: ¹H-NMR spectrum of 5 (400 MHz, CDCl₃, 298 K).

brominated ppaoeme

MALDI

21-Jul-2016 20:36:35

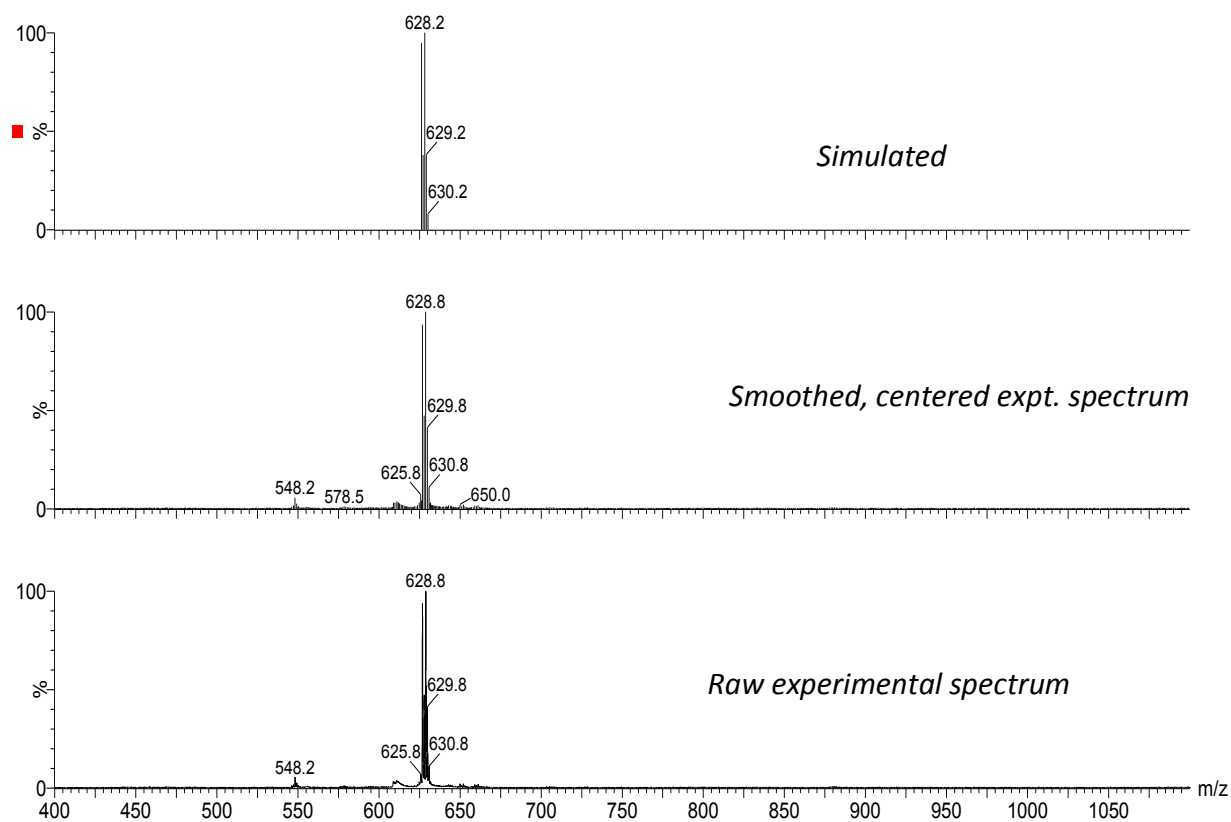


Figure S3: MALDI ToF mass spectrum of 5.

(E)-3²-(4-(*N,N*-diethylaminophenyl) pyrropephorbide-a methyl ester 2a

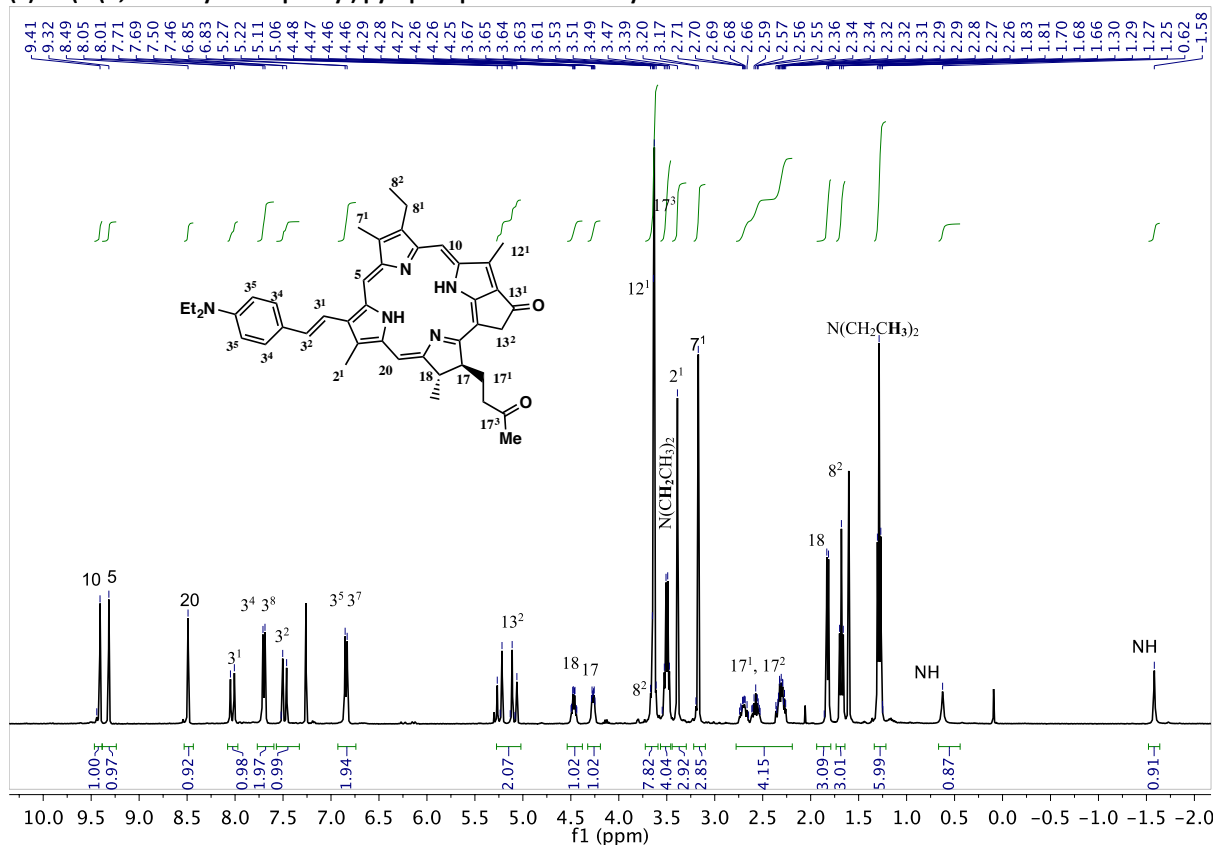


Figure S4: ¹H-NMR spectrum of 2a (400 MHz, CDCl₃, 298 K).

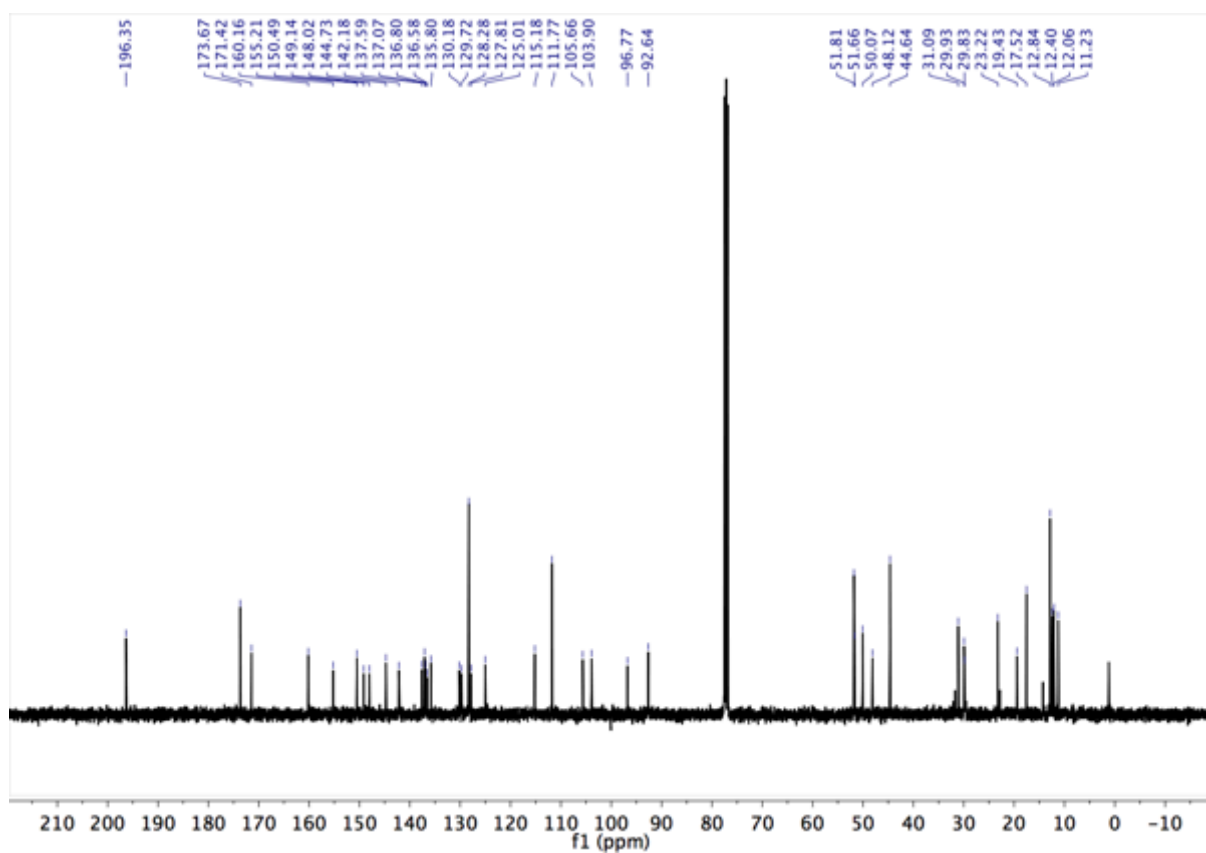


Figure S5: ¹³C NMR of spectrum of 2a (100 MHz, CDCl₃, 298 K).

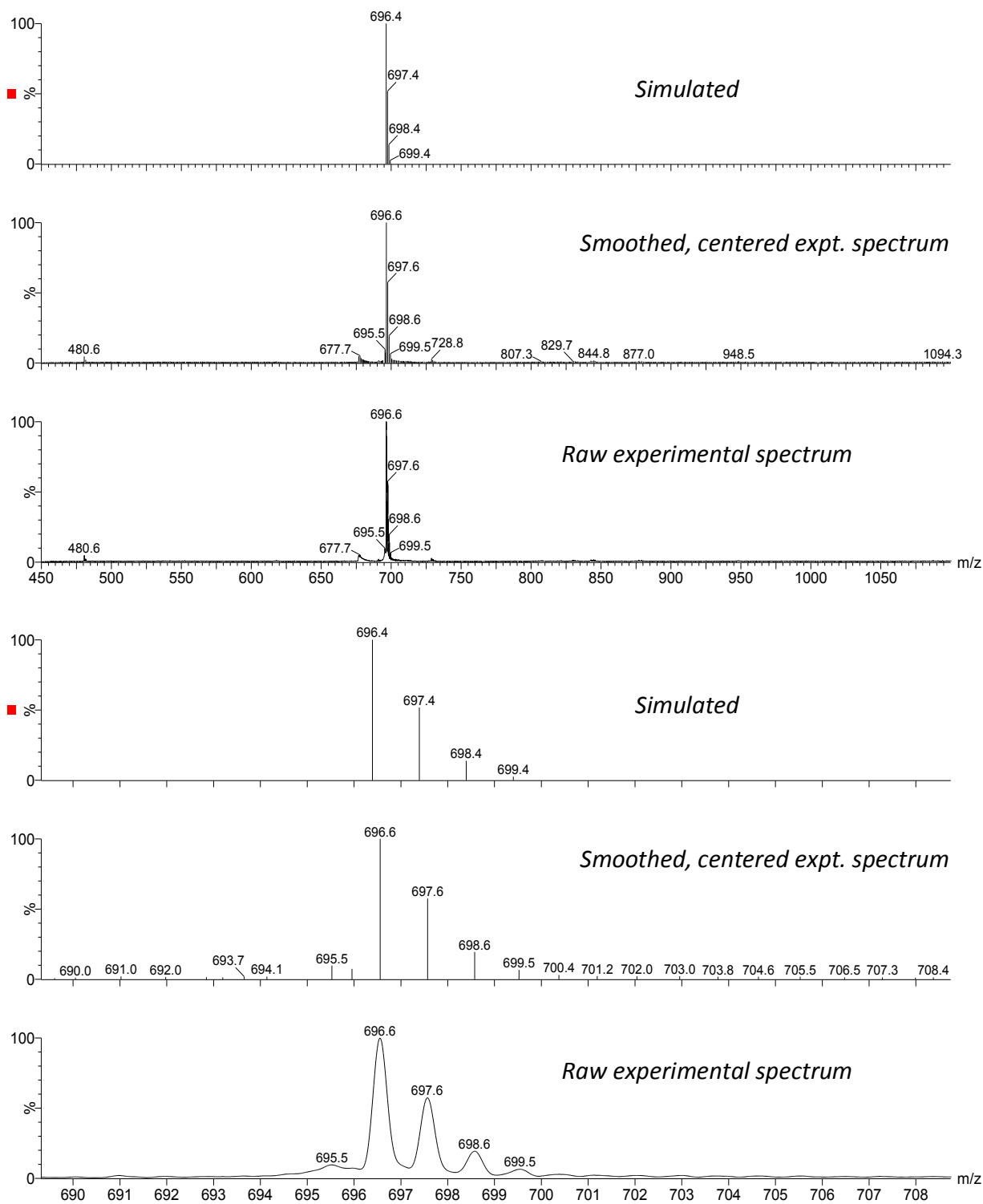
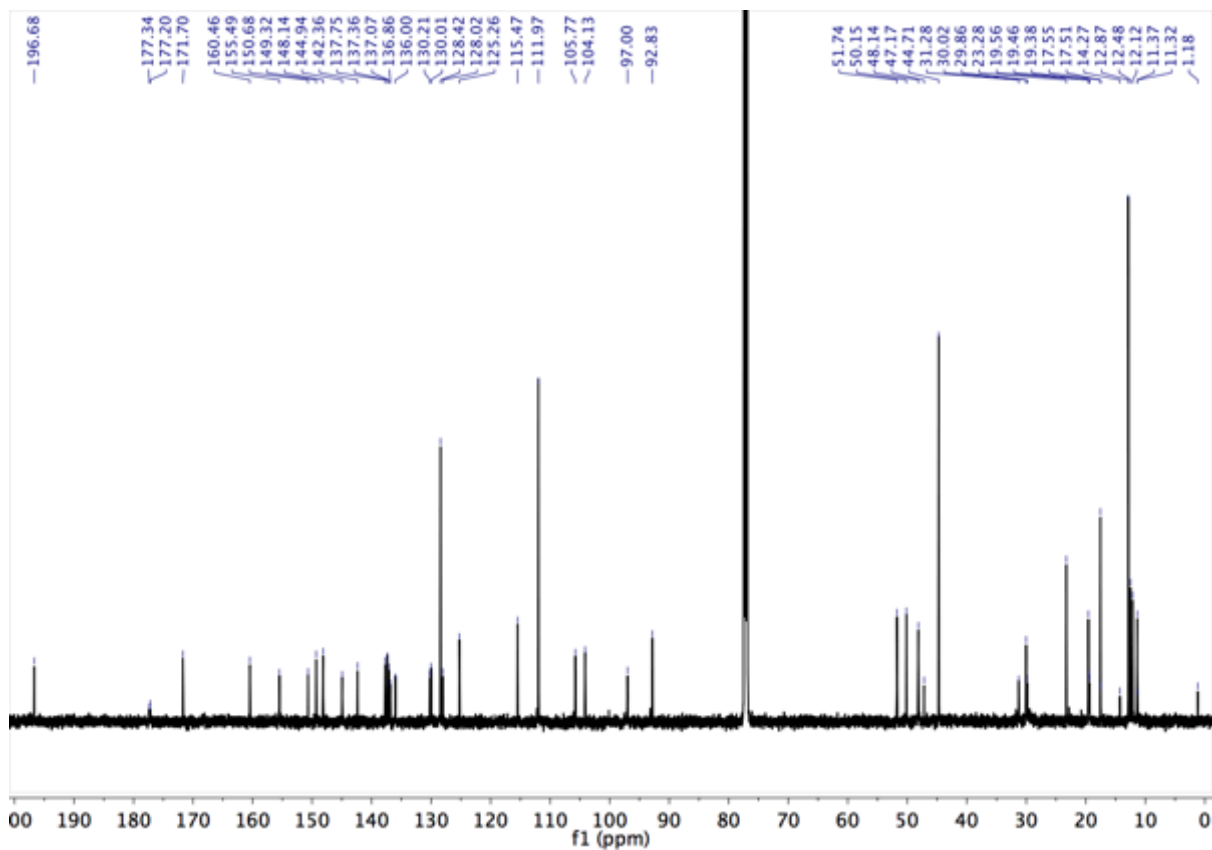
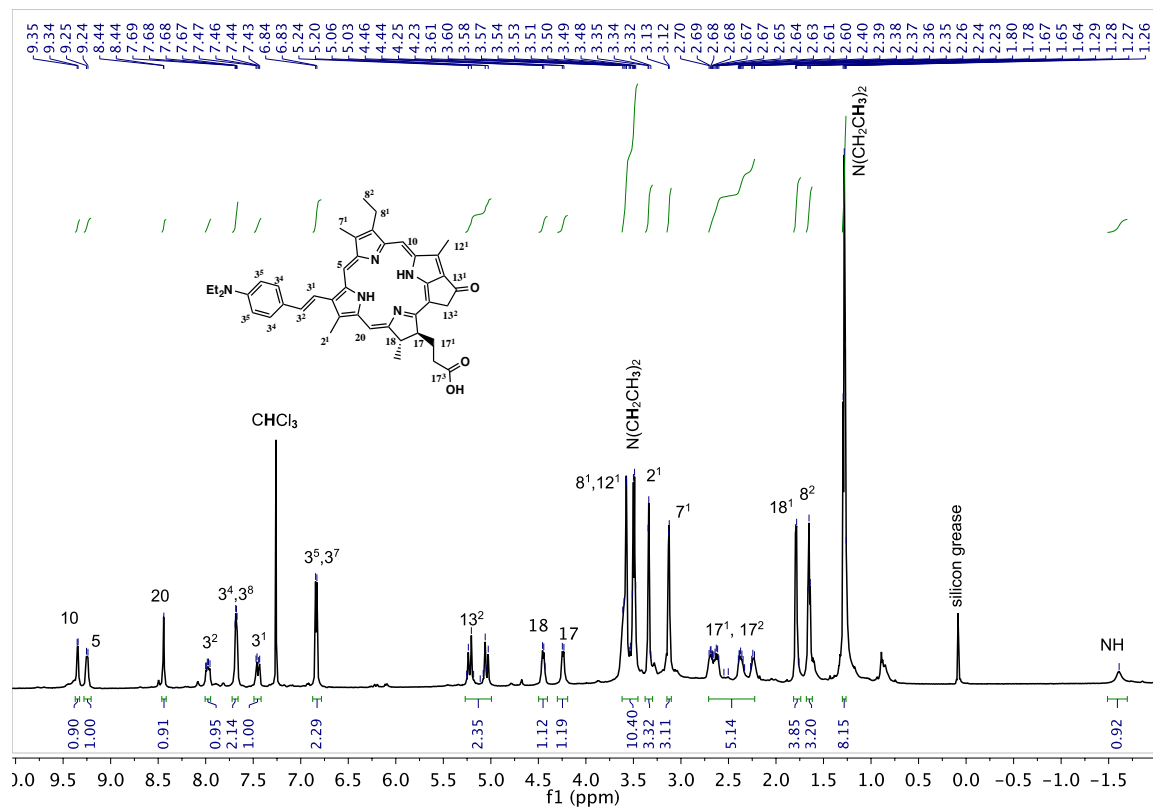


Figure S6: MALDI ToF mass spectrum of 2a.

(E)-3²-(4-(N,N-diethylaminophenyl)) pyropheorbide -a 2b



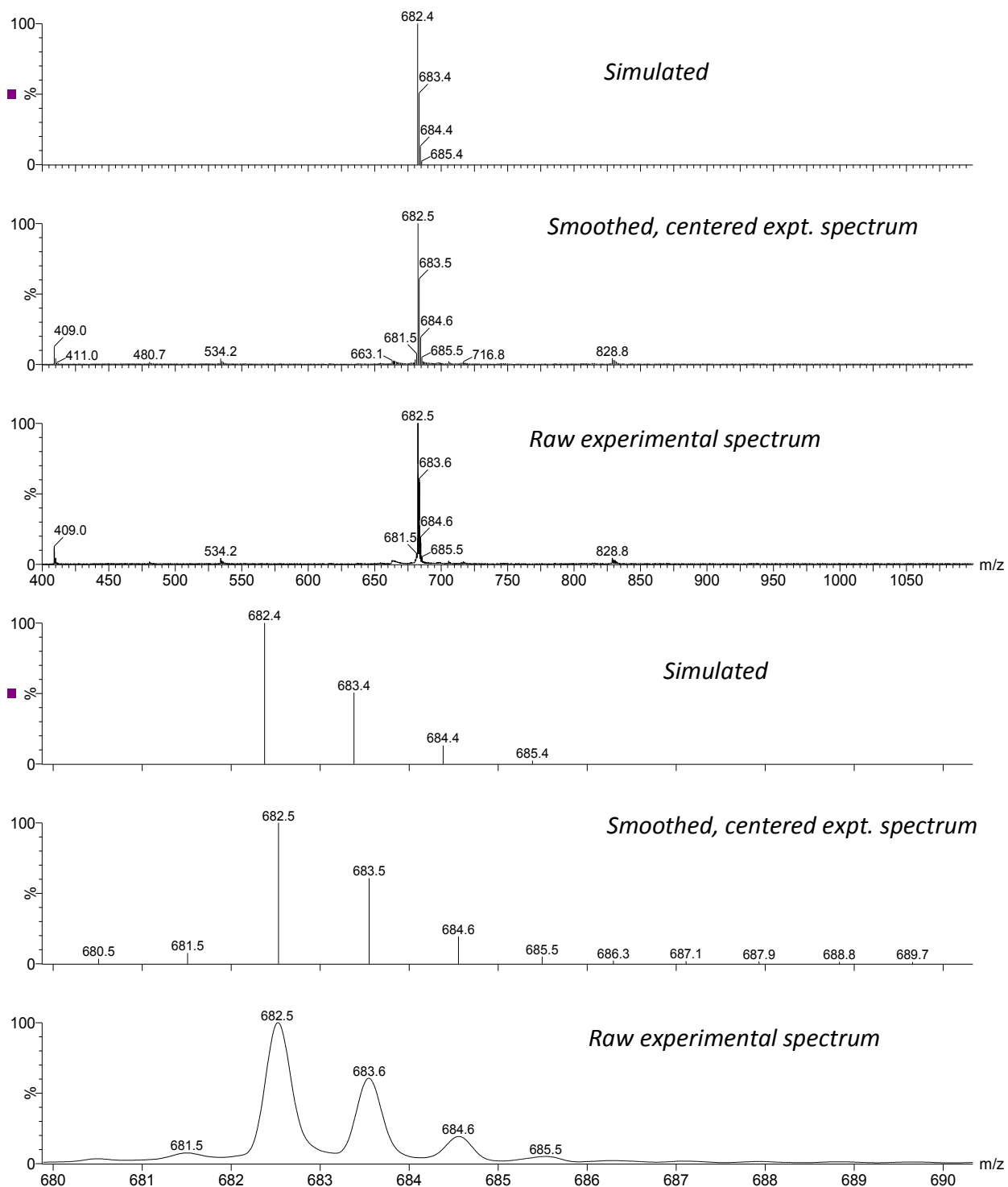
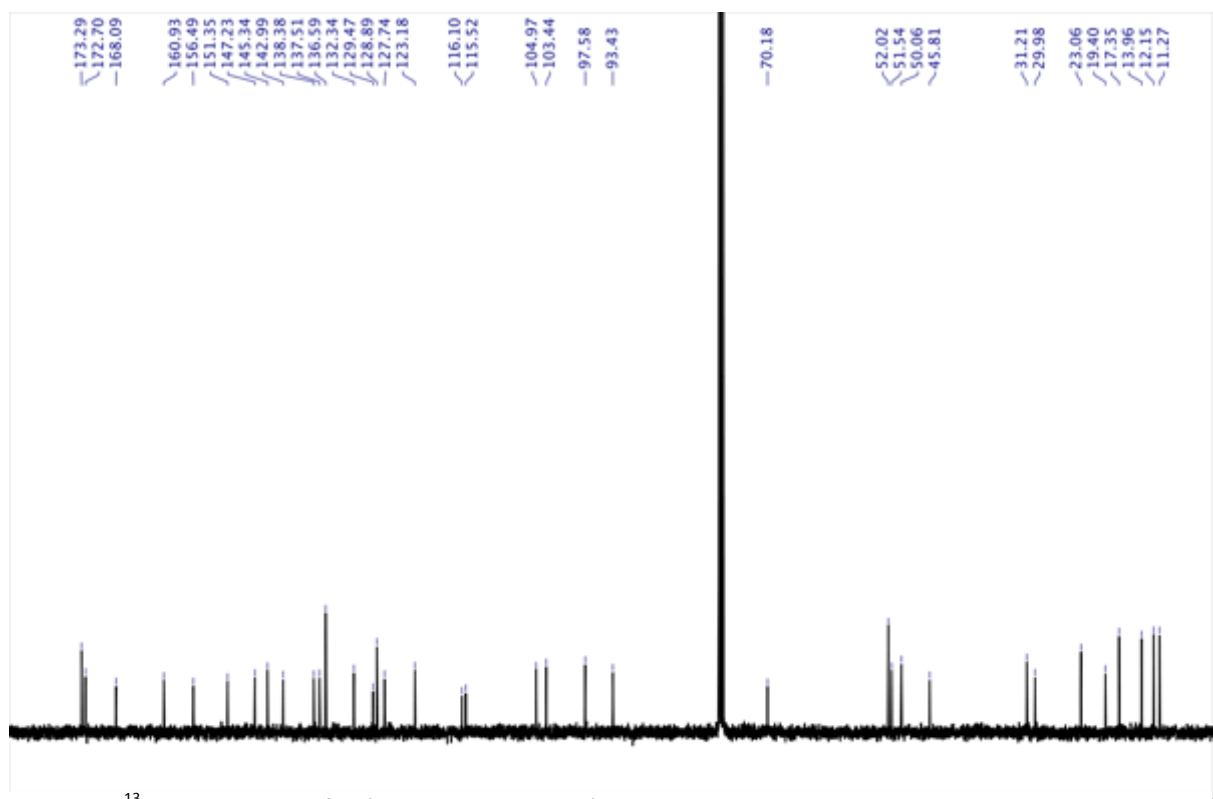
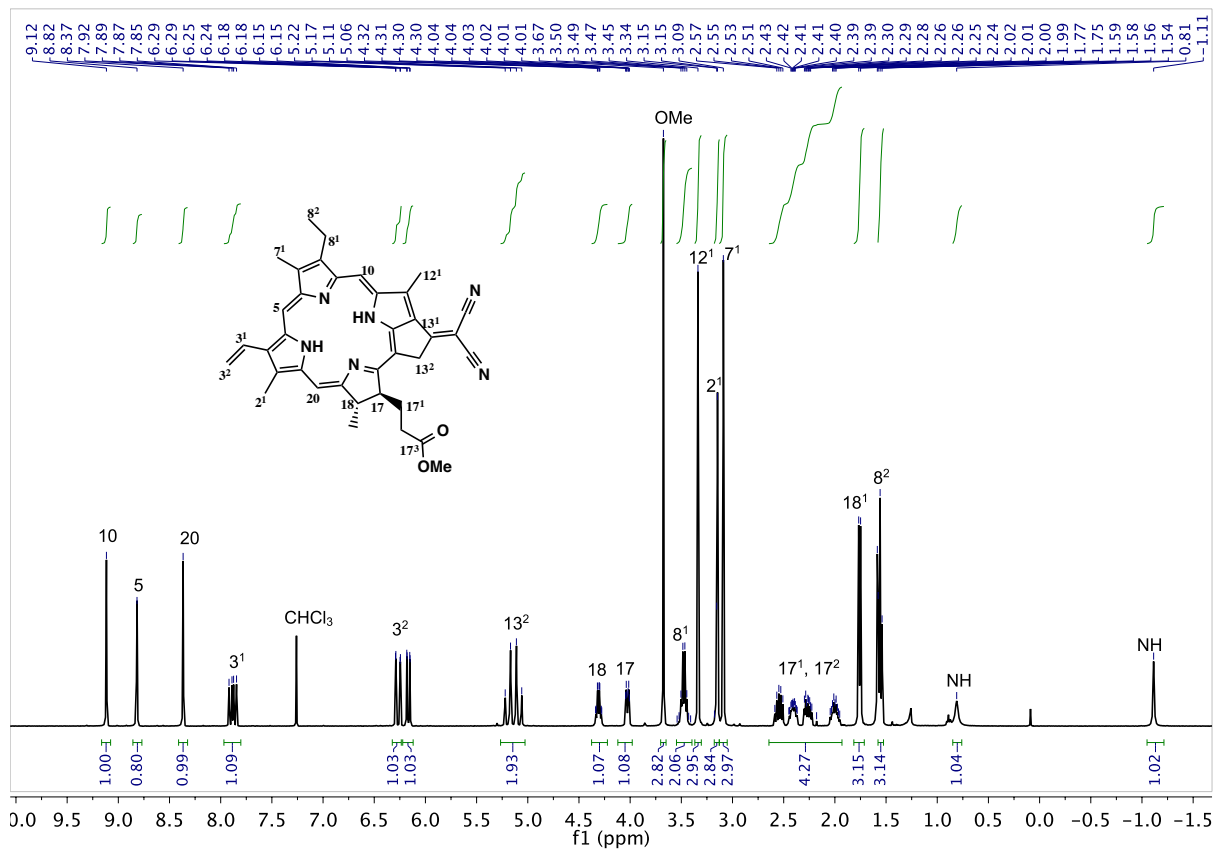


Figure S9: MALDI ToF mass spectrum of 2b.

Methyl-13¹-Deoxo-13¹-(dicyanomethylene)pyropheophorbide-a **3a**



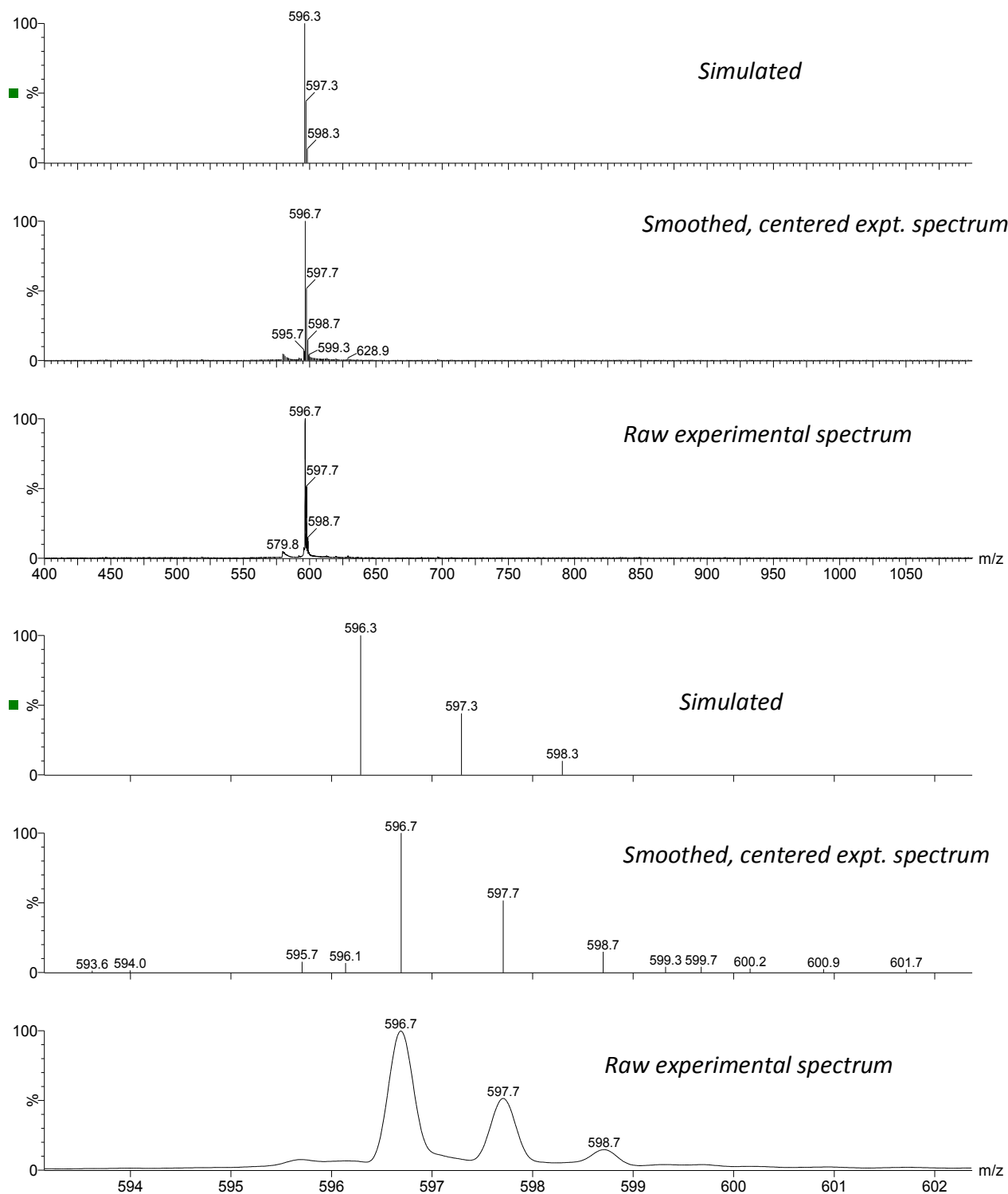


Figure S12: MALDI ToF mass spectrum of **3a**.

¹³C-Deoxy-¹³C-(dicyanomethylene)pyropheophorbide-a 3b

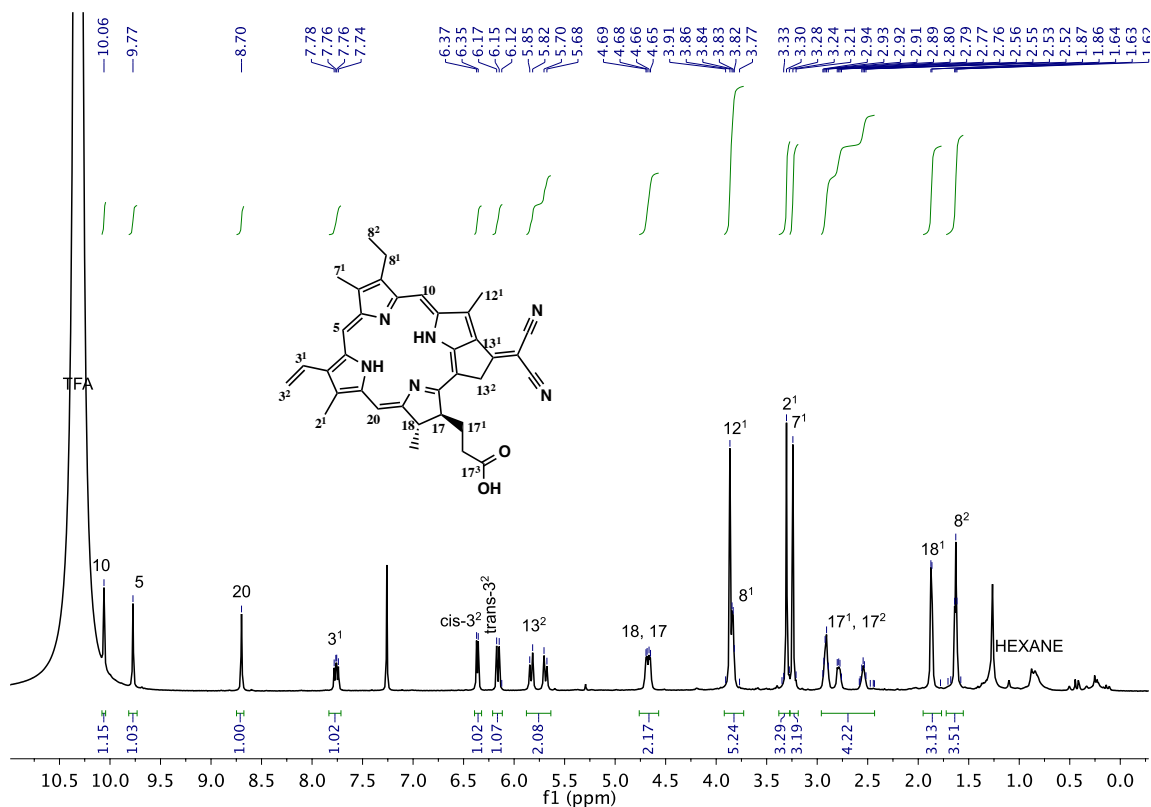


Figure S13: ¹H-NMR spectrum of **3b** (700 MHz, CDCl₃, TFA, 298 K).

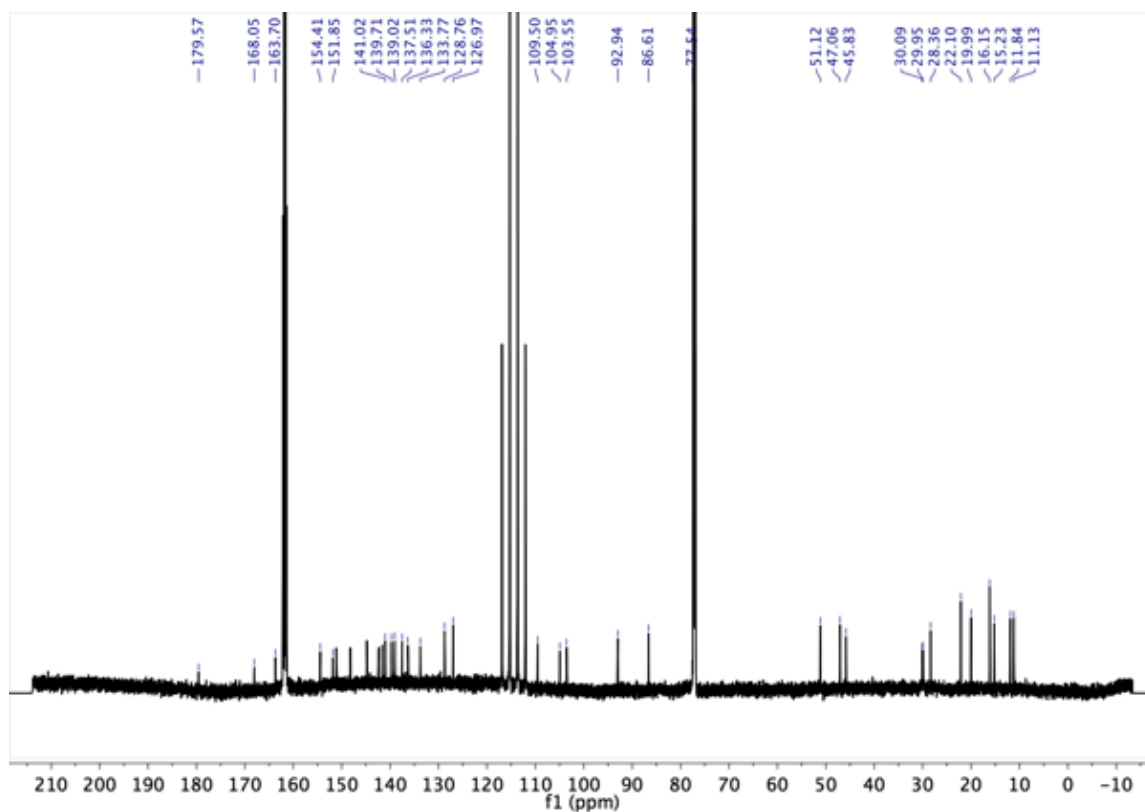


Figure S14: ¹³C-NMR spectrum of **3b** (175 MHz, CDCl₃, TFA, 298 K).

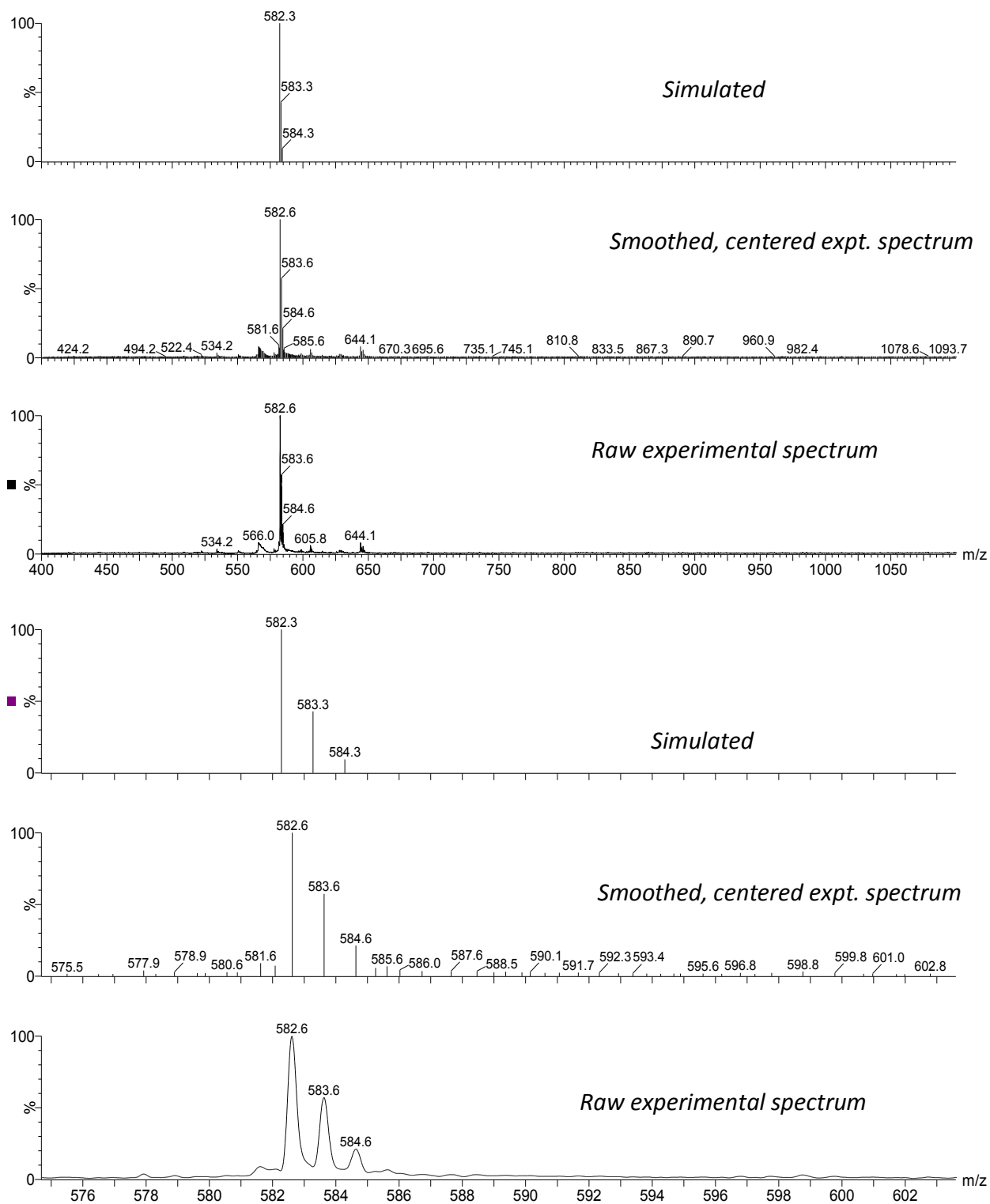


Figure S15: MALDI ToF mass spectrum of **3b**.

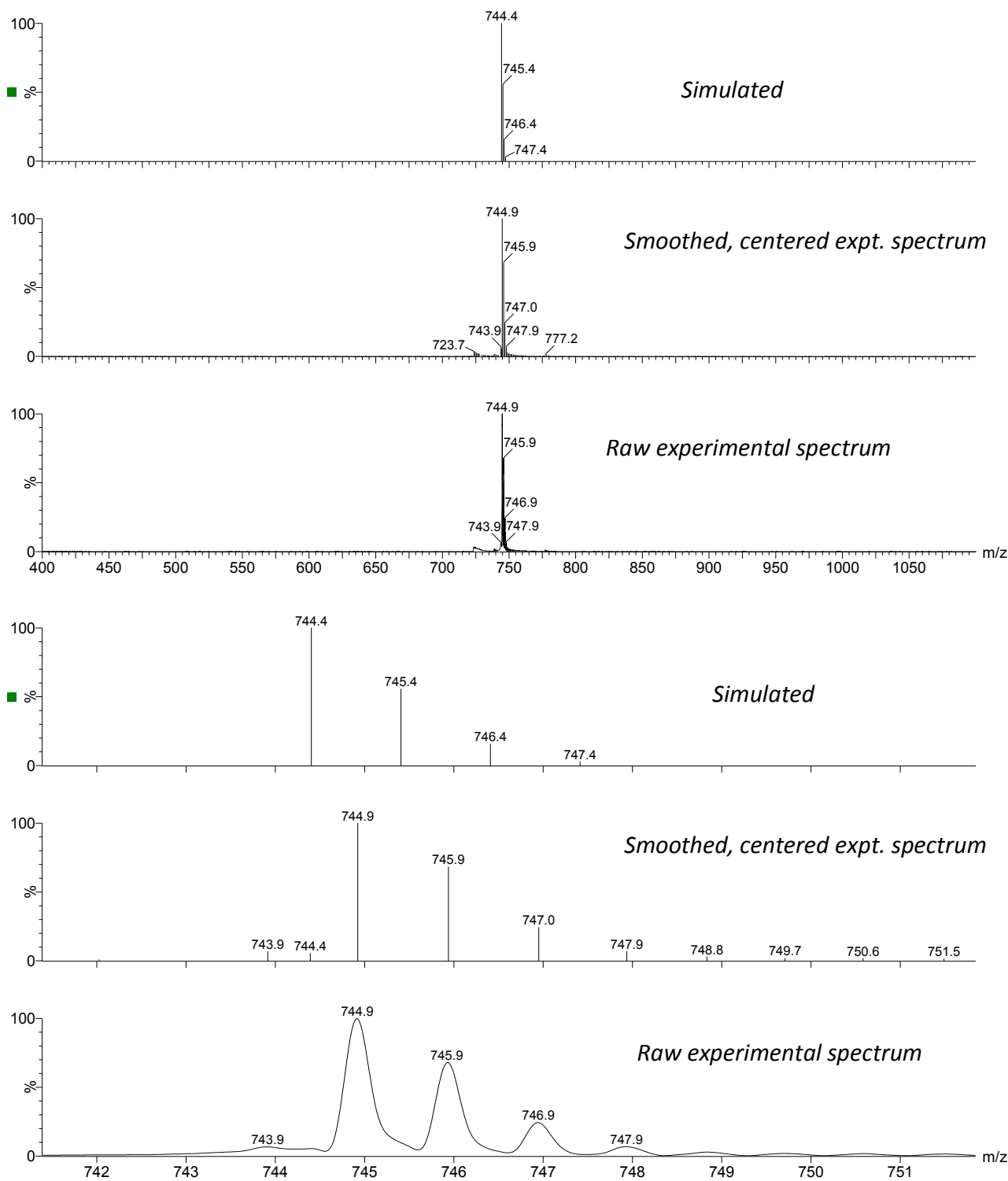


Figure S18: MALDI ToF mass spectrum of 4a.

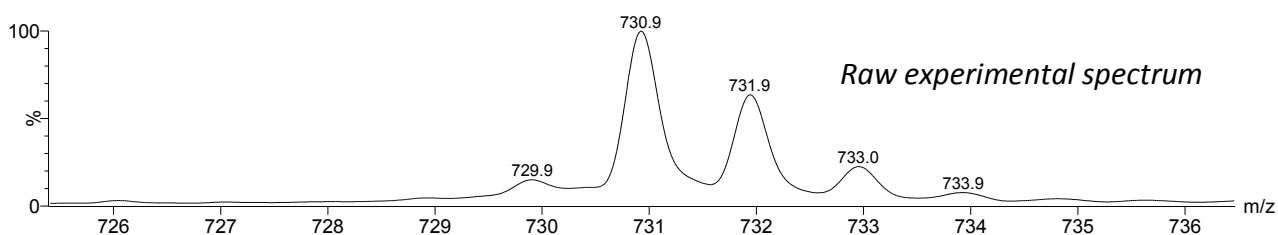
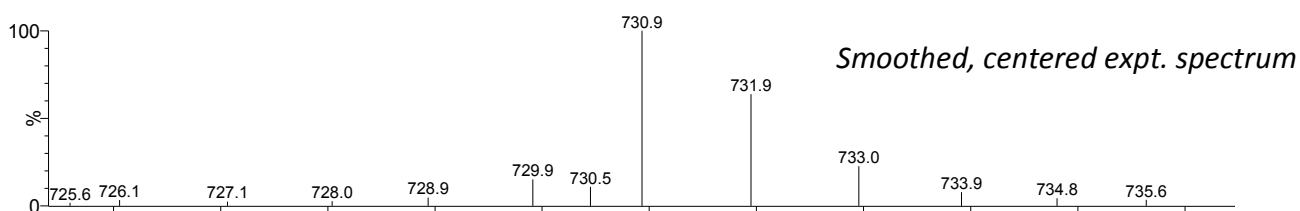
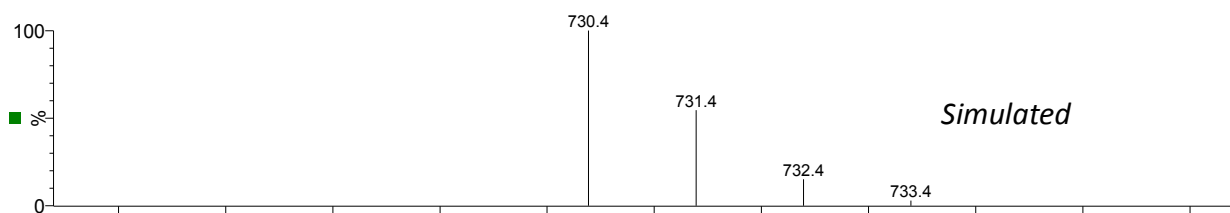
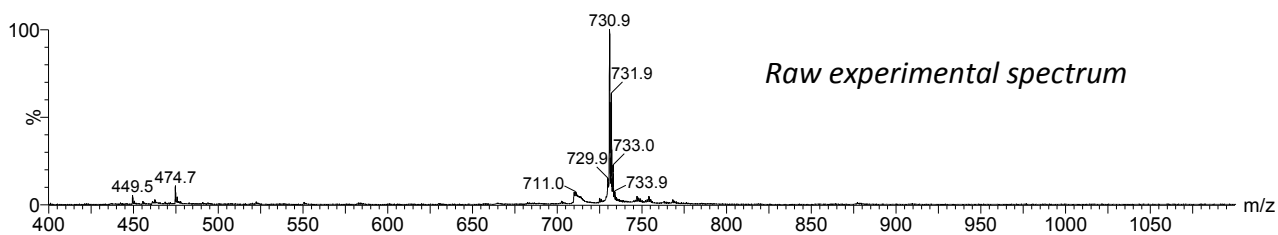
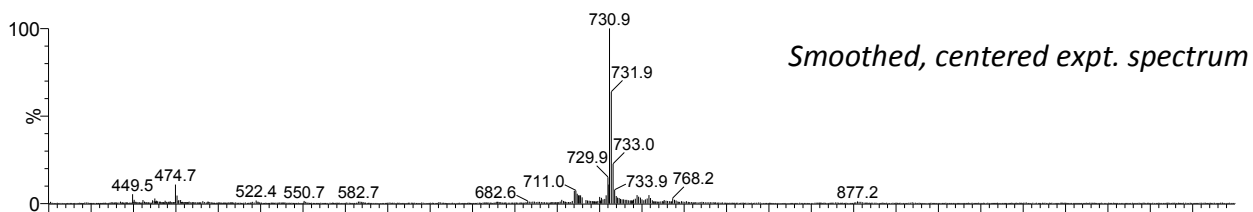
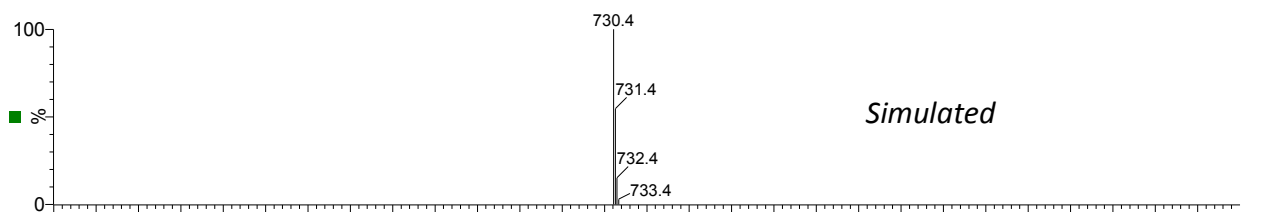


Figure S21: MALDI ToF mass spectrum of 4b.

^{17}O -bis-(TEG)amide pyropheophorbide-a 1c

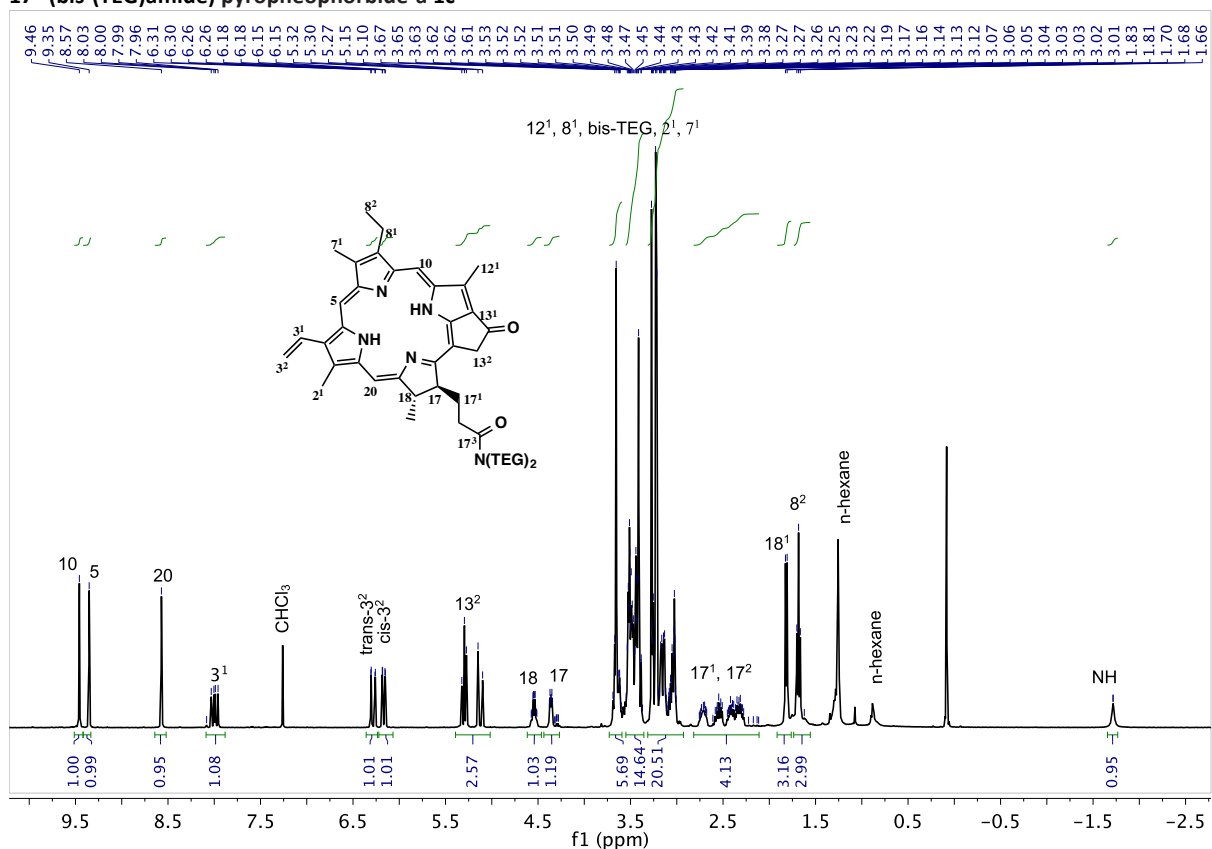


Figure S22: ^1H -NMR spectrum of **1c** (400 MHz, CDCl_3 , 298 K).

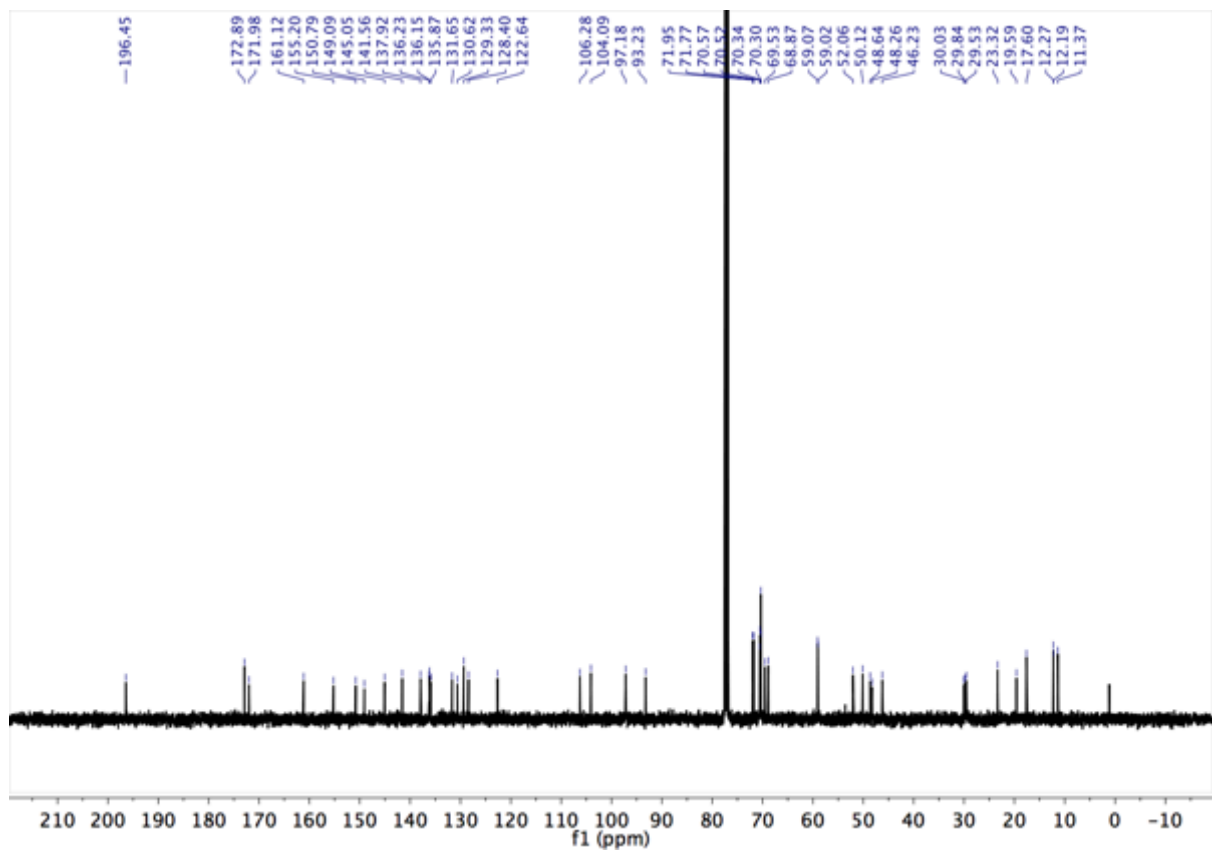


Figure S23: ^{13}C -NMR spectrum of **1c** (100 MHz, CDCl_3 , 298 K).

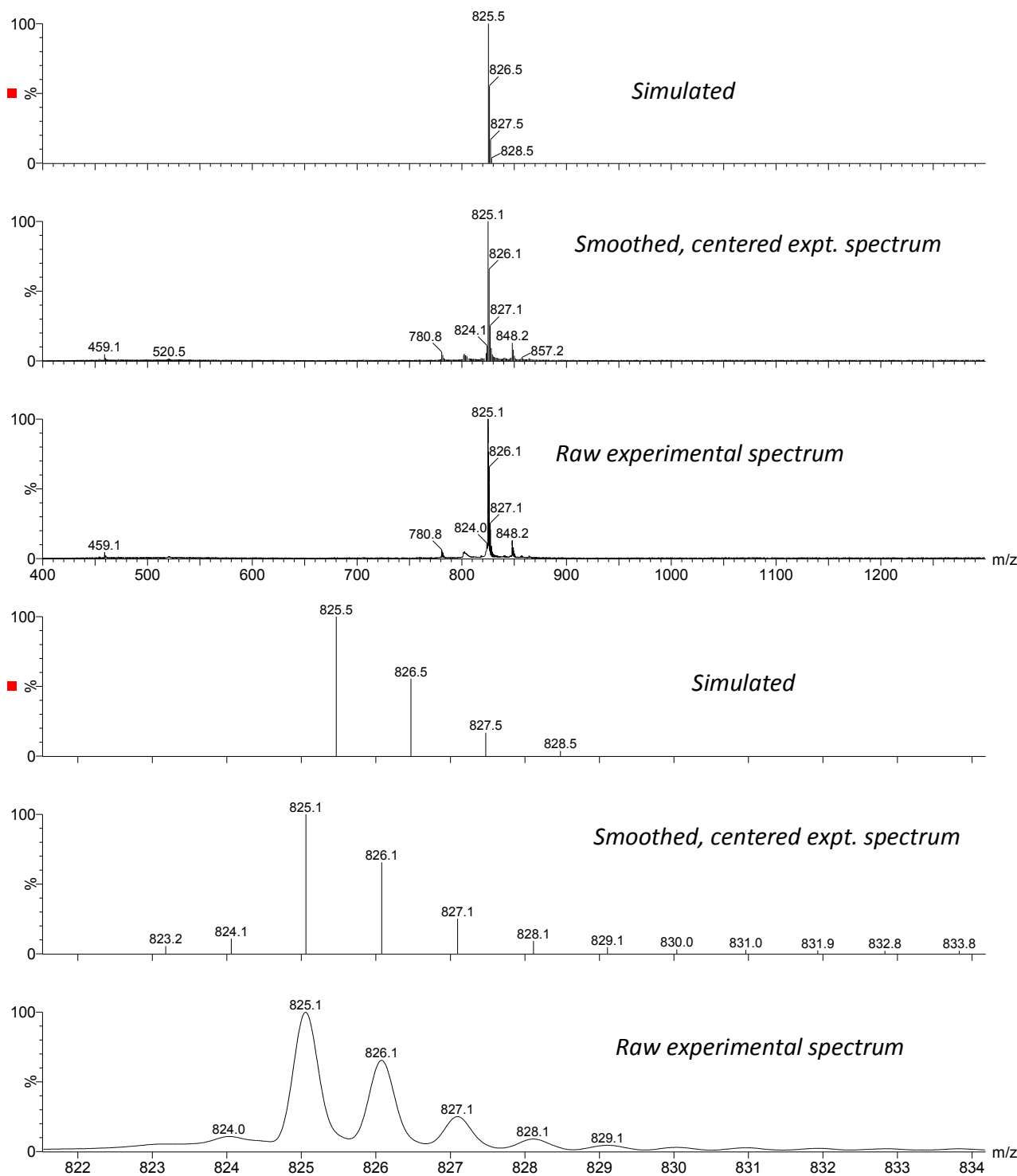


Figure S24: MALDI ToF mass spectrum of 1c.

(E)-3²-(4-(N,N-diethylaminophenyl))-17³-(bis-(TEG)amide) pyrropephorbide-a 2c

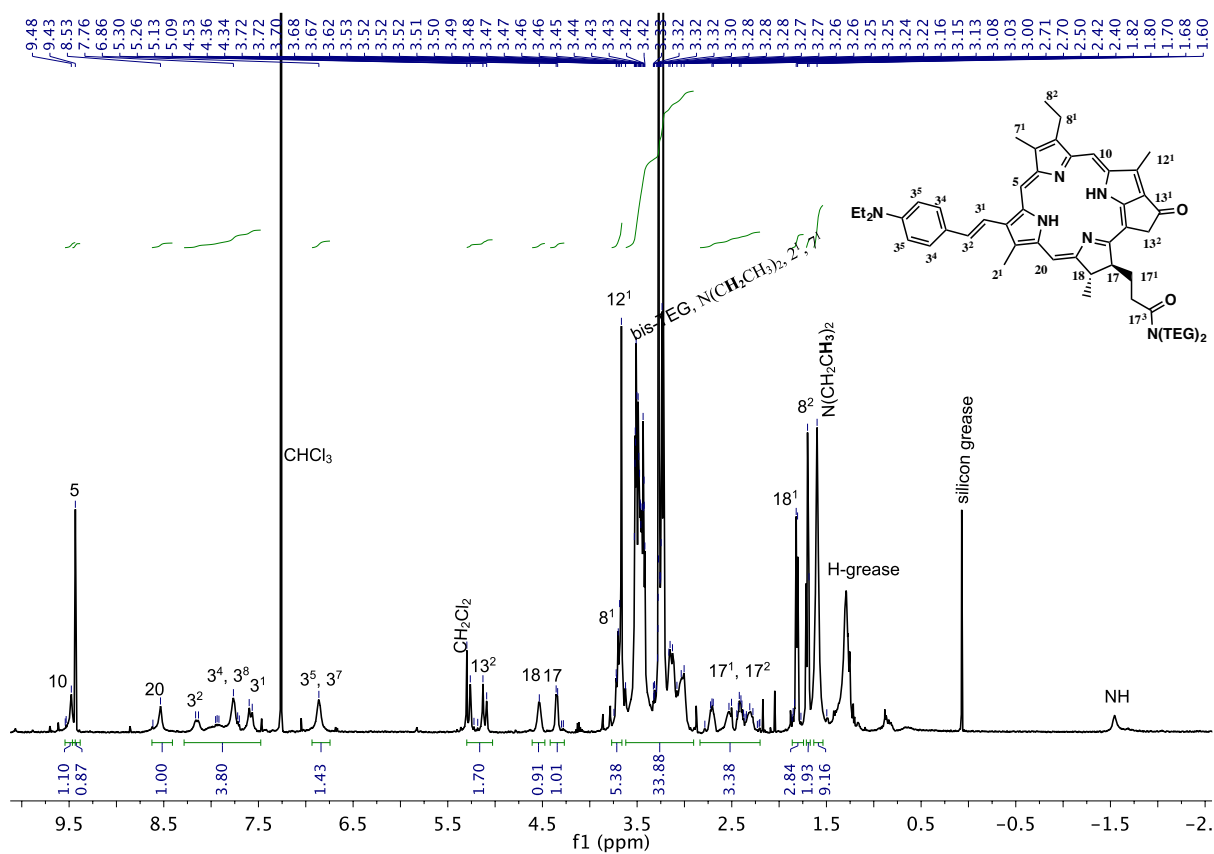


Figure S25: ¹H-NMR spectrum of 2c (600MHz, CDCl₃, 298 K).

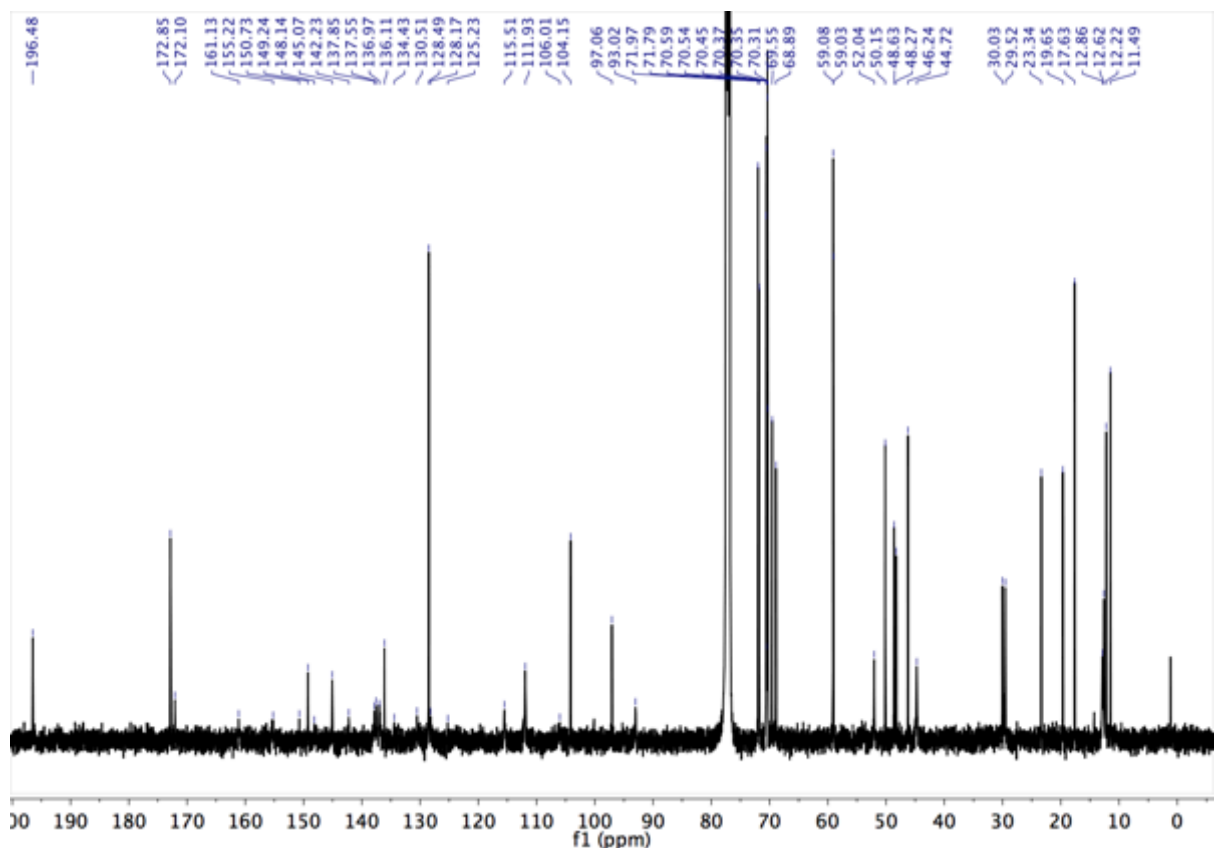


Figure S26: ¹³C NMR spectrum of 2c (150 MHz, CDCl₃, 298 K).

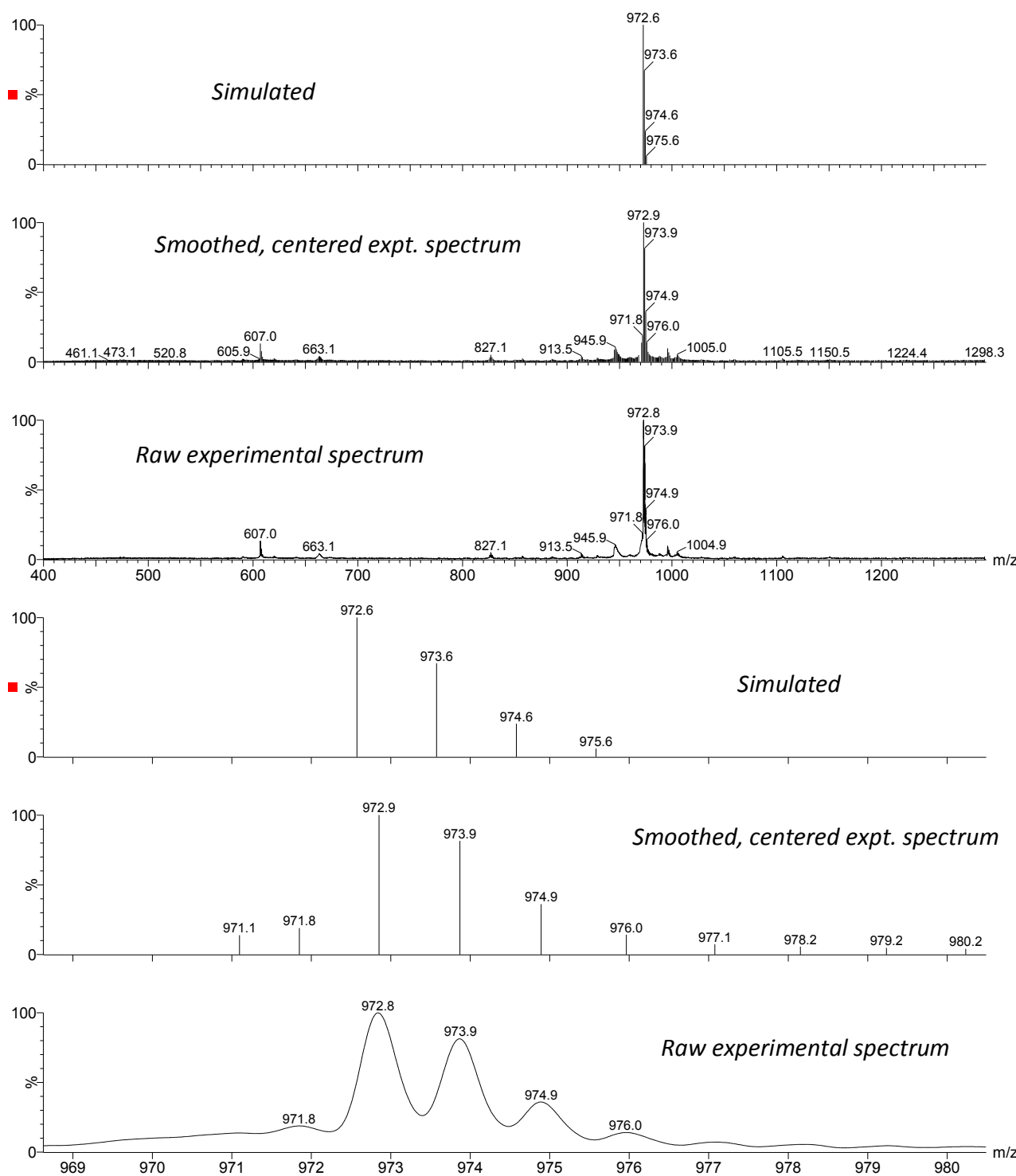


Figure S27: MALDI ToF mass spectrum of 2c.

¹³C-Deoxy-¹³C¹-(dicyanomethylene)-¹⁷C³-(bis-(TEG)amide) pyropheophorbide-a **3c**

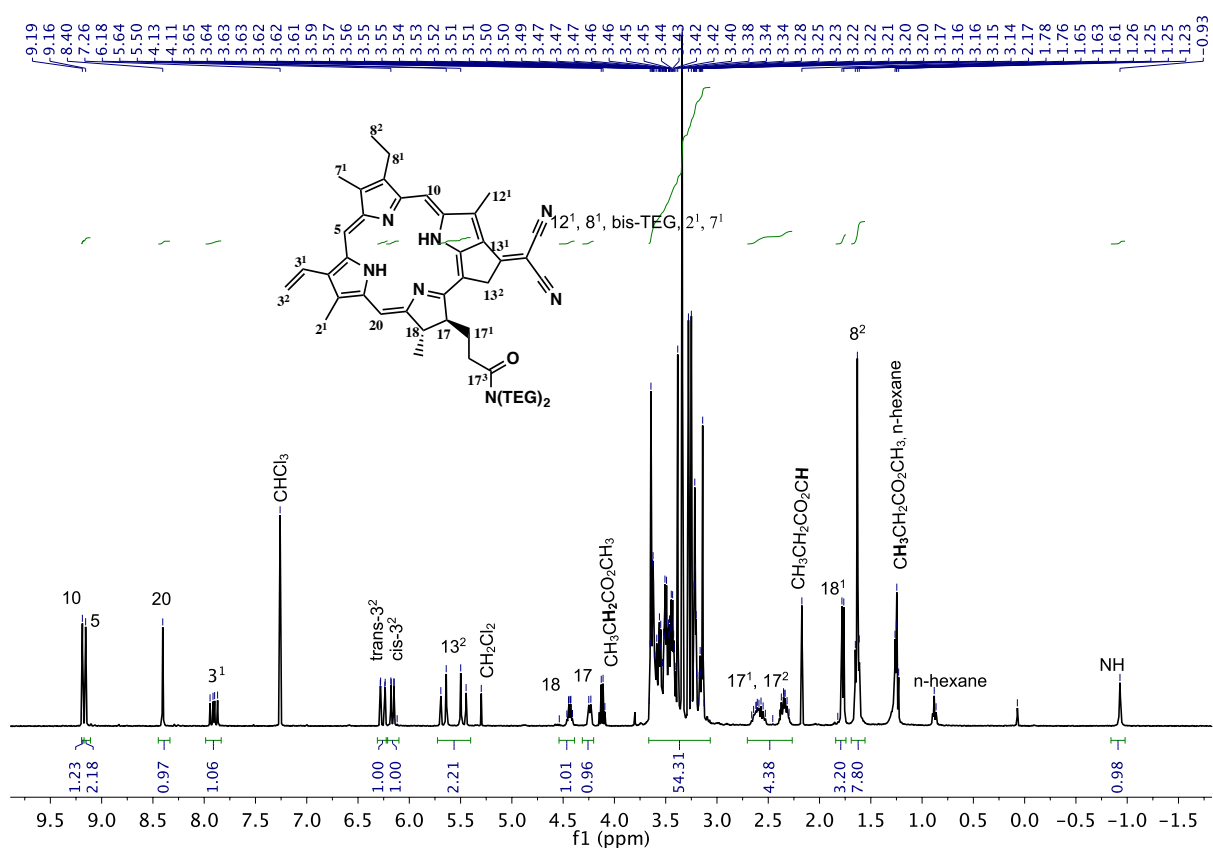
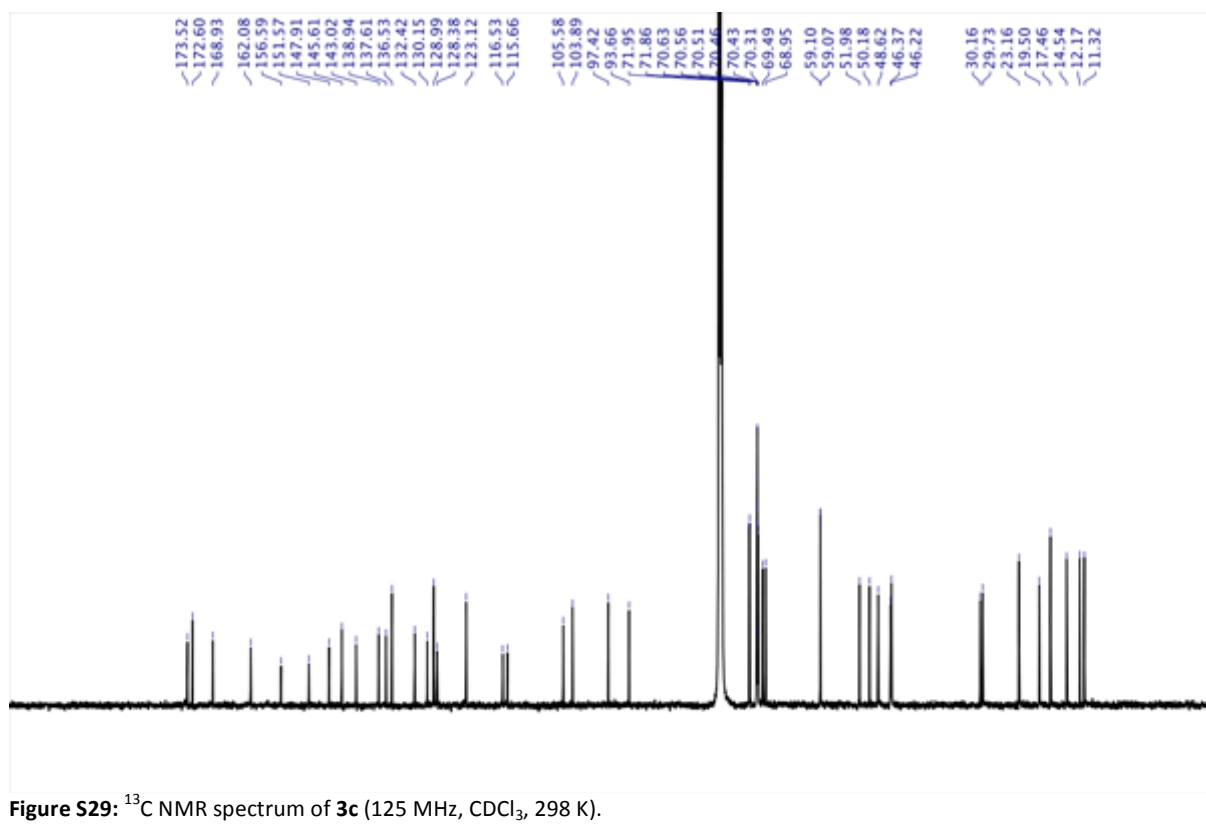


Figure S28: ¹H-NMR spectrum of **3c** (400MHz, CDCl₃, 298 K).



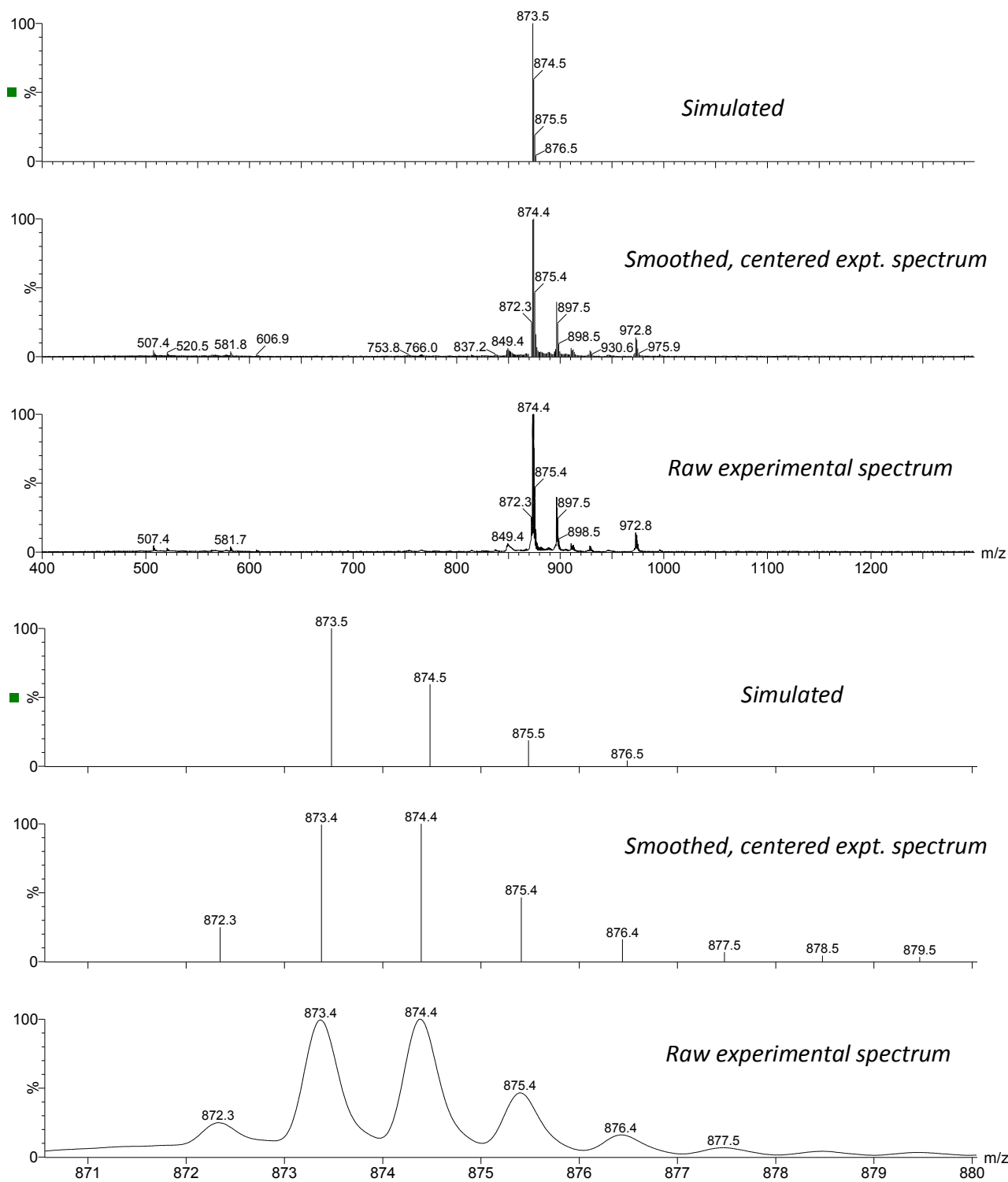


Figure S30: MALDI ToF mass spectrum of 3c.

¹³C-Deoxo-13¹-(dicyanomethylene)-(E)-3²-(4-(N,N-diethylaminophenyl))-17³-(bis-(TEG)amide)-pyropheophorbide-a 4c

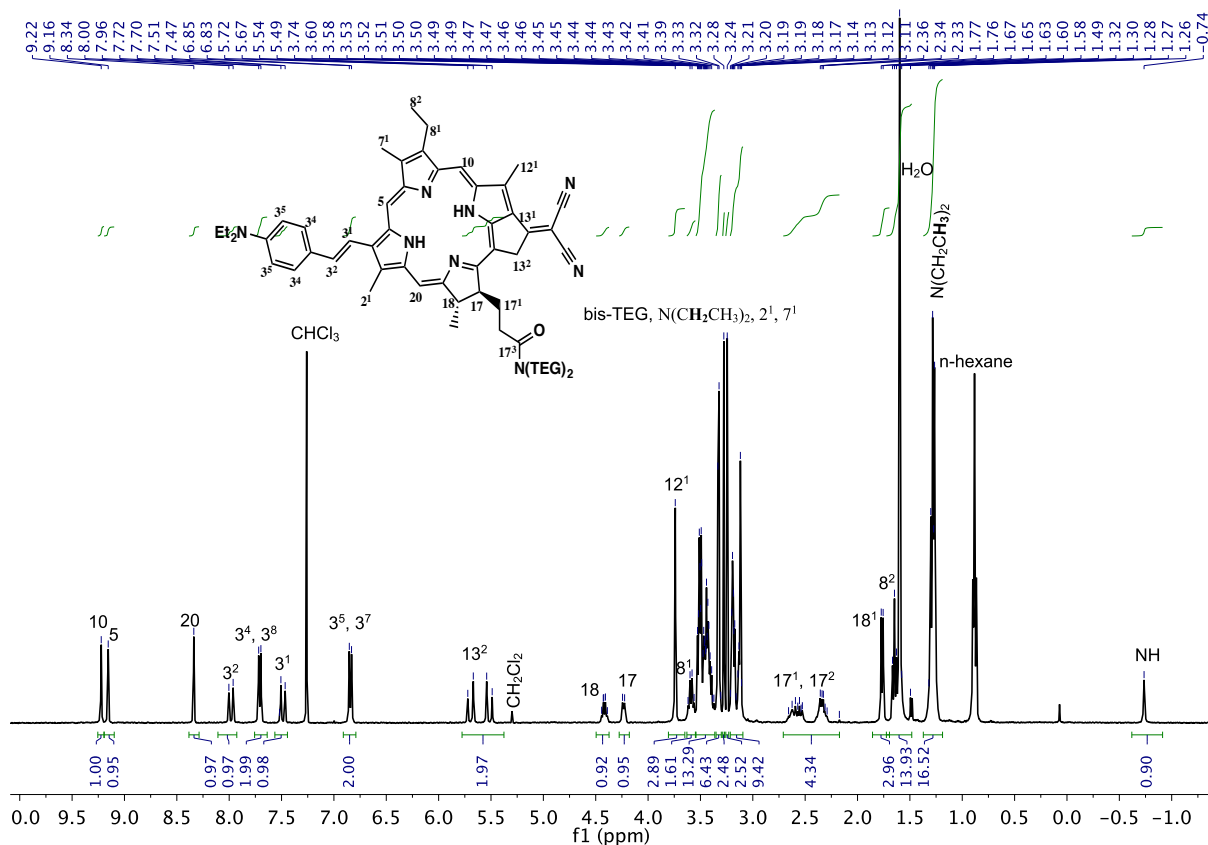


Figure S31: ¹H-NMR spectrum of **4c** (500 MHz, CDCl₃, 298 K).

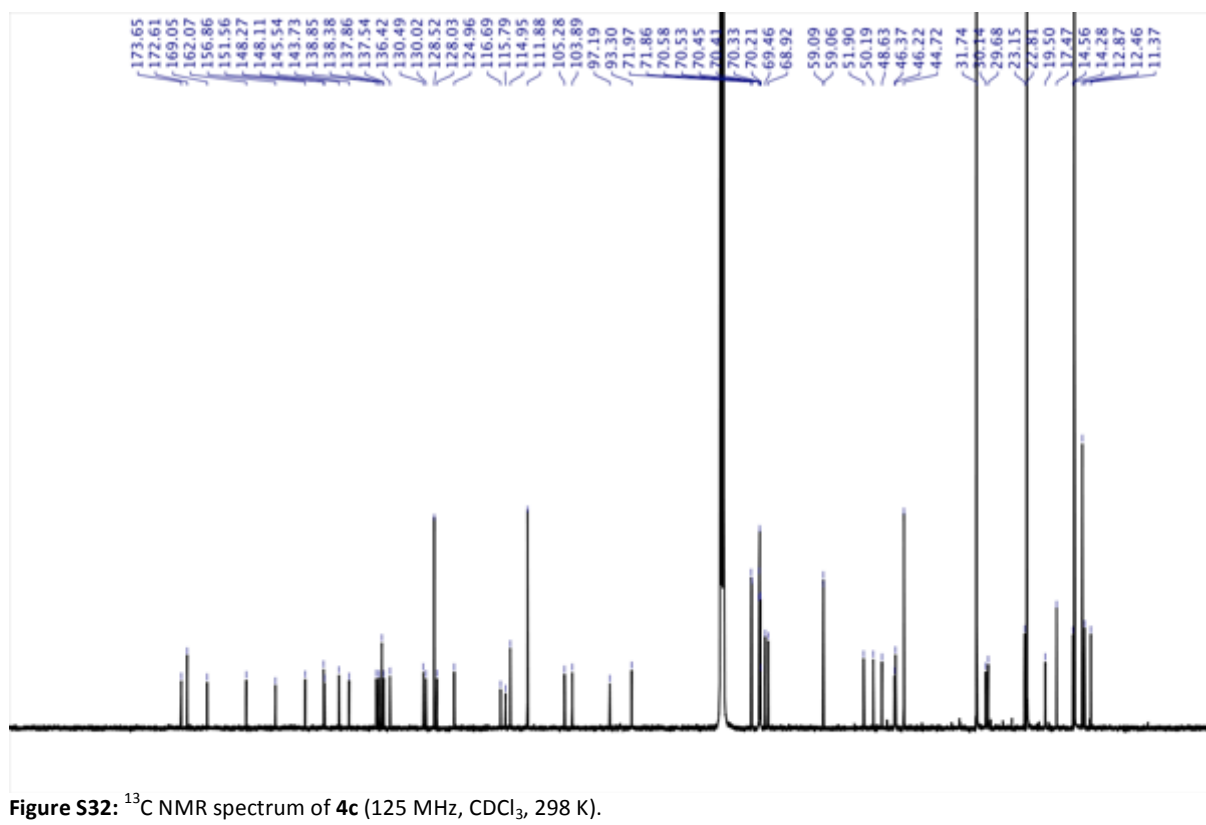


Figure S32: ¹³C NMR spectrum of **4c** (125 MHz, CDCl₃, 298 K).

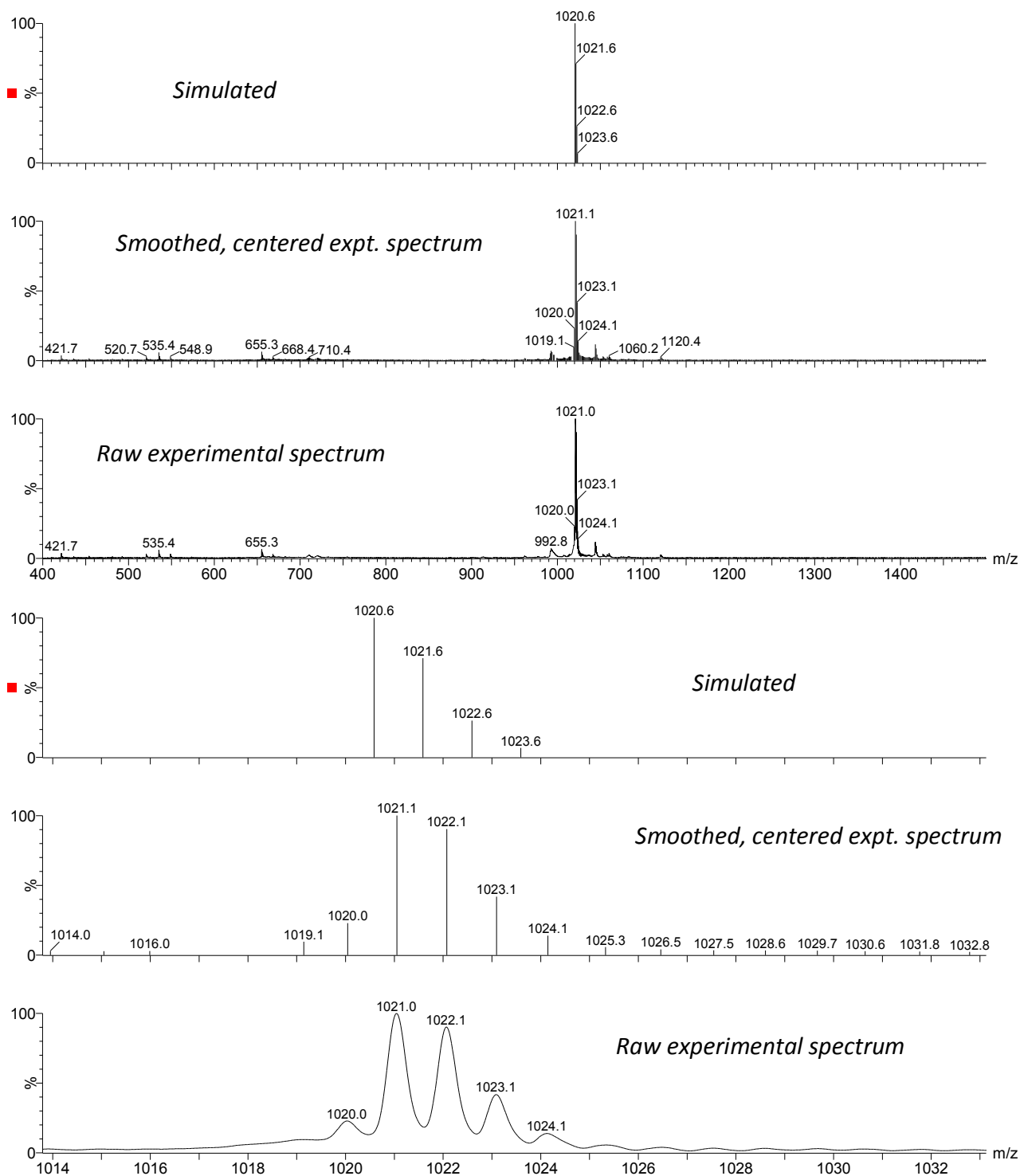


Figure S33: MALDI ToF mass spectrum of 4c.

3.0 Absorption and fluorescence measurements

3.1 Determination of molar absorptivity

For all the compounds, the absorption spectra were measured at five or six different concentrations to calculate the molar absorptivity, ϵ .

General protocol: The compound was weighed (~1–2 mg, weighed with 0.01 mg precision) and dissolved in CH_2Cl_2 (1.00 mL) to prepare the stock solution. A blank measurement of pure CH_2Cl_2 (450 μL) was taken before taking the absorbance measurements. The absorption spectra of the dyes were measured for five or six different concentrations (by incrementally adding 1 μL of stock solution using a 5 μL Hamilton glass syringe to the sample before taking the absorbance measurements). An absorbance vs. concentration graph was drawn to calculate the extinction coefficient at a particular wavelength. According to Beer-Lambert law:

$$A = \epsilon CL,$$

where A is the absorbance, ϵ is the molar absorptivity in $\text{M}^{-1} \text{cm}^{-1}$, C is the concentration in M and L is the length of the light path (1.00 cm in all cases). The slope of the graph is the molar absorption coefficient at the particular wavelength. For example, the graph of **4a** at 716 nm is shown below (Fig S34).

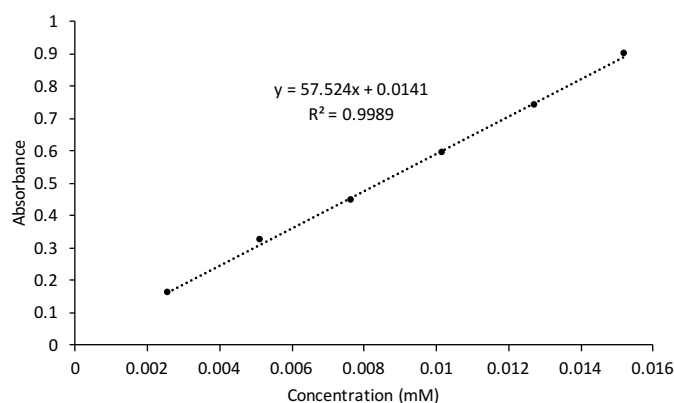


Figure S34: Absorbance vs. concentration graph for **4a** at 716 nm.

3.2 Measurement of quantum yield

The quantum yield of a compound is given by the equation:

$$\phi_C = \phi_R \frac{I_C \cdot A_R}{I_R \cdot A_C}$$

where ϕ_C is the quantum yield of the compound, ϕ_R is the quantum yield of the reference compound, I_C is the fluorescence intensity of the compound, I_R is the fluorescence intensity of the reference compound, A_C is the absorbance of the compound (<0.1) and A_R is the absorbance of the reference compound (<0.1). The reference and the unknown compound were analyzed in the same solvent (CH_2Cl_2).

The quantum yields of studied family of dyes were calculated by measuring their absorbances and fluorescence intensities and then comparing them with the absorbance and fluorescence intensity of the reference compound, **1a** per the above equation. For each compound, five measurements were done at different absorbances (<0.1). The reported quantum yield of **1a** ($\phi = 0.22$ in CH_2Cl_2) was used as a reference.¹ The total fluorescence intensity vs. absorbance graphs used to measure the quantum yields are given in Figure S35.

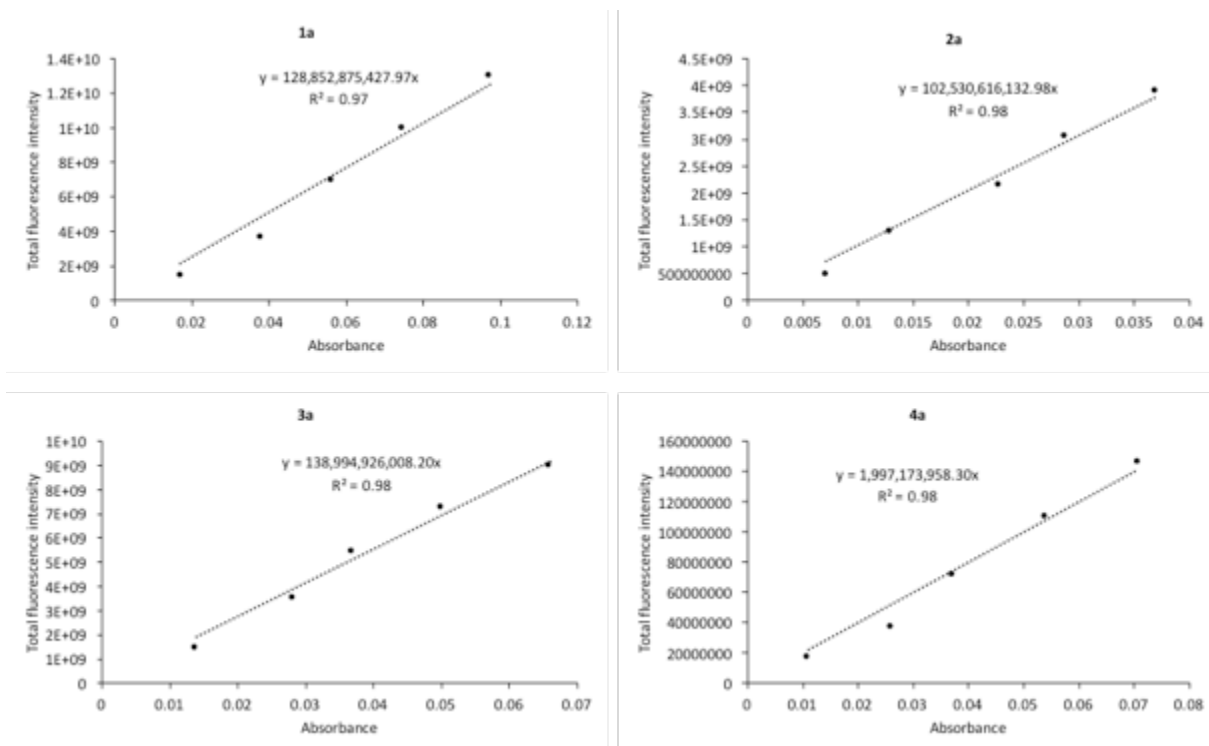


Figure S35: Total fluorescence intensity vs. absorbance graphs for **1a**, **2a**, **3a**, and **4a** for calculating their respective quantum yields. **1a** was taken as reference. **1a** was excited at 414 nm, **2a** was excited at 450 nm, **3a** was excited at 454 nm and **4a** was excited at 459 nm.

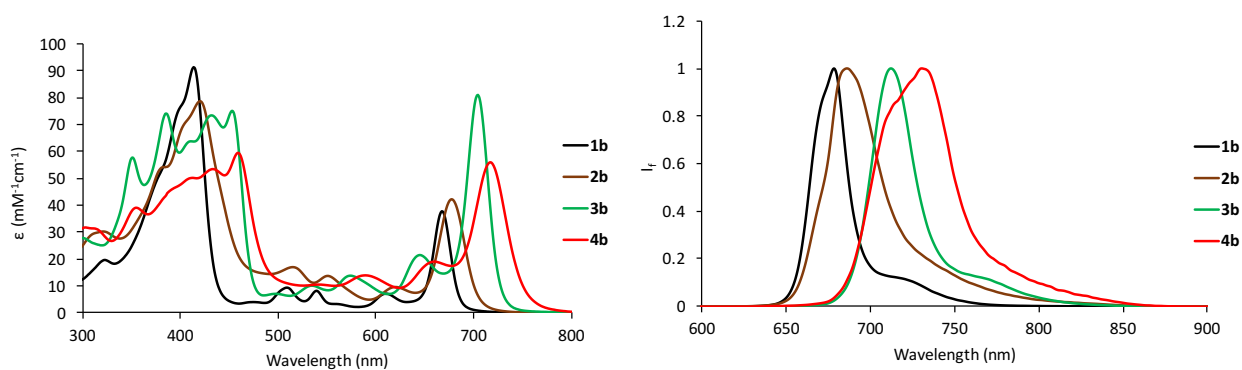


Figure S36: Absorption and normalized emission spectra of PPa family of dyes (**1b**, **2b**, **3b**, and **4b**) in CH_2Cl_2 .

4.0 Electrochemistry

The square-wave voltammograms of **1a**, **2a**, **3a** and **4a** measured in THF with 0.1 M NBu_4PF_6 as electrolyte, are given below in Figures S37–S40. The scan rate of each measurement was 0.05 V/s at 10 Hz with voltage step of 0.005 V. In all the voltammograms, ferrocene (Fc/Fc^+ 0 V) was used as an internal reference.

In **3a**, a bump or a small peak is visible at around 0.75 V. The bump is visible when the measurement is done from -1.5 V to 1.5 V; however, its size reduces drastically when the measurements are done from 0 V to -1.5 V and 0 V to 1.5 V. The bump is also present in **2a** and **4a** but their sizes are negligible in comparison to oxidation and reduction peaks.

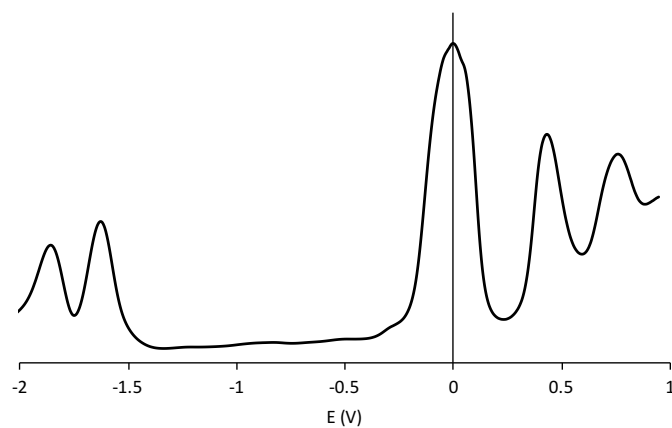


Figure S37: Square wave voltammogram of **1a**.

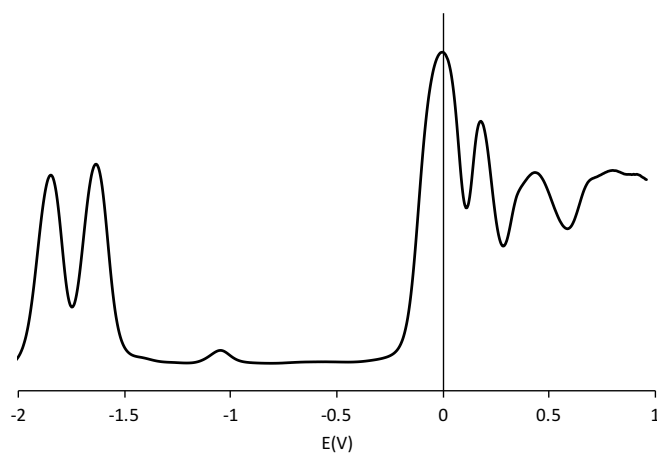


Figure S38: Square wave voltammogram of **2a**.

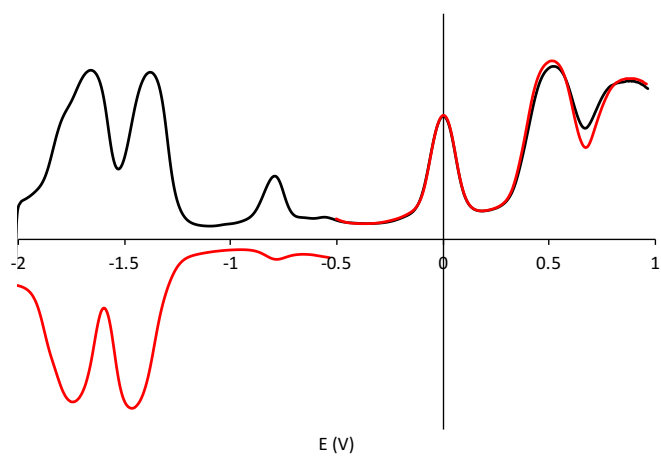


Figure S39: Square wave voltammogram of **3a**.

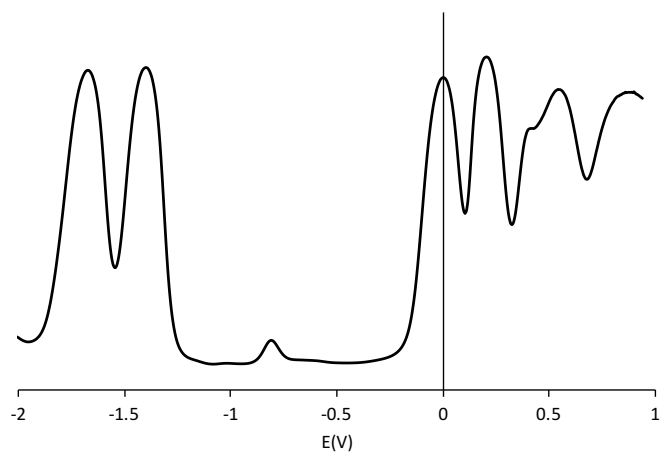


Figure S40: Square wave voltammogram of **4a**.

5.0 Hyper-Rayleigh scattering

The first hyperpolarizabilities (β) of the compounds were quantified using a HRS setup with high-frequency demodulation of two-photon fluorescence.⁴ Measurements were carried out at a fundamental wavelength of 800 nm and 840 nm using a tunable mode-locked femtosecond titanium-sapphire laser (Spectra-Physics, Tsunami) pumped by a diode laser (Spectra-Physics, Millennia). To correct for the self-absorbance of the HRS light in the cuvette, a Lambert-Beer correction factor was used. We used the correct bandpass filters (400 nm and 420 nm, 10 nm FWHM) to collect only the signal at the second-harmonic wavelength. The intensity of scattered light at twice the frequency was plotted against the varying intensities of the fundamental laser light. The quadratic dependences were determined for different concentrations. The magnitude of the slope of the linear dependence of QC against concentration was compared to that of the reference compound crystal violet (i.e. the external reference method) with a β_{HRS} of 209×10^{-30} esu at 800 nm and 226×10^{-30} esu at 840 nm.

A concentration series of compounds **1a**, **2a**, **3a** and **4a** were made in chloroform with maximum concentrations of 12.2, 12.6, 13.6 and 24.9 μM , respectively. Sample solutions were filtered through 0.2 μm PTFE filters to remove dust. UV-VIS spectra were taken before and after each experiment to exclude photodegradation of the compounds. Fundamental wavelengths of 800 and 840 nm were used. The signal was demodulated at 80, 160, 240 and 320 MHz, and in all cases, no significant phase shift or decrease in the apparent β_{HRS} was observed (see Figure S41–S44). This indicates that no multiphoton fluorescence contributes to the HRS signal. Hence, β_{HRS} was calculated by averaging apparent values at different demodulation frequencies. Because β_{zzz} was assumed to be the dominating tensor component and was calculated from $\langle \beta_{HRS} \rangle^2 = (6/35) \langle \beta_{zzz} \rangle^2$.⁵

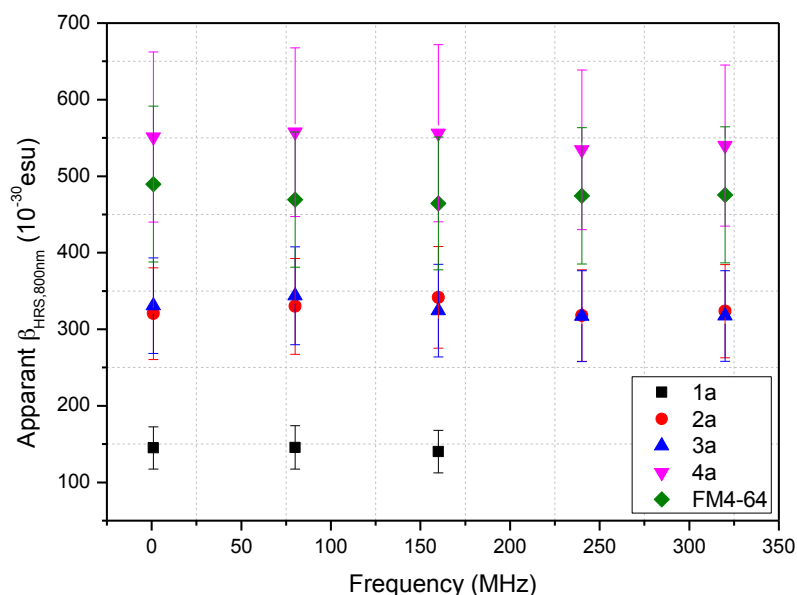


Figure S41: Apparent hyperpolarizability as a function of the induced AM frequency at 800 nm for compounds **1a–4a** and FM4-64 in CHCl_3 .

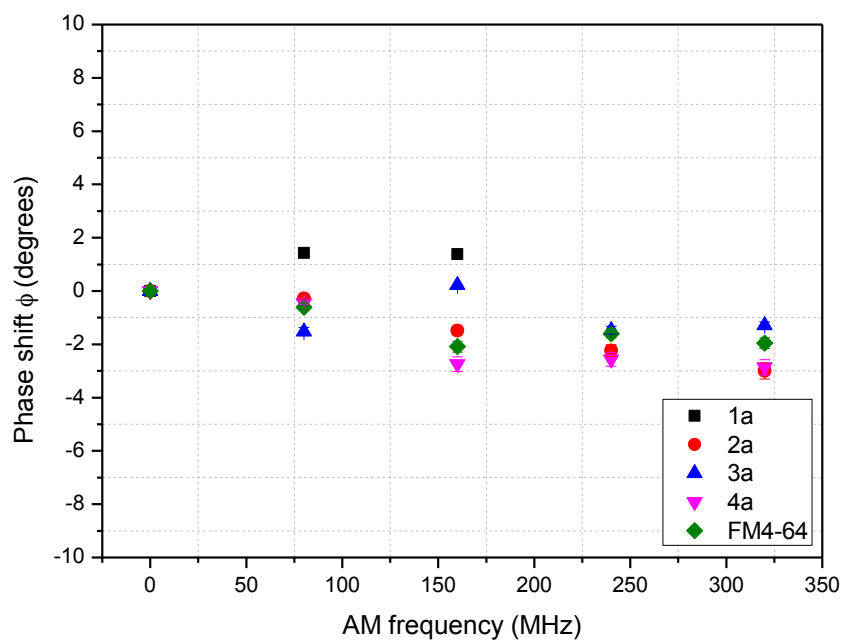


Figure S42: Observed phase shift ϕ of compounds **1a–4a** and FM4-64 compared to the reference molecule crystal violet at different induced AM frequencies in the HRS experiment at 800 nm.

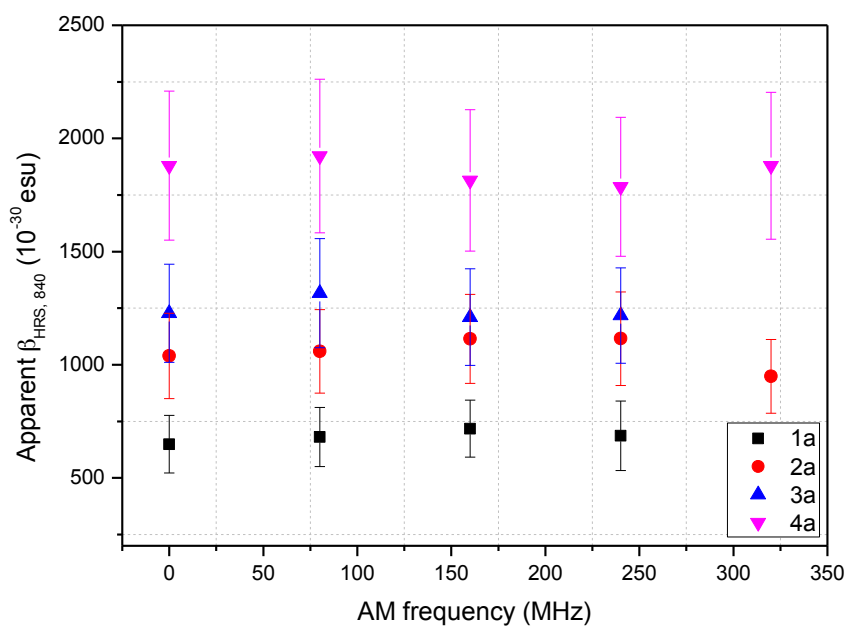


Figure S43: Observed phase shift ϕ of compounds **1a–4a** compared to the reference molecule crystal violet at different induced AM frequencies in the HRS experiment at 840 nm.

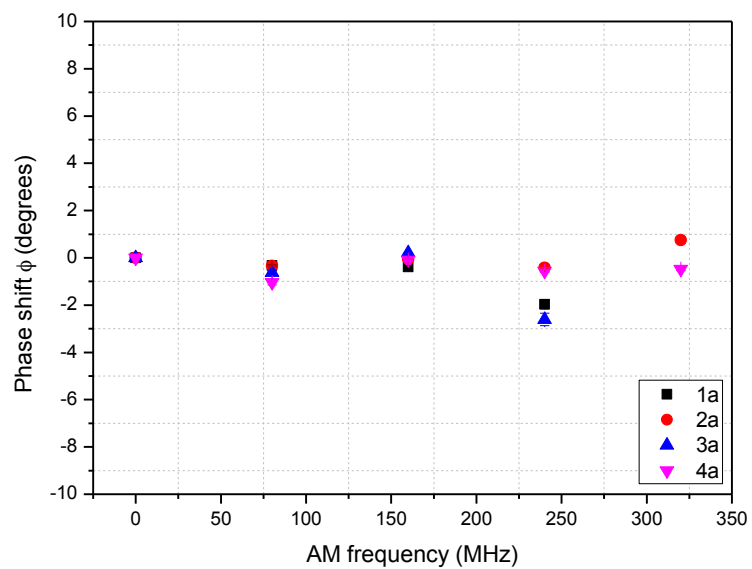


Figure S44: Observed phase shift ϕ of compounds **1a-4a** compared to the reference molecule crystal violet at different induced AM frequencies in the HRS experiment at 840 nm.

6.0 Microscopy

6.1 Droplet experiments

The dye (20 μM) was added to a mixture of 1,2-diphytanoyl-*sn*-glycero-3-phosphocholine (DPhPC, Avanti lipids) (0.5 mg/mL) and phosphate buffer (1 mL, 50 mM H_2KPO_4 , 50 mM NaCl, pH 7.0) and sonicated until the dye was fully dissolved. The phosphate buffer (10 μL) solution was then added to a solution of DPhPC lipid (5 mg/mL) in dodecane (0.5 mL) and gently shaken. The droplets are then imaged in a 35 mm glass bottom well dish (MatTek[®]).

6.2 Microscopy

The microscopy experiments were done using an Olympus FV1200MPE-BX61WI microscope equipped with Mai Tai[®] eHP DeepSee™ Ti:Sapphire laser from Spectra-Physics. The numerical aperture of the objective (UPLSAPO 10X2) is 0.4 (10X) and of condenser (air based) is 0.9. The light pulses were passed through a long pass 690 nm dichroic mirror. For TPEF, the reflected light was passed through a 750 nm short pass filter before passing through a 540 nm long pass (LP) filter and then detected by a PMT detector (Hamamatsu IR sensitive PMT-R10699). For SHG, the light in the transmitted direction was passed through a band-pass filter (420 ± 15 nm) before being detected through a PMT detector (Hamamatsu R3896). All the dyes were excited at 840 nm.

6.3 Tilt angle experiments

Two-photon excited fluorescence and second harmonic generation images of one droplet of each of the dye **1c**, **2c** and **4c** are shown in Figures S45–S50. (A) The angular part of the model (black line) is plotted over data. (B) The surface representation of the image. (C) The parameterized model of the surface of the image. (D) The image in grayscale map. (E) The parameterized model of the image in grayscale map.

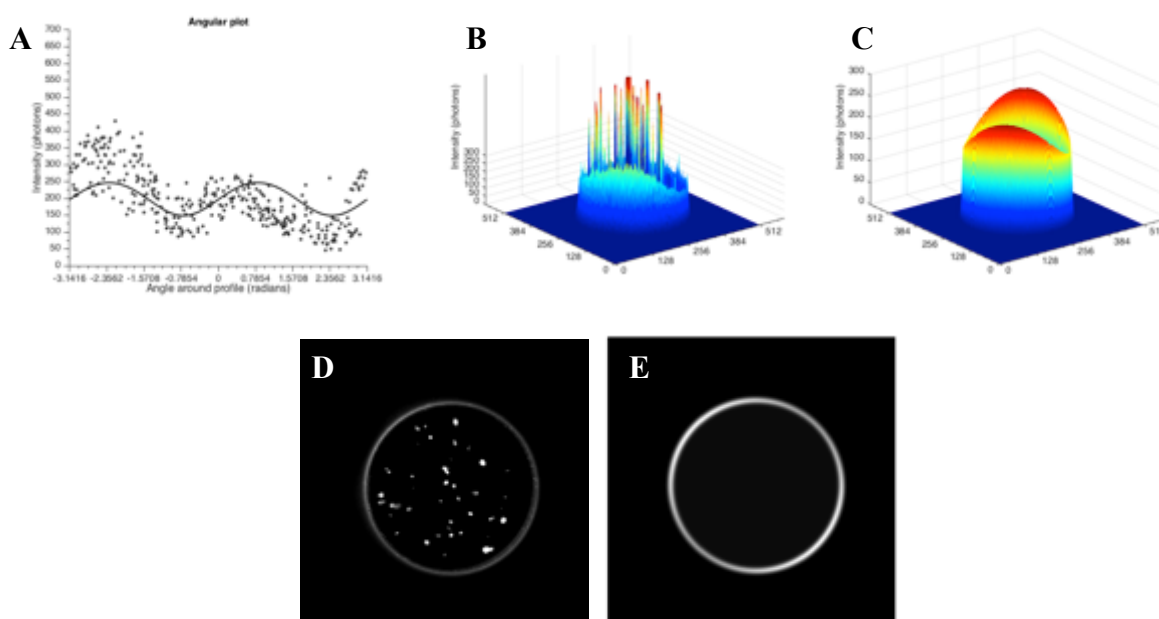


Figure S45: Analysis of **1c** in monolayer droplet by two-photon microscopy. (A) Angular plot of tilt-angle, (B) the image plotted as a surface, (C) the parameterized model plotted as a surface with photon counts on the z-axis, (D) the image plotted as a linear grayscale intensity map and (E) the parameterized model plotted as a linear grayscale intensity map. Droplet diameter: 250 μm .

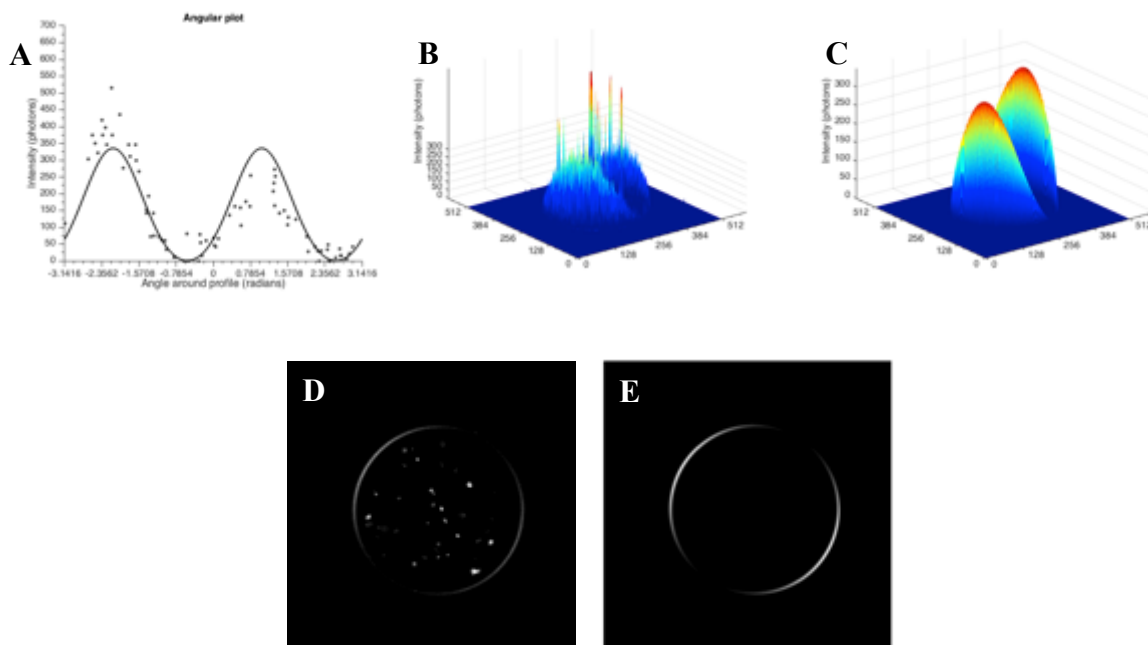


Figure S46: Analysis of **1c** in monolayer droplet by second harmonic generation microscopy. (A) Angular plot of tilt-angle, (B) the image plotted as a surface, (C) the parameterized model plotted as a surface with photon counts on the z-axis, (D) the image plotted as a linear grayscale intensity map and (E) the parameterized model plotted as a linear grayscale intensity map. Droplet diameter: 250 μm .

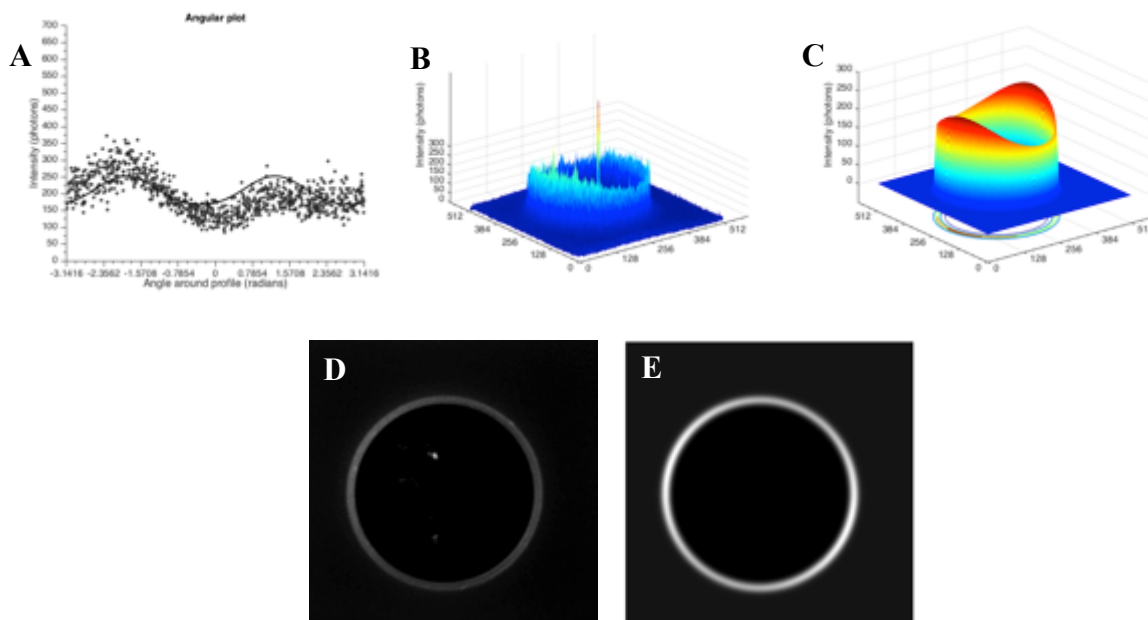


Figure S47: Analysis of **2c** in monolayer droplet by two-photon microscopy. (A) Angular plot of tilt-angle, (B) the image plotted as a surface, (C) the parameterized model plotted as a surface with photon counts on the z-axis, (D) the image plotted as a linear grayscale intensity map and (E) the parameterized model plotted as a linear grayscale intensity map. Droplet diameter: 130 μm .

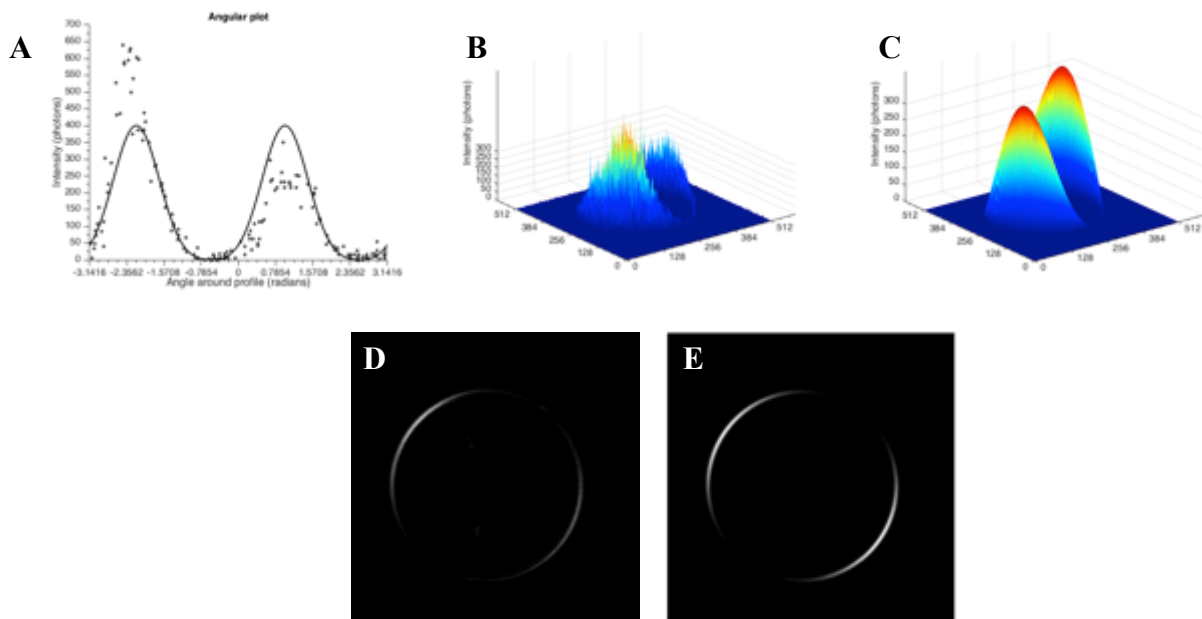


Figure S48: Analysis of **2c** in monolayer droplet by second harmonic generation microscopy. (A) Angular plot of tilt-angle, (B) the image plotted as a surface, (C) the parameterized model plotted as a surface with photon counts on the z-axis, (D) the image plotted as a linear grayscale intensity map and (E) the parameterized model plotted as a linear grayscale intensity map. Droplet diameter: 130 μm .

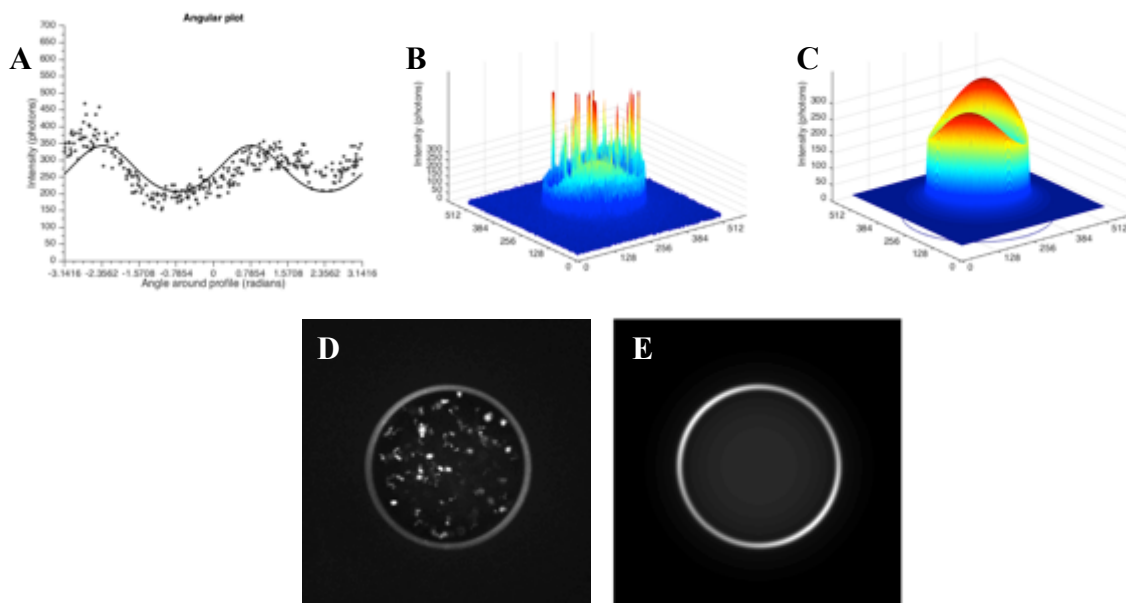


Figure S49: Analysis of **4c** in monolayer droplet by two-photon microscopy. (A) Angular plot of tilt-angle, (B) the image plotted as a surface, (C) the parameterized model plotted as a surface with photon counts on the z-axis, (D) the image plotted as a linear grayscale intensity map and (E) the parameterized model plotted as a linear grayscale intensity map. Droplet diameter: 225 μm .

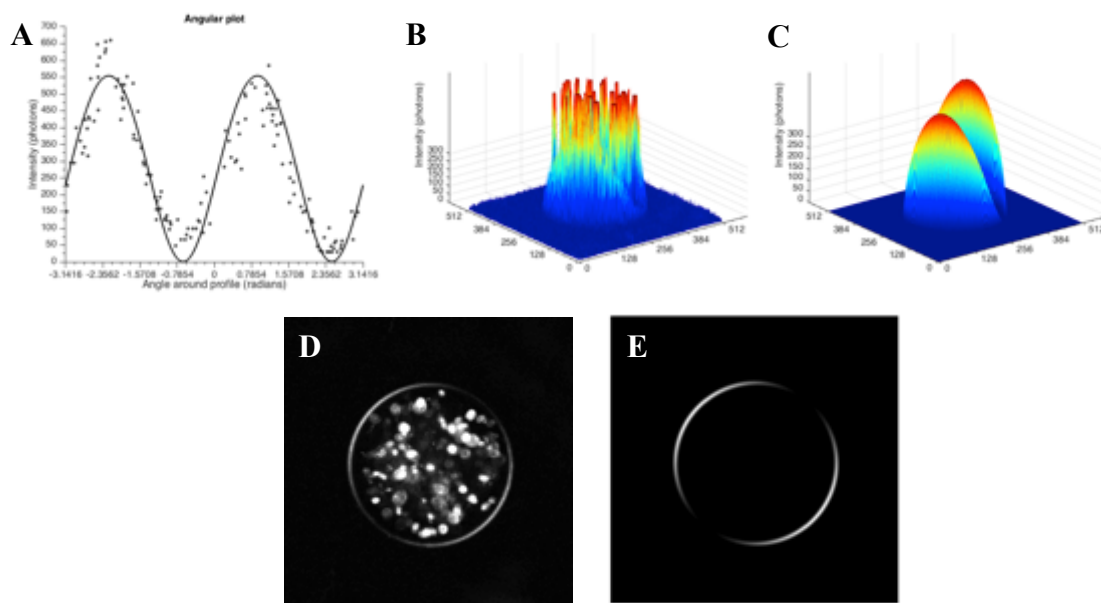


Figure S50: Analysis of **4c** in monolayer droplet by second harmonic microscopy. (A) Angular plot of tilt-angle, (B) the image plotted as a surface, (C) the parameterized model plotted as a surface with photon counts on the z-axis, (D) the image plotted as a linear grayscale intensity map and (E) the parameterized model plotted as a linear grayscale intensity map. Droplet diameter: 225 μm .

6.4 Presence of different transition dipole moments at different wavelengths

Compound **3c** was dissolved in deionized water and then mixed with glycerin in such a way that the concentration of water is 10% v/v. The compound was added in such a way that the total absorbance of the glycerin-water mixture is less than 0.1. The excitation spectrum ($\lambda_{em} = 730$ nm) of the sample is measured by placing it between two polarization filters at parallel directions to each other. After the first measurement, the polarization filter placed between the sample and the detector is rotated by 90° angle and the spectrum was measured again. Both spectra are plotted and then normalized at 707 nm for better comparison (Figure S51).

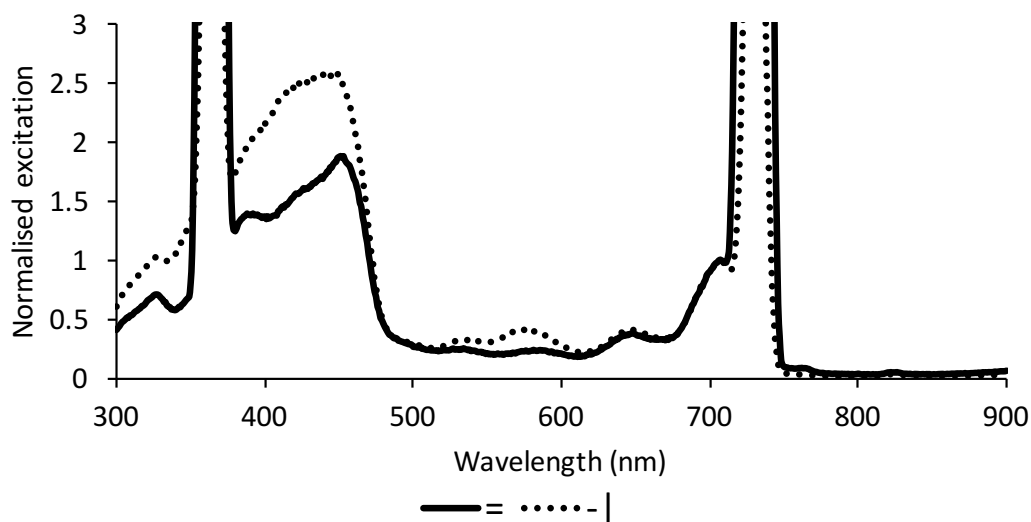


Figure S51: Excitation spectra comparison of **3c** (in glycerin mixed with 10% v/v deionized water) at different orientations of polarization filters. The solid curve depicts the spectrum when both the filters placed at either side of the sample are in same orientation (=). The dotted curve depicts the spectrum when the orientation of only the filter placed between the sample and the detector is rotated by 90° angle. The difference in the change in intensities is not constant, when the curves are normalized at 707 nm. The peaks at 730 nm and 365 nm are scattering peaks. $\lambda_{em} = 730$ nm.

7.0 Computational studies of pyropheophorbide a derivatives.

The molecular structures of compounds **1a**, **2a**, **3a** and **4a** were optimized at the DFT B3LYP/6-31G(d) level of theory using the software package Gaussian 09.⁶ Solvation in CH₂Cl₂ was applied using the polarizable continuum model (PCM).⁷ All structures are confirmed ground-state minima according to the analysis of their analytical frequencies computed at the same level, which show no imaginary frequencies. On these minima, the vertical transition energies were calculated by time-dependent density functional theory (TD-DFT) at given level of theory with the PCM solvation in CH₂Cl₂.⁷

7.1 Conformational search of donor-acceptor-substituted pyropheophorbide a

Conformational search was split into two parts concerned as the regions with most degrees of freedom. The first part was the methyl propionate group. Two conformations were optimized (Figure S52) and, expectedly, the one where the group lays at the smaller angle to the plain of the macrocycle is the lower energy conformation. This geometry was used in further studies.

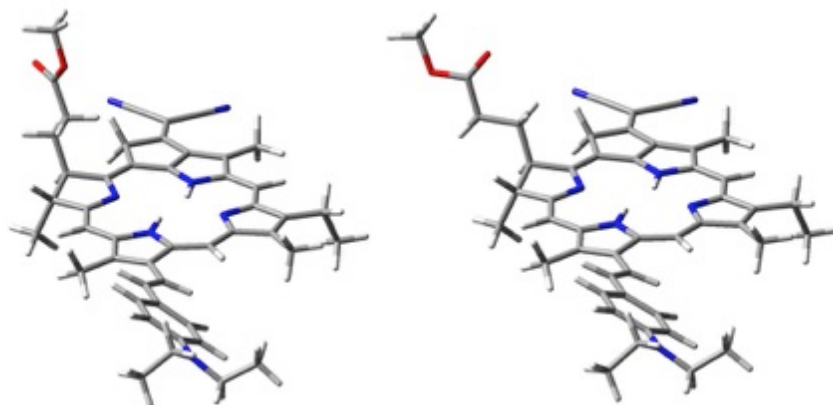


Figure S52: Two possible conformations of the methyl propionate group in **4a**.

The second part of conformational search was aiming to study the geometry of the 4-(*N,N*-diethylaminophenyl) group. Four different conformations were optimized (Figure S49). Interestingly, the lowest energy conformation changed after applying solvation in CH₂Cl₂. The lowest energy conformation in solvation was used in further studies. Additionally, the redundant coordinate scan for the rotation around the torsion angle between olefin and pyrrole was performed (Figure S50). The energy barrier for this rotation as low as 3.5 kcal/mol shows that this part of the molecule exists in a dynamic mixture of conformers at ambient conditions.

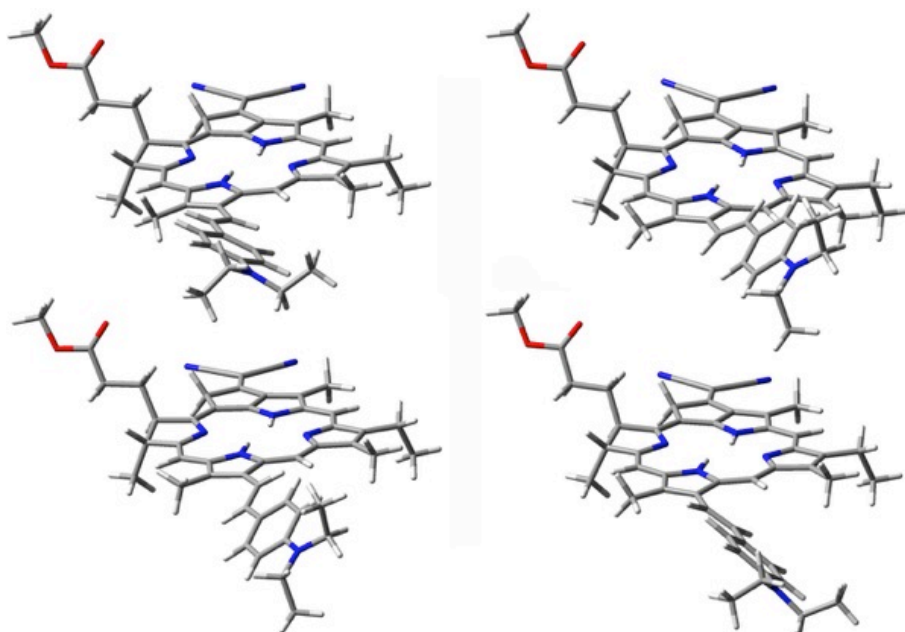


Figure S53: Four possible conformations of 4-(*N,N*-diethylaminophenyl) moiety in **4a**.

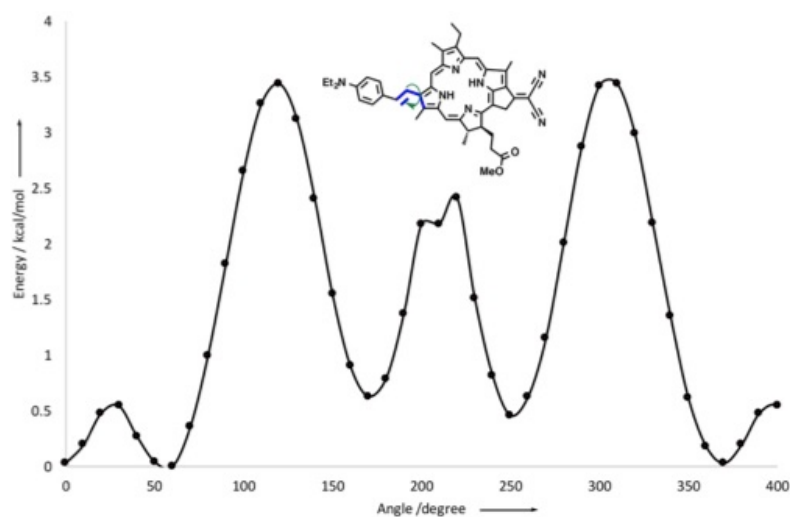


Figure S54: Rotational scan around the dihedral angle between olefin and pyrrole.

7.2 Calculated Optical and Electronic Properties of **1a**, **2a**, **3a**, and **4a**.

We performed a screening for the best method for calculating the electronic spectra of studied compounds (Figure S55). For this purpose, we compared experimental UV-Vis spectrum of **4a** to obtained theoretical results. The push-pull-substituted derivative **4a** was selected because it is known that TD-DFT methods are uncertain in describing charge transfer excited states.⁸⁻¹¹ From the methods tested, B3LYP using both 6-31G and LANL2DZ basis sets are describing best electronic transitions in this system. Additionally, LANL2DZ was used in the literature to compute electronic excitations of chlorins.¹² Hence, B3LYP/LANL2DZ was applied in this study. Electronic transition spectra were calculated for first 40 vertical transitions and the peak half-width was set to 0.1 eV.

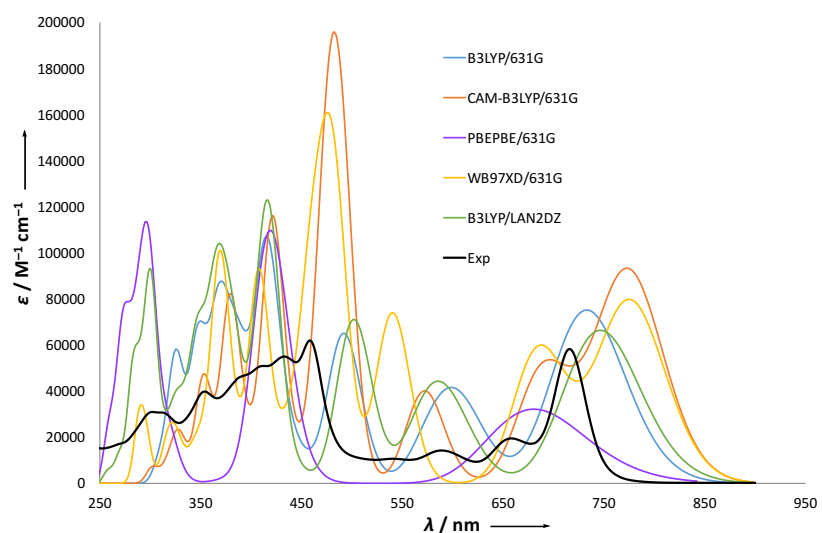


Figure S55: Comparison of UV-vis spectra obtained with different methods overlaid with the experimental one (black).

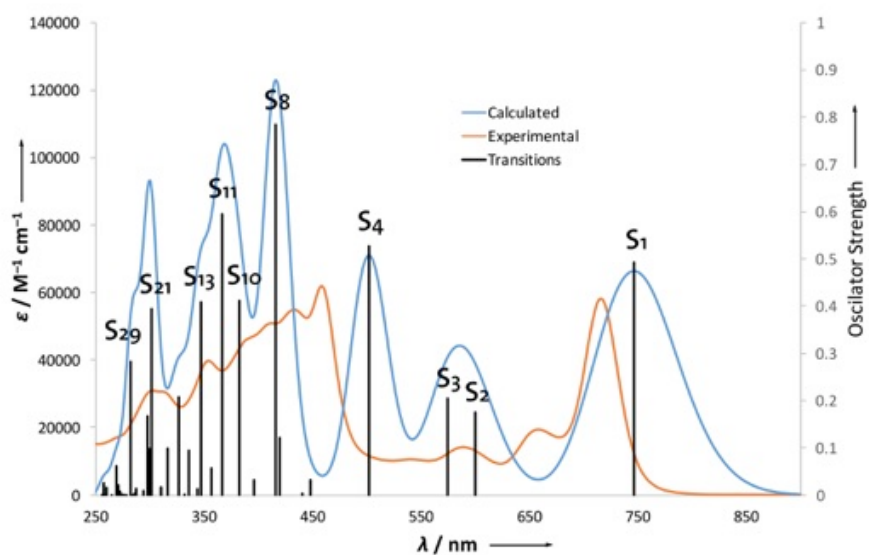


Figure S56: Comparison between the measured and calculated UV/Vis spectra of **4a**, TD-DFT B3LYP/LANL2DZ level of theory. Vertical bars represent oscillator strength of particular transitions.

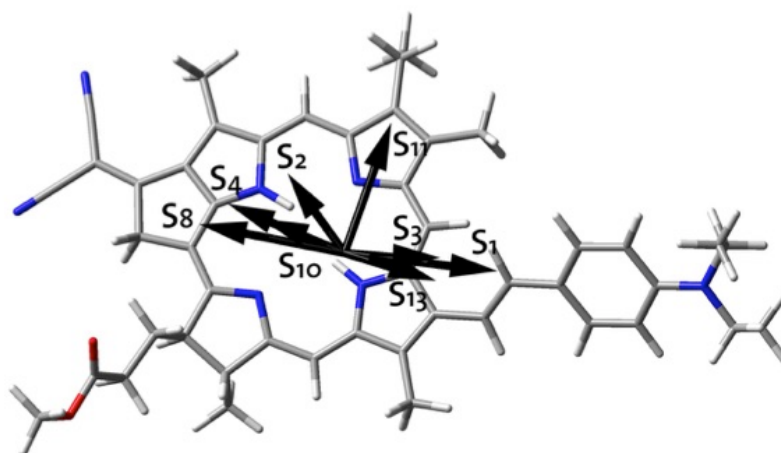


Figure S57: Visualization of calculated electric transition dipole moments for the main electronic transitions in **4a**. TD-DFT B3LYP/LANL2DZ level of theory.

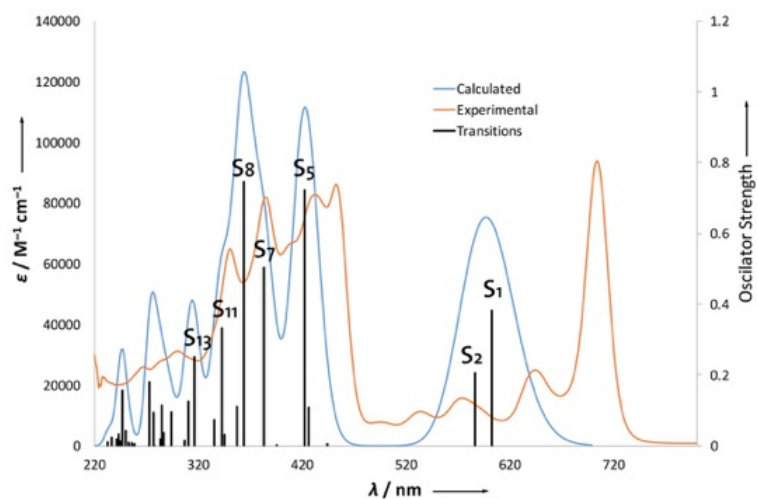


Figure S58: Comparison between the measured and calculated UV/Vis spectra of **3a**, TD-DFT B3LYP/LANL2DZ level of theory. Vertical bars represent oscillator strength of particular transitions.

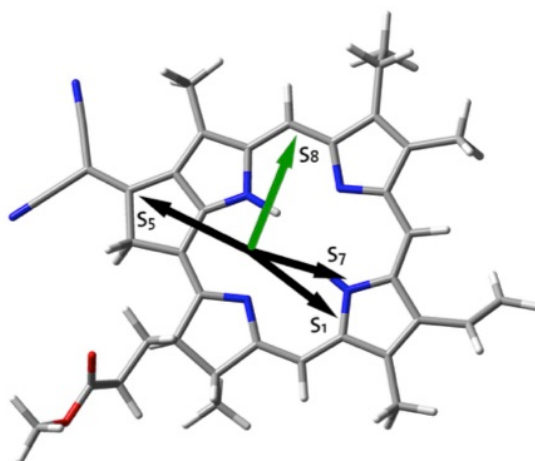


Figure S59: Visualization of calculated electric transition dipole moments for the main electronic transitions in **3a**. Colors of vectors are applied to highlight different direction of S4. TD-DFT B3LYP/LANL2DZ level of theory.

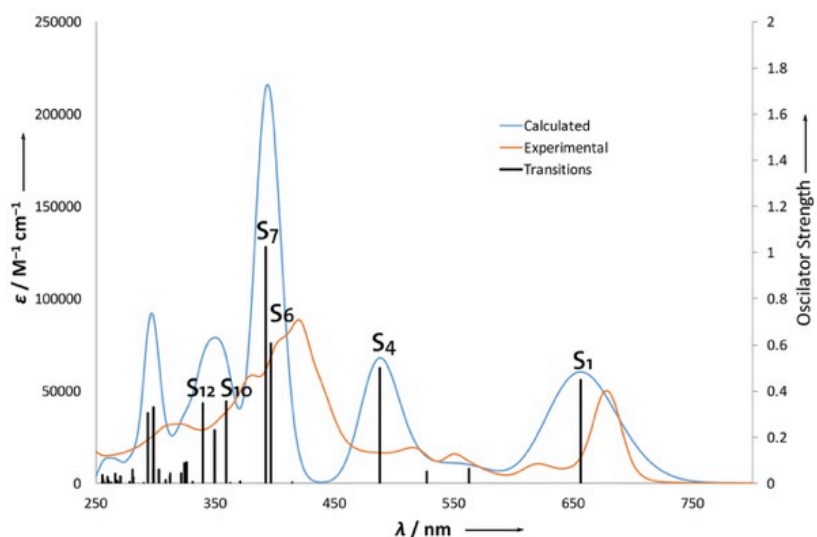


Figure S60: Comparison between the measured and calculated UV/Vis spectra of **2a**, TD-DFT B3LYP/LANL2DZ level of theory. Vertical bars represent oscillator strength of particular transitions.

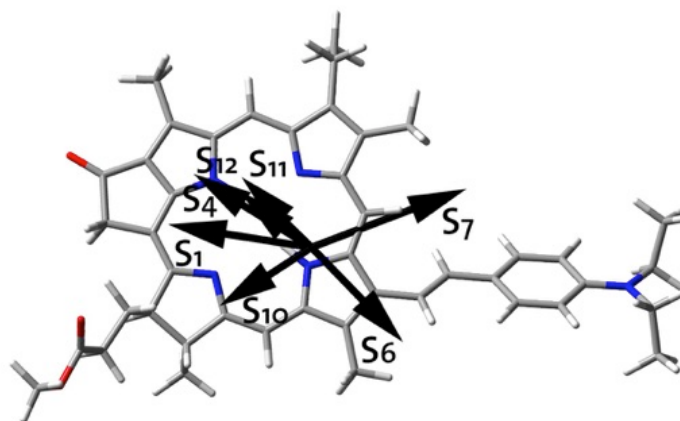


Figure S61: Visualisation of calculated electric transition dipole moments for the main electronic transitions in **2a**. TD-DFT B3LYP/LANL2DZ level of theory.

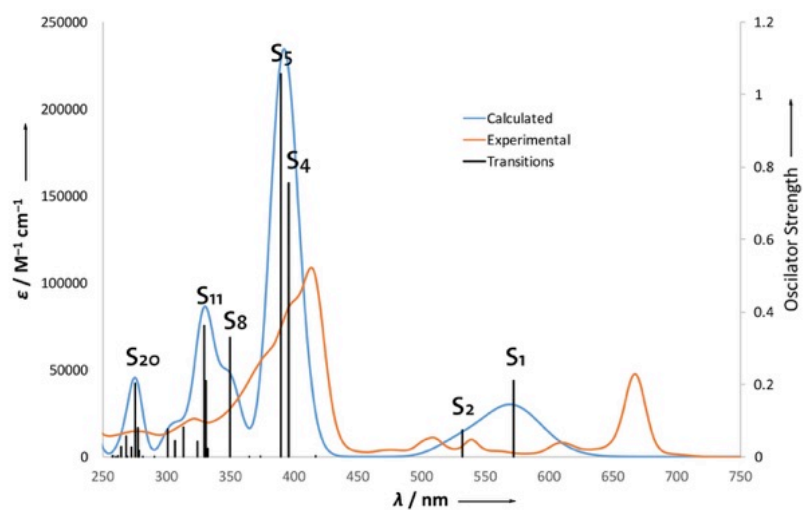


Figure S62: Comparison between the measured and calculated UV/Vis spectra of **1a**, TD-DFT B3LYP/LANL2DZ level of theory. Vertical bars represent oscillator strength of particular transitions.

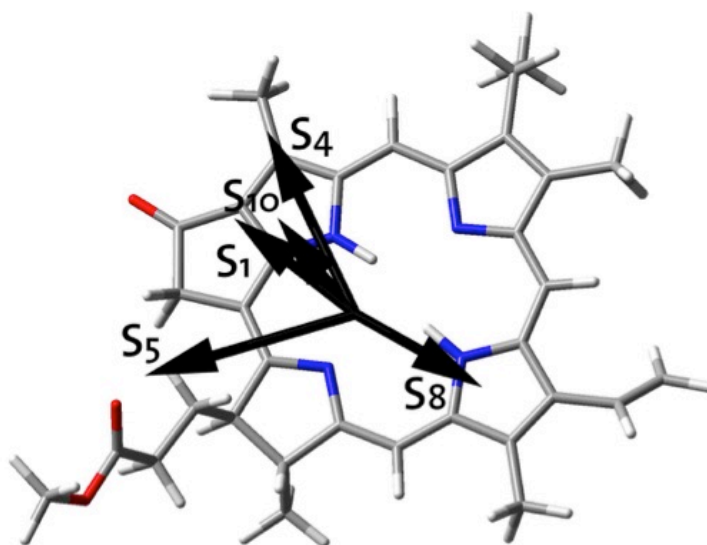
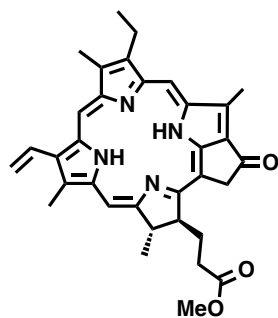


Figure S63: Visualization of calculated electric transition dipole moments for the main electronic transitions in **1a**. TD-DFT B3LYP/LANL2DZ level of theory.

Table S2. Depiction of calculated HOMOs and LUMOs and electrostatic potential (ESP) map on total density surface over optimized ground-state geometries, transition energies (E), and oscillator strengths (f) for 1a.



Experimental:

$\lambda_{\text{max}} = 413 \text{ nm}$

$\lambda_{\text{end}} = 667 \text{ nm}$

Excited state	ΔE (eV)	λ (nm)	f	assignments
1	2.17	572	0.210	H \rightarrow L
4	3.13	396	0.756	H-2 \rightarrow L+1 H-1 \rightarrow L+1 H \rightarrow L
5	3.18	390	1.057	H-2 \rightarrow L+1 H-1 \rightarrow L+1 H-2 \rightarrow L+2 H \rightarrow L H \rightarrow L+1

Orbital		E (eV)
HOMO-1		-5.25

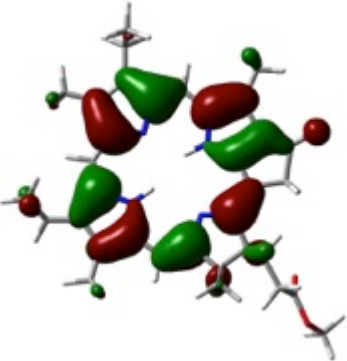
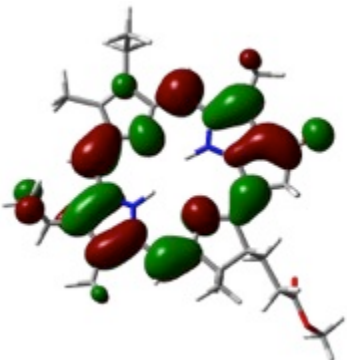
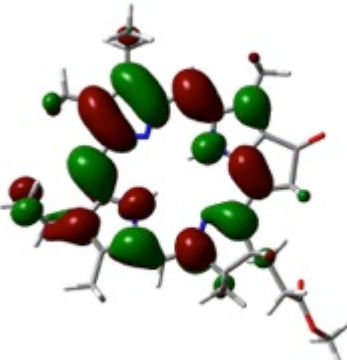
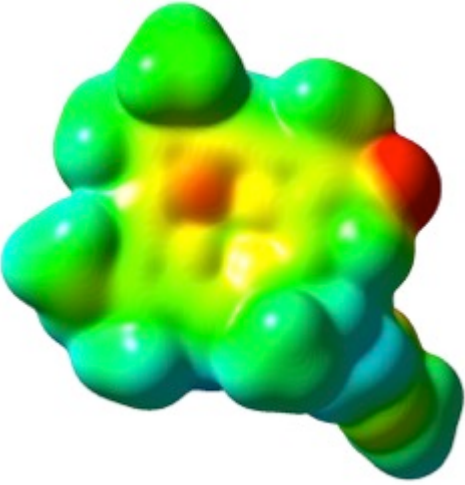
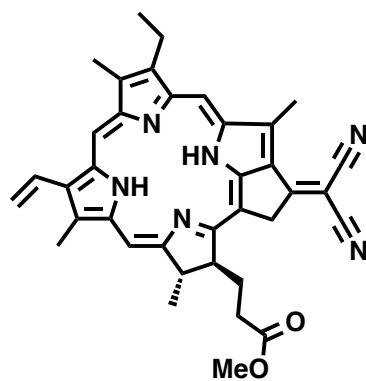
HOMO		-5.09
LUMO		-2.60
LUMO+1		-1.91
ESP		

Table S3. Depiction of calculated HOMOs and LUMOs and electrostatic potential map on total density surface over optimized ground-state geometries, transition energies (E), and oscillator strengths (f) for 3a.

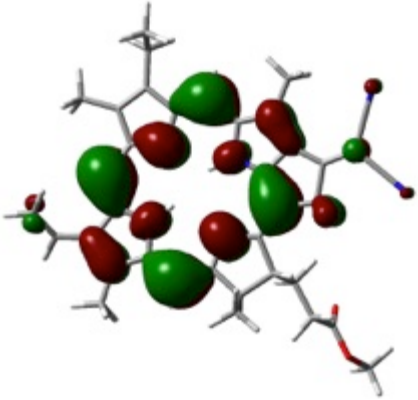
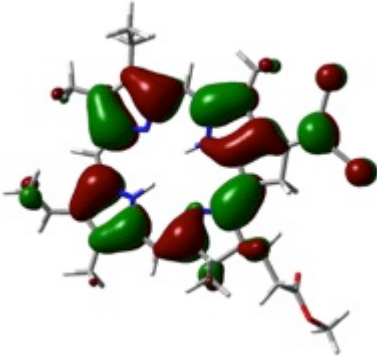
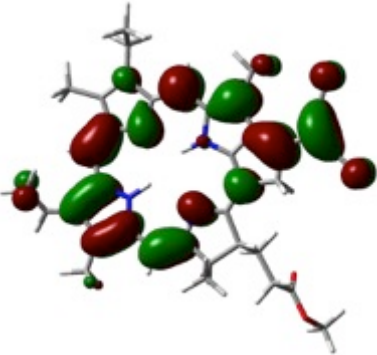


Experimental:

$$\lambda_{\max} = 453 \text{ nm}$$

$$\lambda_{\text{end}} = 704 \text{ nm}$$

Excited state	ΔE (eV)	λ (nm)	f	assignments
1	2.06	603	0.382	H-1 \rightarrow L+1 H \rightarrow L
2	3.11	586	0.205	H-1 \rightarrow L H \rightarrow L
5	2.94	422	0.722	H-1 \rightarrow L+1 H \rightarrow L+2
7	3.24	383	0.503	H-4 \rightarrow L H \rightarrow L H \rightarrow L+2
8	3.41	363	0.746	H-4 \rightarrow L H-2 \rightarrow L+1 H-1 \rightarrow L H-1 \rightarrow L+2 H \rightarrow L+1

Orbital		<i>E</i> (eV)
HOMO-1		-5.37
HOMO		-5.25
LUMO		-2.94

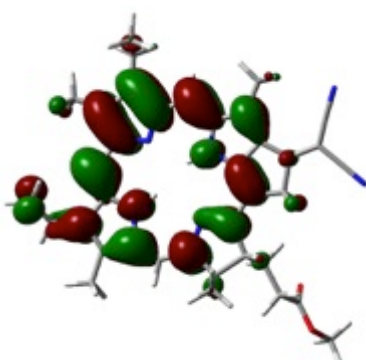
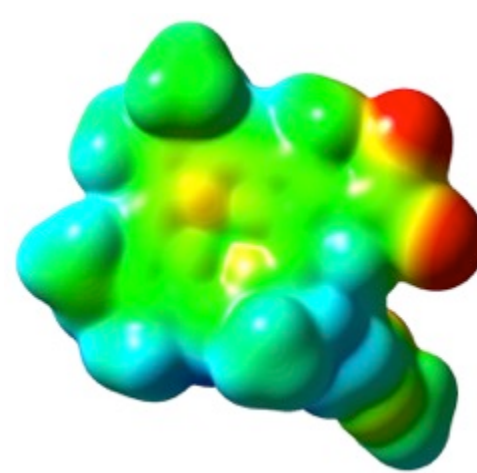
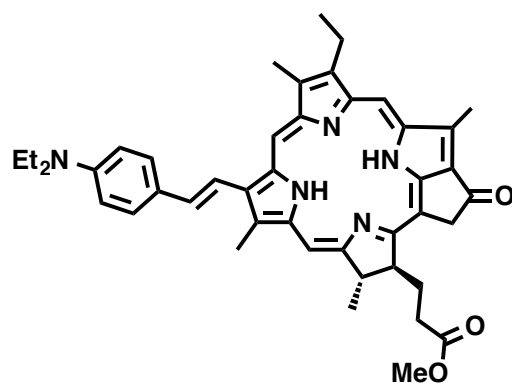
LUMO+1		-2.00
ESP		

Table S4. Depiction of calculated HOMOs and LUMOs and electrostatic potential map on total density surface over optimized ground-state geometries, transition energies (E), and oscillator strengths (f) for 2a.



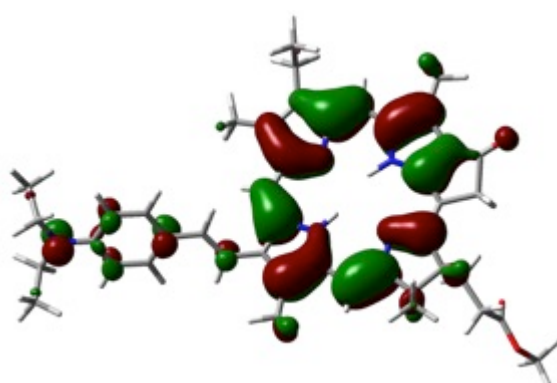
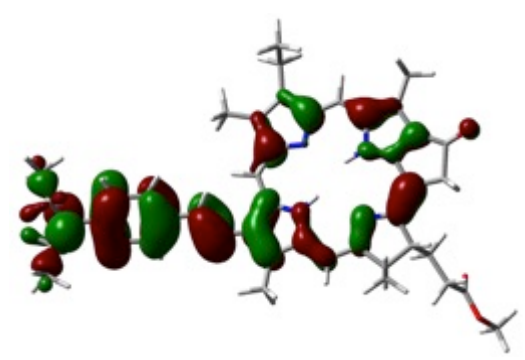
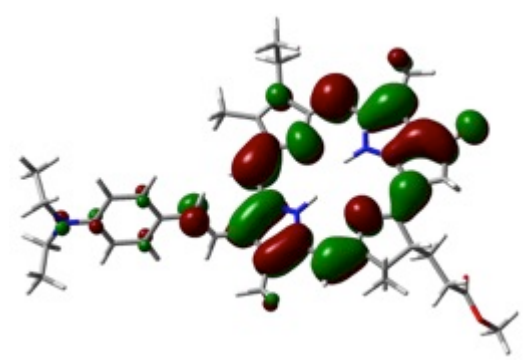
Experimental:

$$\lambda_{\max} = 419 \text{ nm}$$

$$\lambda_{\text{end}} = 678 \text{ nm}$$

Excited state	ΔE (eV)	λ (nm)	f	assignments
1	1.890	656	0.447	H \rightarrow L
4	2.54	488	0.500	H-2 \rightarrow L+1 H-1 \rightarrow L H \rightarrow L+1
6	3.13	396	0.606	H-3 \rightarrow L H-3 \rightarrow L+1

				H-2 → L+1
7	3.16	392	1.024	H-2 → L H-1 → L+1

Orbital		<i>E</i> (eV)
HOMO-1		-5.09
HOMO		-4.79
LUMO		-2.54

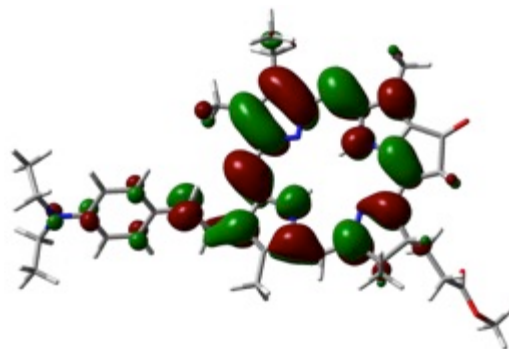
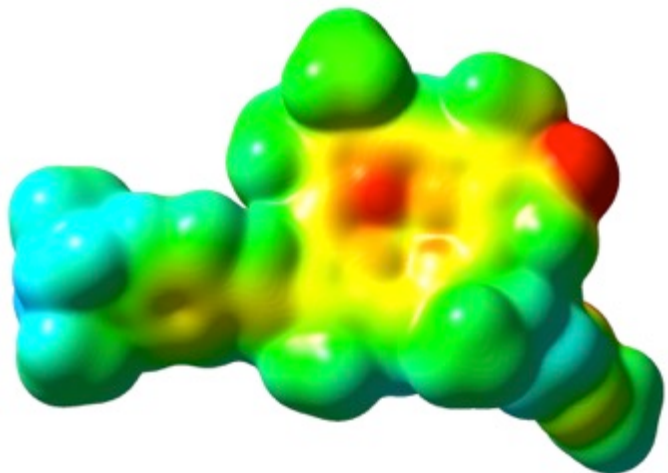
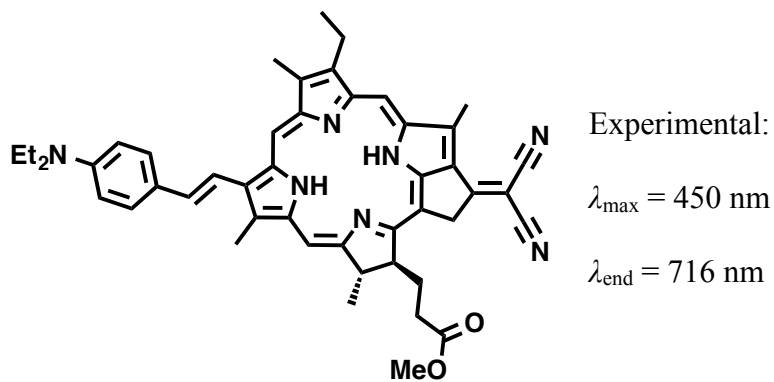
LUMO+1		-1.88
ESP		

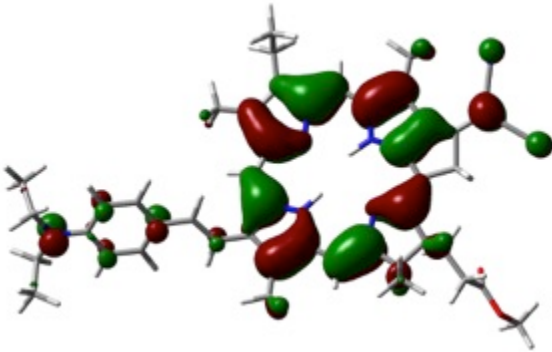
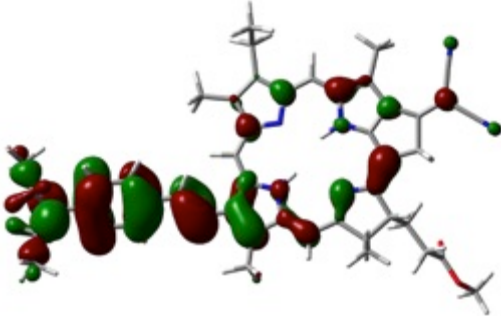
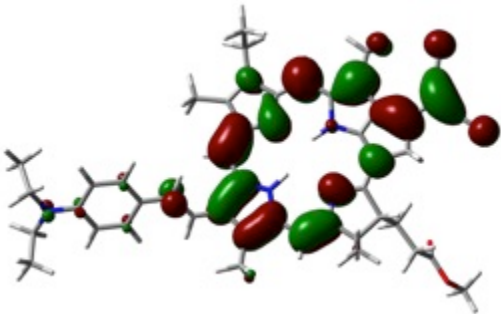
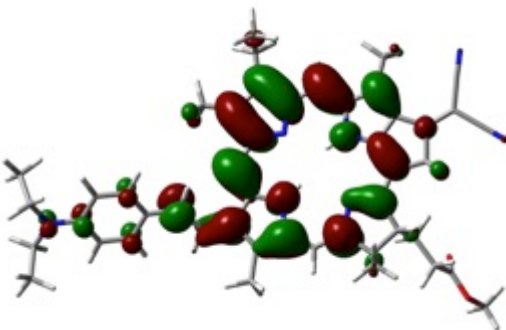
Table S5. Depiction of calculated HOMOs and LUMOs and electrostatic potential map on total density surface over optimized ground-state geometries, transition energies (E), and oscillator strengths (f) for 4a.

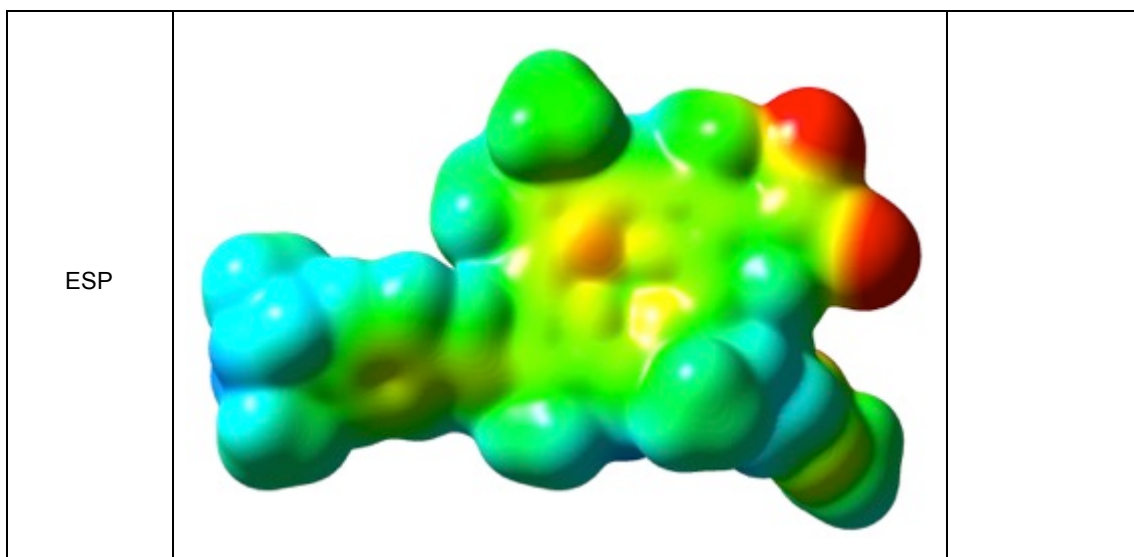


Excited state	ΔE (eV)	λ (nm)	f	assignments
1	1.66	746	0.492	H \rightarrow L
2	2.07	600	0.175	H-2 \rightarrow L H-1 \rightarrow L
3	2.15	574	0.205	H-2 \rightarrow L H-1 \rightarrow L+1

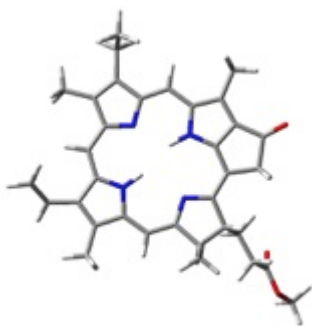
4	2.47	502	0.527	H-1 → L H → L+1
7	2.95	420	0.121	H-2 → L+1 H → L+2
8	2.98	415	0.784	H-2 → L+1 H-2 → L+2 H-1 → L H-1 → L+1
10	3.24	382	0.412	H-3 → L+1 H-2 → L+1 H-1 → L+2
11	3.38	366	0.595	H-6 → L H-2 → L H-2 → L+1 H-2 → L+2 H-1 → L+2 H-1 → L+3
13	3.57	347	0.408	H-3 → L+1 H → L+3
17	3.80	326	0.208	H-6 → L H-2 → L+1 H-1 → L+2 H → L+3 H → L+5
21	4.11	302	0.394	H-3 → L+2 H-2 → L+3 H-1 → L+1 H-1 → L+3

Orbital		<i>E</i> (eV)
---------	--	---------------

HOMO-1		-5.24
HOMO		-4.86
LUMO		-2.89
LUMO+1		-1.98



7.3 Cartesian Coordinates and Structural Parameters of Compounds

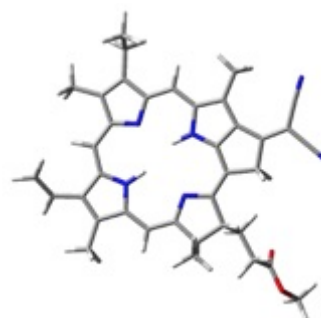


B3LYP/6-31G(d)

Atom type, (x,y,z) coordinates:

Symbol	X	Y	Z
C	3.055109	1.718531	-1.200871
C	3.424156	0.232971	-0.944436
C	3.243532	2.15473	-2.664622
C	4.333225	0.034939	0.289563
C	5.761833	0.532672	0.056301
C	6.661927	0.323393	1.258029
O	7.882962	0.854095	1.043958
O	6.351121	-0.24814	2.284574
C	8.832723	0.699997	2.116293
H	3.643622	2.388672	-0.562079
H	3.922512	-0.207344	-1.81835
H	2.673328	1.508252	-3.341743
H	2.905786	3.185323	-2.817949
H	3.894495	0.555144	1.149844
H	4.370527	-1.02445	0.561263
H	6.219989	0.013403	-0.796456
H	5.785936	1.598785	-0.199755
H	9.747215	1.179165	1.767402
H	8.467882	1.187585	3.023706
H	9.009938	-0.35867	2.321427
C	-4.83769	4.996195	-0.163111
C	-3.560394	5.102882	0.231392
C	-2.501245	4.106102	0.060355
C	-2.640729	2.661607	0.148742
C	-1.172696	4.384915	-0.217127
C	-0.473803	3.12998	-0.341723
N	-1.392922	2.137156	-0.11838
C	-3.77187	1.935291	0.487934
C	-3.940688	0.535746	0.55353
N	-2.978829	-0.383887	0.295449
C	-5.215432	-0.103264	0.890642
C	-4.994193	-1.453111	0.817993
C	-3.586418	-1.608532	0.447748
C	-2.932757	-2.834766	0.284376
C	-1.579312	-2.99555	-0.030728
N	-0.737444	-1.897554	-0.203745
C	-0.800129	-4.18533	-0.213349
C	0.496965	-3.743094	-0.485435
N	1.066924	0.534062	-0.587644
C	1.586307	1.756542	-0.779655
C	0.877507	2.955845	-0.65077
C	2.049245	-0.397412	-0.743438
C	0.509266	-2.324712	-0.46807
C	1.775315	-1.753517	-0.703769
C	2.728637	-2.927437	-0.918078
C	1.853034	-4.207258	-0.775915
C	-1.290892	-5.597387	-0.123144
C	-6.485015	0.620405	1.229318
C	-5.973523	-2.574163	1.031348

C	-6.58685	-3.11038	-0.277333
C	-0.533416	5.726648	-0.411957
H	-5.217423	4.12494	-0.688178
H	-3.248692	6.035653	0.700224
H	-1.171285	1.149989	-0.114143
H	-4.642681	2.531521	0.733009
H	-3.51258	-3.741787	0.421627
H	-1.094719	-0.949857	-0.113124
H	1.439979	3.870104	-0.81244
H	3.540398	-2.974934	-0.181539
H	3.205115	-2.921169	-1.90725
H	-1.724576	-5.810938	0.861479
H	-2.068579	-5.802029	-0.869268
H	-0.466072	-6.293878	-0.291185
H	-6.343916	1.321111	2.061981
H	-6.858926	1.206284	0.379192
H	-7.277158	-0.077085	1.517182
H	-5.4846	-3.400664	1.563059
H	-6.781753	-2.232891	1.688876
H	-7.285053	-3.929837	-0.071516
H	-7.133256	-2.320398	-0.804356
H	-5.811061	-3.486275	-0.953589
H	-1.237504	6.538069	-0.212798
H	0.329407	5.859906	0.251655
H	-0.17159	5.851832	-1.440472
H	4.300352	2.098096	-2.949224
O	2.271087	-5.351766	-0.891867
H	-5.540887	5.805571	0.010226



B3LYP/6-31G(d)

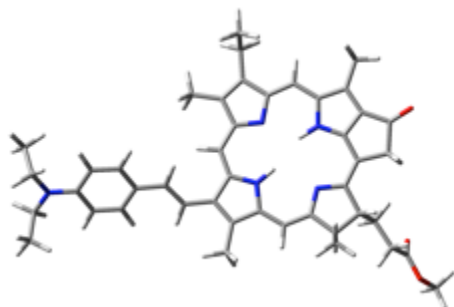
Atom type, (x,y,z) coordinates:

Symbol	X	Y	Z
C	3.055109	1.718531	-1.200871
C	3.424156	0.232971	-0.944436
C	3.243532	2.15473	-2.664622
C	4.333225	0.034939	0.289563
C	5.761833	0.532672	0.056301
C	6.661927	0.323393	1.258029
O	7.882962	0.854095	1.043958
O	6.351121	-0.24814	2.284574
C	8.832723	0.699997	2.116293
H	3.643622	2.388672	-0.562079
H	3.922512	-0.207344	-1.81835
H	2.673328	1.508252	-3.341743
H	2.905786	3.185323	-2.817949
H	3.894495	0.555144	1.149844
H	4.370527	-1.02445	0.561263
H	6.219989	0.013403	-0.796456
H	5.785936	1.598785	-0.199755
H	9.747215	1.179165	1.767402
H	8.467882	1.187585	3.023706
H	9.009938	-0.35867	2.321427
C	-4.83769	4.996195	-0.163111

C	-3.560394	5.102882	0.231392
C	-2.501245	4.106102	0.060355
C	-2.640729	2.661607	0.148742
C	-1.172696	4.384915	-0.217127
C	-0.473803	3.12998	-0.341723
N	-1.392922	2.137156	-0.11838
C	-3.77187	1.935291	0.487934
C	-3.940688	0.535746	0.55353
N	-2.978829	-0.383887	0.295449
C	-5.215432	-0.103264	0.890642
C	-4.994193	-1.453111	0.817993
C	-3.586418	-1.608532	0.447748
C	-2.932757	-2.834766	0.284376
C	-1.579312	-2.99555	-0.030728
N	-0.737444	-1.897554	-0.203745
C	-0.800129	-4.18533	-0.213349
C	0.496965	-3.743094	-0.485435
N	1.066924	0.534062	-0.587644
C	1.586307	1.756542	-0.779655
C	0.877507	2.955845	-0.65077
C	2.049245	-0.397412	-0.743438
C	0.509266	-2.324712	-0.46807
C	1.775315	-1.753517	-0.703769
C	2.728637	-2.927437	-0.918078
C	1.853034	-4.207258	-0.775915
C	-1.290892	-5.597387	-0.123144
C	-6.485015	0.620405	1.229318
C	-5.973523	-2.574163	1.031348
C	-6.58685	-3.11038	-0.277333
C	-0.533416	5.726648	-0.411957
H	-5.217423	4.12494	-0.688178
H	-3.248692	6.035653	0.700224
H	-1.171285	1.149989	-0.114143
H	-4.642681	2.531521	0.733009
H	-3.51258	-3.741787	0.421627
H	-1.094719	-0.949857	-0.113124
H	1.439979	3.870104	-0.81244
H	3.540398	-2.974934	-0.181539
H	3.205115	-2.921169	-1.90725
H	-1.724576	-5.810938	0.861479
H	-2.068579	-5.802029	-0.869268
H	-0.466072	-6.293878	-0.291185
H	-6.343916	1.321111	2.061981
H	-6.858926	1.206284	0.379192
H	-7.277158	-0.077085	1.517182
H	-5.4846	-3.400664	1.563059
H	-6.781753	-2.232891	1.688876
H	-7.285053	-3.929837	-0.071516
H	-7.133256	-2.320398	-0.804356
H	-5.811061	-3.486275	-0.953589
H	-1.237504	6.538069	-0.212798
H	0.329407	5.859906	0.251655
H	-0.17159	5.851832	-1.440472
H	4.300352	2.098096	-2.949224
O	2.271087	-5.351766	-0.891867
H	-5.540887	5.805571	0.010226

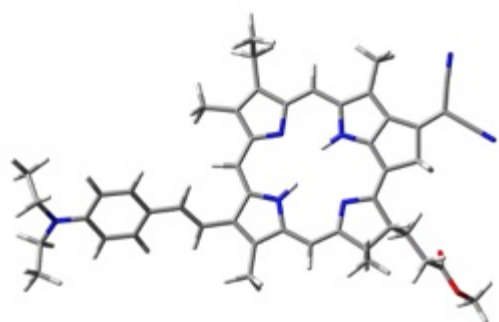
Atom type, (x,y,z) coordinates:

Symbol	X	Y	Z
C	-3.949173	-2.843273	-1.247722
C	-5.124708	-1.872745	-0.956803
C	-3.86512	-3.280266	-2.720953
C	-5.950874	-2.270657	0.286972
C	-6.806524	-3.518328	0.053957
C	-7.640563	-3.896217	1.262032
O	-8.306099	-5.048971	1.045084
O	-7.721226	-3.260558	2.294754
C	-9.150761	-5.501395	2.120797
H	-4.014065	-3.742932	-0.623576
H	-5.802771	-1.8038	-1.817823
H	-3.79442	-2.409701	-3.383355
H	-2.987472	-3.911246	-2.898147
H	-5.273521	-2.437308	1.13349
H	-6.6066	-1.445012	0.579891
H	-7.494088	-3.365902	-0.789153
H	-6.195774	-4.388117	-0.216963
H	-9.595021	-6.433036	1.771027
H	-8.56065	-5.674748	3.024053
H	-9.928489	-4.763552	2.333212
C	4.363865	-0.791182	-0.304898
C	3.402767	-1.670317	0.071188
C	1.965497	-1.489496	-0.068956
C	1.217627	-0.243259	0.055411
C	1.048667	-2.497041	-0.341217
C	-0.257069	-1.89945	-0.431767
N	-0.102435	-0.556272	-0.197054
C	1.695824	1.003455	0.423706
C	0.998244	2.227661	0.53033
N	-0.32318	2.402578	0.289175
C	1.647174	3.489095	0.896755
C	0.667058	4.445629	0.858185
C	-0.561	3.745201	0.480416
C	-1.816363	4.34635	0.345494
C	-3.004926	3.679431	0.02671
N	-3.031905	2.300282	-0.179245
C	-4.339848	4.176981	-0.125178
C	-5.125259	3.056567	-0.412043
N	-3.044507	-0.718741	-0.616506
C	-2.738662	-2.007662	-0.831628
C	-1.455528	-2.554816	-0.728541
C	-4.390609	-0.550798	-0.750061
C	-4.292343	1.908869	-0.433297
C	-4.975256	0.701328	-0.681867
C	-6.442448	1.084189	-0.865652
C	-6.496032	2.630609	-0.687937
C	-4.782559	5.601755	0.006245
C	3.101289	3.652065	1.227451
C	0.79203	5.923681	1.106273
C	0.961988	6.749145	-0.184423
C	1.323201	-3.955099	-0.557052
H	4.054394	0.130623	-0.794802
H	3.708506	-2.635463	0.471075
H	-0.866624	0.105861	-0.164813
H	2.751665	1.038538	0.662716
H	-1.887793	5.416563	0.51156
H	-2.180379	1.74852	-0.112406
H	-1.370613	-3.623156	-0.901294
H	-7.113115	0.623711	-0.129483
H	-6.83684	0.818756	-1.855489
H	-4.560754	6.001578	1.003392
H	-4.277051	6.249534	-0.720501
H	-5.85966	5.678211	-0.160217
H	3.415601	2.969155	2.026799
H	3.742587	3.44415	0.36056
H	3.3231	4.670717	1.559324
H	-0.089343	6.287259	1.650281



B3LYP/6-31G(d)

H	1.648358	6.113265	1.764379
H	1.042644	7.817786	0.045779
H	1.866071	6.446951	-0.72456
H	0.109623	6.609724	-0.85855
H	2.396182	-4.161428	-0.563342
H	0.867263	-4.573719	0.226704
H	0.91738	-4.301141	-1.515654
H	-4.756835	-3.851373	-3.003675
C	5.806917	-0.951496	-0.174773
C	6.667523	-0.014756	-0.779576
C	8.049188	-0.112309	-0.702061
C	8.671598	-1.17627	-0.000132
C	7.805393	-2.119041	0.617658
C	6.427759	-2.001842	0.532363
N	10.04395	-1.289562	0.083622
C	10.938107	-0.402669	-0.661367
C	11.294001	0.890363	0.083191
C	10.687857	-2.305388	0.917204
C	10.908792	-3.64544	0.204165
H	6.236055	0.821177	-1.326604
H	8.64681	0.656339	-1.17685
H	8.214658	-2.961025	1.162701
H	5.820237	-2.750379	1.033937
H	11.852878	-0.966536	-0.874041
H	10.493228	-0.174758	-1.635224
H	10.401271	1.488961	0.291111
H	11.982014	1.497009	-0.516977
H	11.782289	0.668491	1.038713
H	10.103836	-2.448399	1.831785
H	11.65254	-1.898316	1.239091
H	11.531102	-3.513909	-0.688075
H	9.959237	-4.091378	-0.109267
H	11.416318	-4.35176	0.871321
O	-7.514914	3.304558	-0.770287

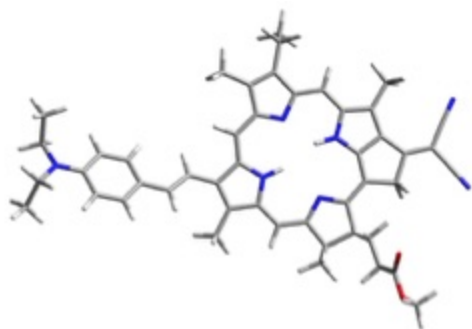


B3LYP/6-31G(d)

Atom type, (x,y,z) coordinates:

\ Symbol	X	Y	Z
C	3.055109	1.718531	-1.200871
C	3.424156	0.232971	-0.944436
C	3.243532	2.15473	-2.664622
C	4.333225	0.034939	0.289563
C	5.761833	0.532672	0.056301
C	6.661927	0.323393	1.258029
O	7.882962	0.854095	1.043958
O	6.351121	-0.24814	2.284574
C	8.832723	0.699997	2.116293
H	3.643622	2.388672	-0.562079
H	3.922512	-0.207344	-1.81835
H	2.673328	1.508252	-3.341743
H	2.905786	3.185323	-2.817949
H	3.894495	0.555144	1.149844
H	4.370527	-1.02445	0.561263
H	6.219989	0.013403	-0.796456
H	5.785936	1.598785	-0.199755
H	9.747215	1.179165	1.767402
H	8.467882	1.187585	3.023706

H	9.009938	-0.35867	2.321427
C	-4.83769	4.996195	-0.163111
C	-3.560394	5.102882	0.231392
C	-2.501245	4.106102	0.060355
C	-2.640729	2.661607	0.148742
C	-1.172696	4.384915	-0.217127
C	-0.473803	3.12998	-0.341723
N	-1.392922	2.137156	-0.11838
C	-3.77187	1.935291	0.487934
C	-3.940688	0.535746	0.55353
N	-2.978829	-0.383887	0.295449
C	-5.215432	-0.103264	0.890642
C	-4.994193	-1.453111	0.817993
C	-3.586418	-1.608532	0.447748
C	-2.932757	-2.834766	0.284376
C	-1.579312	-2.99555	-0.030728
N	-0.737444	-1.897554	-0.203745
C	-0.800129	-4.18533	-0.213349
C	0.496965	-3.743094	-0.485435
N	1.066924	0.534062	-0.587644
C	1.586307	1.756542	-0.779655
C	0.877507	2.955845	-0.65077
C	2.049245	-0.397412	-0.743438
C	0.509266	-2.324712	-0.46807
C	1.775315	-1.753517	-0.703769
C	2.728637	-2.927437	-0.918078
C	1.853034	-4.207258	-0.775915
C	-1.290892	-5.597387	-0.123144
C	-6.485015	0.620405	1.229318
C	-5.973523	-2.574163	1.031348
C	-6.58685	-3.11038	-0.277333
C	-0.533416	5.726648	-0.411957
H	-5.217423	4.12494	-0.688178
H	-3.248692	6.035653	0.700224
H	-1.171285	1.149989	-0.114143
H	-4.642681	2.531521	0.733009
H	-3.51258	-3.741787	0.421627
H	-1.094719	-0.949857	-0.113124
H	1.439979	3.870104	-0.81244
H	3.540398	-2.974934	-0.181539
H	3.205115	-2.921169	-1.90725
H	-1.724576	-5.810938	0.861479
H	-2.068579	-5.802029	-0.869268
H	-0.466072	-6.293878	-0.291185
H	-6.343916	1.321111	2.061981
H	-6.858926	1.206284	0.379192
H	-7.277158	-0.077085	1.517182
H	-5.4846	-3.400664	1.563059
H	-6.781753	-2.232891	1.688876
H	-7.285053	-3.929837	-0.071516
H	-7.133256	-2.320398	-0.804356
H	-5.811061	-3.486275	-0.953589
H	-1.237504	6.538069	-0.212798
H	0.329407	5.859906	0.251655
H	-0.17159	5.851832	-1.440472
H	4.300352	2.098096	-2.949224
O	2.271087	-5.351766	-0.891867
H	-5.540887	5.805571	0.010226

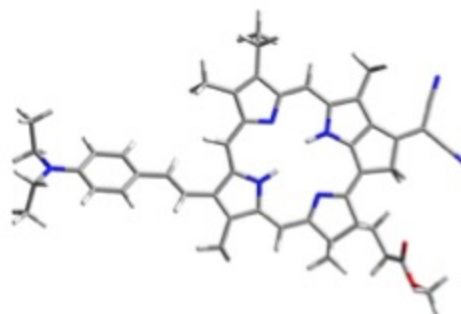


B3LYP/6-31G(d)

Atom type, (x,y,z) coordinates:

Symbol	X	Y	Z
C	-2.812143	-3.271129	-1.343935
C	-4.131673	-2.601536	-0.878023
C	-2.78667	-3.596898	-2.848004
C	-4.710928	-3.227611	0.411303
C	-5.298064	-4.62196	0.178955
C	-5.877662	-5.232509	1.439735
O	-6.333666	-6.47943	1.205406
O	-5.939153	-4.689833	2.525424
C	-6.923277	-7.155644	2.33279
H	-2.616059	-4.195112	-0.786399
H	-4.897867	-2.646279	-1.663293
H	-2.978722	-2.698609	-3.446054
H	-1.814655	-4.002044	-3.149022
H	-3.924808	-3.277245	1.17445
H	-5.49297	-2.581705	0.822592
H	-6.0978	-4.588082	-0.572955
H	-4.54955	-5.319237	-0.21696
H	-7.237279	-8.129364	1.957479
H	-6.190188	-7.273153	3.134734
H	-7.782719	-6.594937	2.708282
C	5.129667	-1.384255	-0.119912
C	4.167446	-0.461515	-0.378788
C	2.743055	-0.711851	-0.466887
C	1.740567	0.32899	-0.24537
C	2.061978	-1.880618	-0.789587
C	0.649815	-1.590606	-0.755075
N	0.511618	-0.26453	-0.429131
C	1.969846	1.649801	0.089813
C	1.035429	2.696675	0.278428
N	-0.305635	2.576714	0.180076
C	1.432987	4.073444	0.595173
C	0.272646	4.793243	0.680614
C	-0.80992	3.840513	0.41914
C	-2.165143	4.158811	0.42164
C	-3.216633	3.25241	0.193463
N	-2.95295	1.905812	-0.05629
C	-4.62498	3.452146	0.176332
C	-5.186837	2.176876	-0.08696
N	-2.324475	-1.03375	-0.646923
C	-1.774075	-2.21267	-0.974778
C	-0.399497	-2.474579	-1.015475
C	-3.681786	-1.161347	-0.653663
C	-4.107597	1.248442	-0.218762
C	-4.512651	-0.073194	-0.464903
C	-6.034752	-0.02676	-0.507154
C	-6.403784	1.444722	-0.272652
C	-7.729523	1.842839	-0.271704
C	-5.302085	4.767765	0.40499
C	2.844774	4.547832	0.771313
C	0.101368	6.263496	0.944082
C	-0.028902	7.10445	-0.341275
C	2.640392	-3.209435	-1.170417
H	4.822272	-2.406796	0.086623
H	4.470481	0.57421	-0.51543

H	-0.381649	0.200307	-0.329298
H	3.011152	1.92326	0.217538
H	-2.438724	5.188702	0.621952
H	-1.996157	1.558196	-0.081118
H	-0.111476	-3.488667	-1.270806
H	-6.503541	-0.652946	0.262743
H	-6.439071	-0.372779	-1.467776
H	-4.575618	5.559973	0.601464
H	-5.898646	5.066472	-0.463085
H	-5.98664	4.720567	1.258109
H	3.379451	3.959419	1.527652
H	3.419319	4.467901	-0.160936
H	2.876992	5.594985	1.085836
H	-0.782323	6.429919	1.573238
H	0.955219	6.631519	1.525126
H	-0.156165	8.165574	-0.098455
H	0.864665	7.001804	-0.96671
H	-0.891143	6.786252	-0.937725
H	3.587156	-3.079322	-1.705194
H	2.846298	-3.840602	-0.295476
H	1.962913	-3.769444	-1.822004
H	-3.554666	-4.339466	-3.091976
C	-8.18359	3.178706	-0.074975
C	-8.760983	0.87969	-0.486809
N	-9.599277	0.088584	-0.663181
N	-8.610734	4.252765	0.077047
C	6.565592	-1.162604	-0.040672
C	7.408861	-2.221424	0.351929
C	8.784516	-2.081618	0.452575
C	9.419658	-0.845991	0.163419
C	8.5718	0.223593	-0.236816
C	7.200265	0.06278	-0.335662
N	10.785236	-0.689133	0.262632
C	11.645587	-1.743924	0.800865
C	12.12697	-2.750105	-0.25189
C	11.457281	0.540725	-0.159943
C	11.54278	1.609458	0.936825
H	6.96724	-3.189216	0.580721
H	9.369894	-2.946005	0.741229
H	8.990539	1.197297	-0.460345
H	6.608567	0.91805	-0.650638
H	12.509729	-1.254867	1.263306
H	11.122373	-2.258419	1.6131
H	11.284634	-3.268562	-0.721144
H	12.777823	-3.500884	0.210892
H	12.696616	-2.247018	-1.041193
H	10.957986	0.940561	-1.04805
H	12.46677	0.26467	-0.482942
H	12.082602	1.228689	1.810954
H	10.54671	1.923547	1.265323
H	12.076364	2.492015	0.565629



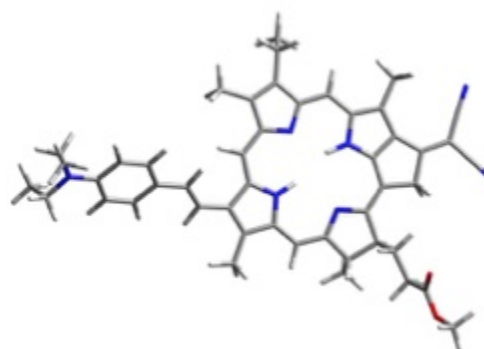
B3LYP/6-31G(d)

Atom type, (x,y,z) coordinates:

Symbol	X	Y	Z
C	-3.212039	-3.28206	-1.207298
C	-4.44372	-2.400603	-0.871272

C	-3.127548	-3.677565	-2.692498
C	-5.208359	-2.875935	0.385008
C	-5.984411	-4.173737	0.148567
C	-6.751104	-4.630782	1.373985
O	-7.36863	-5.806856	1.143791
O	-6.818683	-4.033266	2.430132
C	-8.144155	-6.336291	2.236543
H	-3.201333	-4.198077	-0.603954
H	-5.145688	-2.36363	-1.714689
H	-3.13332	-2.789162	-3.334591
H	-2.211003	-4.239574	-2.901395
H	-4.499309	-3.011812	1.210622
H	-5.910511	-2.102721	0.711916
H	-6.706296	-4.052514	-0.670257
H	-5.324399	-4.994069	-0.158875
H	-8.559083	-7.275594	1.871664
H	-7.507918	-6.51194	3.107466
H	-8.945385	-5.644356	2.507716
C	4.95166	-0.671373	-0.338587
C	4.058103	-1.626131	0.021815
C	2.611355	-1.546139	-0.098159
C	1.7756	-0.356218	0.057886
C	1.765398	-2.611117	-0.372544
C	0.417677	-2.105875	-0.435621
N	0.478329	-0.758846	-0.182728
C	2.168239	0.912118	0.441899
C	1.38276	2.082387	0.582744
N	0.051869	2.165735	0.370371
C	1.951784	3.381018	0.961453
C	0.908997	4.266703	0.961609
C	-0.277143	3.488802	0.593461
C	-1.565574	4.007217	0.495365
C	-2.721526	3.270447	0.180031
N	-2.648873	1.89714	-0.052637
C	-4.078139	3.681828	0.059208
C	-4.807128	2.504443	-0.246121
N	-2.438461	-1.114308	-0.549713
C	-2.053628	-2.375761	-0.79524
C	-0.734411	-2.839102	-0.724278
C	-3.795527	-1.036366	-0.656067
C	-3.875834	1.420942	-0.2966
C	-4.460676	0.171106	-0.556178
C	-5.950584	0.448059	-0.711497
C	-6.105331	1.962858	-0.516447
C	-7.350579	2.558405	-0.618271
C	-4.562332	5.086989	0.240378
C	3.398292	3.63555	1.264451
C	0.935263	5.744608	1.236997
C	0.999272	6.60366	-0.041408
C	2.136427	-4.042884	-0.615301
H	4.574069	0.240788	-0.79754
H	4.435383	-2.578231	0.390089
H	-0.332511	-0.156143	-0.127888
H	3.22192	1.021129	0.666486
H	-1.695913	5.066197	0.688585
H	-1.758539	1.405841	-0.008317
H	-0.580974	-3.895998	-0.917453
H	-6.563992	-0.084047	0.026656
H	-6.333273	0.149421	-1.69659
H	-3.742838	5.758693	0.506987
H	-5.02697	5.470598	-0.673892
H	-5.318576	5.148913	1.029445
H	3.769057	2.975893	2.059164
H	4.033474	3.464236	0.385402
H	3.562433	4.667141	1.58916
H	0.049857	6.031659	1.818868
H	1.798481	5.982794	1.86933
H	1.006907	7.670609	0.208849
H	1.905273	6.380773	-0.615649
H	0.137946	6.412299	-0.690768

H	3.22044	-4.178554	-0.618197
H	1.71697	-4.704877	0.152992
H	1.759377	-4.394677	-1.583573
H	-3.981892	-4.304724	-2.970931
C	-7.606221	3.952044	-0.470379
C	-8.499478	1.760043	-0.902261
N	-9.434328	1.103072	-1.134852
N	-7.871821	5.082114	-0.363084
C	6.402732	-0.735741	-0.227872
C	7.18904	0.288127	-0.791973
C	8.574451	0.286153	-0.726557
C	9.277181	-0.763075	-0.079752
C	8.48573	-1.795624	0.49434
C	7.103117	-1.773311	0.422197
N	10.653869	-0.781744	-0.006868
C	11.477176	0.207035	-0.704223
C	11.734932	1.483975	0.105521
C	11.373442	-1.784993	0.779537
C	11.68109	-3.075273	0.009583
H	6.694114	1.116575	-1.29479
H	9.111724	1.117523	-1.166303
H	8.9588	-2.632557	0.993322
H	6.55254	-2.588178	0.887476
H	12.431653	-0.274274	-0.943323
H	11.014529	0.448939	-1.666283
H	10.799787	2.00217	0.341293
H	12.374259	2.17017	-0.461794
H	12.239873	1.251835	1.049839
H	10.807457	-2.006383	1.689976
H	12.309905	-1.325877	1.114102
H	12.28867	-2.864882	-0.877648
H	10.76242	-3.571228	-0.320119
H	12.238473	-3.772655	0.64558



B3LYP/6-31G(d)

Atom type, (x,y,z) coordinates:

Symbol	X	Y	Z
C	-3.241253	-3.195221	-1.471417
C	-4.433208	-2.406026	-0.867945
C	-3.377995	-3.453669	-2.982677
C	-4.969385	-3.019628	0.445629
C	-5.734556	-4.325495	0.217692
C	-6.277932	-4.921192	1.501557
O	-6.87251	-6.108141	1.266431
O	-6.205545	-4.41429	2.603739
C	-7.446941	-6.763728	2.413621
H	-3.106264	-4.159321	-0.966482
H	-5.263015	-2.332813	-1.583231
H	-3.5175	-2.513932	-3.529335
H	-2.485823	-3.947805	-3.381981
H	-4.131882	-3.193384	1.132154
H	-5.63179	-2.308008	0.948492
H	-6.584414	-4.165003	-0.459448
H	-5.110251	-5.085983	-0.266845
H	-7.871342	-7.693724	2.035997
H	-6.677599	-6.970376	3.161701

H	-8.226733	-6.141164	2.859226	H	-5.245083	5.049858	1.513311
C	4.864147	-0.713029	0.056525	H	3.983578	3.319483	0.698141
C	4.073513	-1.405345	-0.801595	H	3.843755	3.783903	-0.996998
C	2.623452	-1.343466	-0.871077	H	3.590043	4.988161	0.269801
C	1.777541	-0.179629	-0.607183	H	0.139538	6.215548	1.187905
C	1.783165	-2.395795	-1.206527	H	1.860007	6.241952	0.868296
C	0.423303	-1.932379	-1.098277	H	0.658912	7.821958	-0.642324
N	0.47331	-0.614179	-0.720917	H	1.419485	6.53284	-1.596453
C	2.176542	1.12563	-0.390128	H	-0.322862	6.49468	-1.291783
C	1.379222	2.274554	-0.16454	H	3.24637	-3.935767	-1.562737
N	0.031256	2.292707	-0.092051	H	1.739227	-4.523433	-0.857652
C	1.948912	3.613088	0.029115	H	1.793964	-4.074223	-2.563172
C	0.886695	4.452167	0.228391	H	-4.241741	-4.097036	-3.184423
C	-0.309713	3.609972	0.147702	C	-7.723092	3.758506	0.421047
C	-1.615094	4.070519	0.296016	C	-8.589548	1.547423	0.034906
C	-2.775902	3.28173	0.201387	N	-9.523665	0.857556	-0.071791
N	-2.688229	1.914239	-0.058589	N	-8.011713	4.868732	0.628972
C	-4.148782	3.636844	0.315871	C	6.315806	-0.764205	0.158998
C	-4.871262	2.433491	0.112758	C	6.960554	-0.078748	1.207662
N	-2.448198	-1.056111	-0.748125	C	8.337118	-0.095265	1.374159
C	-2.063469	-2.274113	-1.158332	C	9.175979	-0.807274	0.478452
C	-0.733738	-2.68145	-1.319683	C	8.528933	-1.490663	-0.587768
C	-3.806926	-1.034652	-0.63749	C	7.15216	-1.465944	-0.734328
C	-3.919263	1.391842	-0.116085	N	10.546216	-0.832011	0.628239
C	-4.490673	0.129553	-0.342853	C	11.225882	-0.023915	1.641761
C	-5.995649	0.345182	-0.245324	C	11.345922	-0.713303	3.0066
C	-6.17437	1.844013	0.034581	C	11.402939	-1.670793	-0.211176
C	-7.441463	2.386002	0.163736	C	11.85591	-0.991929	-1.509725
C	-4.65106	5.019485	0.594112	H	6.35773	0.47666	1.92334
C	3.411583	3.943248	-0.000358	H	8.760021	0.436831	2.21751
C	0.896163	5.940478	0.441753	H	9.112772	-2.030064	-1.323694
C	0.64726	6.74575	-0.849102	H	6.719426	-1.996326	-1.578348
C	2.162304	-3.800576	-1.566505	H	12.225546	0.206436	1.257857
H	4.384015	-0.066031	0.788565	H	10.714057	0.938576	1.740551
H	4.538016	-2.127158	-1.470517	H	10.360555	-0.937921	3.427442
H	-0.342262	-0.024235	-0.618146	H	11.881927	-0.068055	3.71215
H	3.245935	1.292648	-0.422428	H	11.898946	-1.655249	2.919983
H	-1.75455	5.127142	0.49574	H	10.887973	-2.611727	-0.429042
H	-1.783869	1.459968	-0.167631	H	12.279918	-1.941153	0.386971
H	-0.575139	-3.704639	-1.645117	H	12.411032	-0.071824	-1.295646
H	-6.460091	-0.239618	0.559018	H	11.001093	-0.730913	-2.1421
H	-6.521774	0.064487	-1.167505	H	12.512489	-1.660463	-2.078438
H	-3.825989	5.727235	0.704566				
H	-5.297857	5.37966	-0.212401				

8.0 References

1. S. Sasaki, M. Yoshizato, M. Kunieda and H. Tamiaki, *Eur. J. Org. Chem.*, 2010, **2010**, 5287-5291.
2. C. Selve, J. C. Ravey, M. J. Stebe, C. El Moudjahid, E. M. Moumni and J. J. Delpuech, *Tetrahedron*, 1991, **47**, 411-428.
3. A. El-Faham and F. Albericio, *J. Pept. Sci.*, 2010, **16**, 6-9.
4. G. Olbrechts, R. Strobbe, K. Clays and A. Persoons, *Rev. Sci. Instrum.*, 1998, **69**, 2233-2241.
5. K. Clays, A. Persoons and L. De Maeyer, in *Modern Nonlinear Optics*, eds. M. Evans and S. Kielich, *John Wiley & Sons, Inc*, New York, 1994, vol. 85, pp. 455-498.
6. Gaussian 09, Revision **D.01**, M. J. Frisch, G. W. Trucks, H. B. Schlegel, G. E. Scuseria, M. A. Robb, J. R. Cheeseman, G. Scalmani, V. Barone, B. Mennucci, G. A. Petersson, H. Nakatsuji, M. Caricato, X. Li, H. P. Hratchian, A. F. Izmaylov, J. Bloino, G. Zheng, J. L. Sonnenberg, M. Hada, M. Ehara, K. Toyota, R. Fukuda, J. Hasegawa, M. Ishida, T. Nakajima, Y. Honda, O. Kitao, H. Nakai, T. Vreven, J. A. Montgomery, Jr., J. E. Peralta, F. Ogliaro, M. Bearpark, J. J. Heyd, E. Brothers, K. N. Kudin, V. N. Staroverov, R. Kobayashi, J. Normand, K. Raghavachari, A. Rendell, J. C. Burant, S. S. Iyengar, J. Tomasi, M. Cossi, N. Rega, J. M. Millam, M. Klene, J. E. Knox, J. B. Cross, V. Bakken, C. Adamo, J. Jaramillo, R. Gomperts, R. E. Stratmann, O. Yazyev, A. J. Austin, R. Cammi, C. Pomelli, J. W. Ochterski, R. L. Martin, K. Morokuma, V. G. Zakrzewski, G. A. Voth, P. Salvador, J. J. Dannenberg, S. Dapprich, A. D. Daniels, Ö. Farkas, J. B. Foresman, J. V. Ortiz, J. Cioslowski, and D. J. Fox, Gaussian, Inc., Wallingford CT, 2009.
7. J. Tomasi, B. Mennucci and R. Cammi, *Chemical Rev.*, 2005, **105**, 2999-3093.
8. E. C. Varkey, J. Hutter, P. A. Limacher and H. P. Lüthi, *J. Org. Chem.*, 2013, **78**, 12681-12689.
9. P. Elliott, F. Furche and K. Burke, *Rev. Comput. Chem.*, Vol 26, 2009, **26**, 91-165.
10. C. J. Jodicke and H. P. Luthi, *J. Chem. Phys.*, 2002, **117**, 4146-4156.
11. C. J. Jodicke and H. P. Luthi, *J. Am. Chem. Soc.*, 2003, **125**, 252-264.
12. A. Kozyrev, M. Ethirajan, P. Chen, K. Ohkubo, B. C. Robinson, K. M. Barkigia, S. Fukuzumi, K. M. Kadish and R. K. Pandey, *J. Org. Chem.*, 2012, **77**, 10260-10271.